## Department of Precision and Microsystems Engineering

# Novel Designs to Improve Support Stiffness during Large Strokes in Compliant Mechanisms

Mridul Gandhi

| | | |
|---|---|---|
| Report no | : | MSD 2020.030 |
| Coach | : | Dr. S.H. Hossein Nia Kani |
| Professor | : | Prof. dr. ir. J. L. Herder |
| Specialisation | : | MSD |
| Type of report | : | MSc. Thesis |
| Date | : | 29 September 2020 |

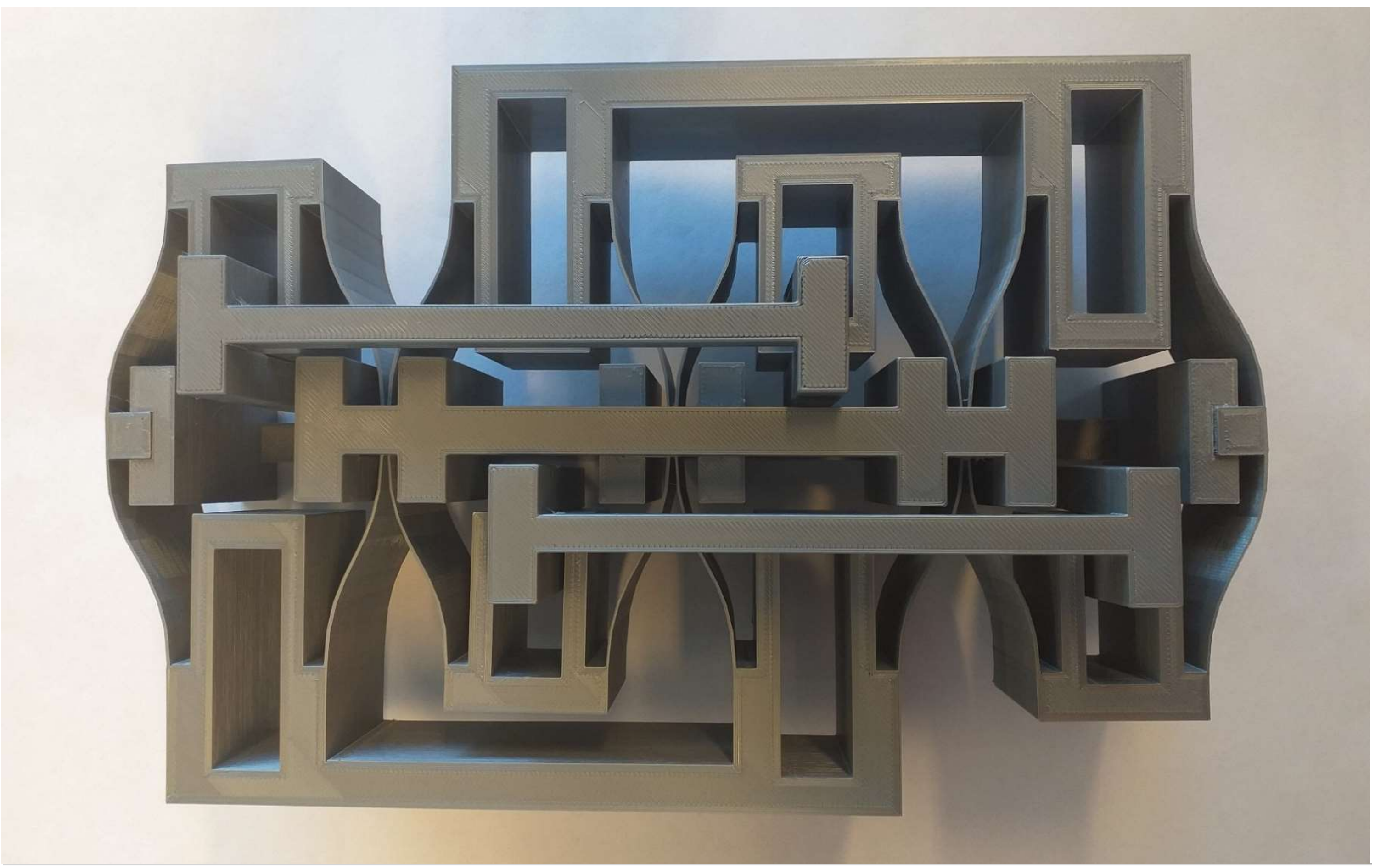

TU Delft Delft University of Technology

# Novel Designs to Improve Support Stiffness during Large Stroke in Compliant Mechanisms

by


**Mridul Gandhi**


to obtain the degree of Master of Science
at the Delft University of Technology,
to be defended publicly on Tuesday September 29, 2020 at 01:00 PM.

| | | |
|---|---|---|
| Student number: | 4861892 | |
| Project duration: | August 1, 2019 – September 29, 2020 | |
| Thesis committee: | Dr. S.H. Hossein Nia Kani (chairman), | TU Delft, supervisor |
| | Prof. dr. Just Herder, | TU Delft |
| | Dr. Andres Hunt, | TU Delft |
| | Dr. Niranjan Saikumar, | TU Delft |

*This thesis is confidential and cannot be made public until September 21, 2022.*

# Contents

# Preface

This is MSc thesis which I did in the last one year as part of my masters in mechanical engineering program. The focus of this thesis is aligned with my specialization of Mechatronics System Design in the High-Tech Engineering track. It is done in the Department of Precision and Microsystems Engineering, faculty of 3mE, TU Delft. Here, I also took several courses in my first year which made me ready to do this thesis, like, Engineering Dynamics (ME46055), Mechatronics System Design (ME46085), Non-Linear Mechanics (ME46000), Compliant Mechanisms (ME46115), Precision Mechanism Design (ME46015), Predictive Modelling (ME46090), and Non-Linear Dynamics (ME46072). It was a wonderful learning experience for me and especially as an international student, coming to one of the most reputed academic places far away from home and country. I thank my family for so much support and motivation. I would like to thank my friends back home and also new ones here who are always there for me.

I would like to thank my supervisor Dr. Hassan HosseinNia for teaching me and introducing me to his vision of the precision mechatronic systems. I am glad for all his support, freedom, feedback, and appreciation throughout the project. Due to this, I could come up with ideas to improve state-of-the-art machines. I want to thank Dr. Niranjan Saikumar and Dr. Andres Hunt who are my daily supervisors and helped me regularly with my doubts and also directing and motivating me to achieve the desired goals. I would like to thank Dr. Niranajan also for taking his time to read my thesis and give detailed feedback. His constructive criticisms have always helped me make the right decisions from day one. I want to thank the technical support staff: Rob, Gideon, Patrick, Spirdon, Bradley, and Jos for providing me the equipment to build my experimental setup and 3D-printing of parts. I would also like to thank my classmate, Madhan, for helping me set up my experiments and the whole MSD research group for fruitful discussions.

*Mridul Gandhi*
*Delft, September 2020*

# SUMMARY

The precision, speed, and stroke of mechatronic machines need continuous improvement. Compliant mechanisms are widely used in the precision machines because it eliminates friction, wear, and backlash. However, compliant mechanisms do not have larger strokes due to their compliance properties. In the present time, various applications also require high speeds and more problems appear due to the dynamics of the compliant mechanisms at such high speeds.

In the first chapter, the problems due to large strokes in static and dynamic situations are discussed. During large strokes, drive stiffness increases and support stiffness decreases. In statics, undesired deflection occurs in the support direction, that is, the load-bearing capacity reduces. In the case of dynamics, the undesired motion in support direction occurs at a reduced frequency. To avoid this, the range of motion or speed is limited. If the range of motion has to be higher then the mechanism has to operate at a lesser speed so that the undesired modes do not appear. If the speed is higher then the range of motion is less so that support stiffness is maintained throughout the stroke. So there is a trade-off between speed and stroke of precision machines. To improve the speed and stroke, support stiffness is required to be maintained or compensated. In this research, it is decided to choose a compliant mechanism which provides a single degree of freedom translation motion. Other mechanisms can be chosen later to improve the performance using the same approaches as taken in the next three chapters.

In the second chapter, a novel single degree of freedom translation stage is made which maintains the support stiffness using a passive method as well as provides amplification in stroke from piezoelectric actuators. The passive method considers only the quasi-static process and different modes can appear at further higher frequencies which cannot be controlled using this method. So in the next two chapters, two different active approaches are taken separately.

In the third chapter, a distributed mechanism is proposed to locally actuate and shape the flexures to improve the support stiffness. The design of a cell, which in series will constitute the flexure, is made to replace the conventional parallel leaf spring mechanism. Besides local control, the cell design is required to accommodate the actuator having the high force and provide amplification.

In the fourth chapter, another approach to solve the same problem is taken. Initially, 1 degree of freedom (DOF) translation stage is designed and then additional DOF in support direction is integrated. It leads to 2 DOF translation motion design, that is an XY stage. This design is further analyzed for potential advantages. In existing XY stages, bandwidth is limited by non-collocation and it further reduces in large strokes. The proposed XY stage does not have this non-collocation. It is also proved with experiments that its yaw rotation is stiff. The yaw rotation frequency does not appear within approximately 9-10 times the X-direction mode frequency.

# Preliminaries

## 0.1. Introduction

Flexure is assumed to follow the principles of finite deformation continuum mechanics. The relative change in the position of end-effector (EE) and ground is due to the deformation of the material between EE and ground. Deformation gives the displacement of material and for each direction, it depends on stiffness in that direction. Stiffness depends on the geometrical and material properties of the flexure. The stiffness required in each direction between the EE and the ground dictates the design of flexure and therefore it is one of the characteristics of flexure. When the required stiffness cannot be achieved, the performance of flexure, and further the compliant mechanism (CM) and mechatronic system gets affected.

The inverse of stiffness is called compliance. DOF is in directions having low stiffness or high compliance. These directions are called compliant directions and the stiffness is called drive stiffness [1]. In other directions, degrees of constraint (DOC) is provided by having high stiffness. These directions are called constraint directions and the stiffness is called support stiffness. A good flexure is required to have a ratio of support stiffness to drive stiffness to be at least 150 [2], so that motion is in compliant direction and not in constraint directions.

In figure 1, DOC is in $y$ direction. $w$ is the displacement of EE along $x$ direction, $\phi$ is the rotation in the counter-clockwise direction (CCW), $F$ is the external force in $x$ direction, $M$ is the moment about EE in CCW direction, $E$ is one of the properties of the material and called as modulus of elasticity, $I$ is a geometrical property and called as area moment of inertia of the cross-section of flexure and $L$ is the length of the flexure. $w$ due to $F$ and $M$ is dependent on the stiffness and stiffness depends on $E$, $I$ and $L$. **Support stiffness is in $y$ direction and it is high** to constrain the motion in $y$ direction.

## 0.2. Synthesis of Flexure Design

Constraint-Based Design (CBD): Many first designs of flexure are based on visualization techniques, experience, and rules of thumb [3]. This design method is called as type synthesis. Type synthesis gives an abstract form of the design without dimensions matching. An example is, where the motion needs to be constrained in a certain direction, more material is placed uniaxially between the ground and the EE in that direction. In this research also this technique will be used to make designs.

An analysis is required, after type synthesis, to find the dimension of the design to provide the required motion and stiffness. Three types of deformations (elongation, compression, and shear) between any two points on the flexure decides the motion and constrain directions. The theories to perform analysis are discussed in appendix 1.1.

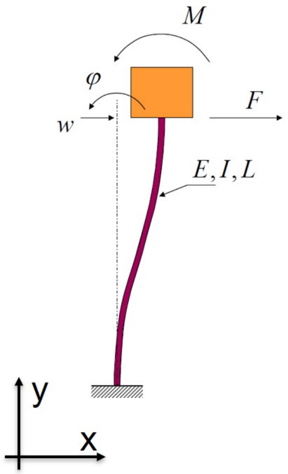


Figure 1: An example of planer flexure adapted from [2]

## 0.3. PARALLEL LEAF SPRINGS MECHANISM

Parallel Leaf Springs Mechanism (PLSM) has only the translational DOF, represented as $x$, as the two parallel leaf springs do not have the common axis of rotation. The set of two flexures has common EE and ground. It has been called plate spring, parallel guiding [4], parallel leaf spring, etc.

Translation can also be provided by using a set of 4 one DOF rotation flexures or cross-flexures as shown in figure 2. But leaf spring flexures have the least stress developed so, **the mechanisms in this research are made up of leaf spring flexures**.

## 0.4. DECREASING SUPPORT STIFFNESS DURING LARGE DEFORMATION

In a motion stage, the desired mode shapes are in the drive direction and for low drive stiffness, the modes occur at lower frequencies. For a linear motion stage, the first desired mode is in the direction of linear motion and the undesired mode is the out of plane motion or motion along support direction. Motion along support direction occurs at large transverse displacement due to reduced support stiffness. A translation stage made of parallel leaf-spring flexures is shown in figure 3. Both the leaf springs have the same EE and ground and undergo the translation along the x-direction.

The extent of motion provided by deformation is called **range of motion (ROM)** or stroke of the flexure. **This is restricted due to the increase in drive stiffness at large displacements or strokes.**. So it is required to reduce the drive stiffness, but due to the elastic behavior of flexure coupled in different directions, reducing the drive stiffness to increase the ROM also reduces support stiffness. Reduction in support stiffness also happens at large deflections and results in the graph shown in 4. Here, the support direction is along the Z-direction, but later in the project it will be marked by Y-direction.

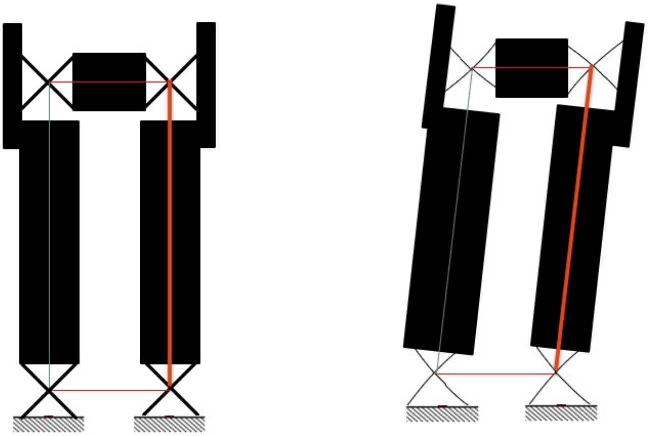

Figure 2: Four Cross flexures to provide single DOF translation motion like rigid body four bar parallelogram mechanism

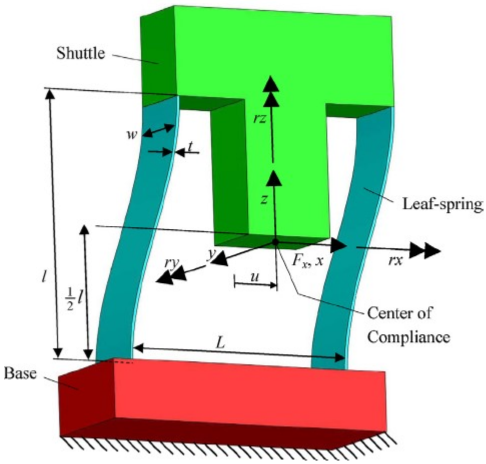


Figure 3: Basic embodiment of parallel leaf-spring flexures in [1]

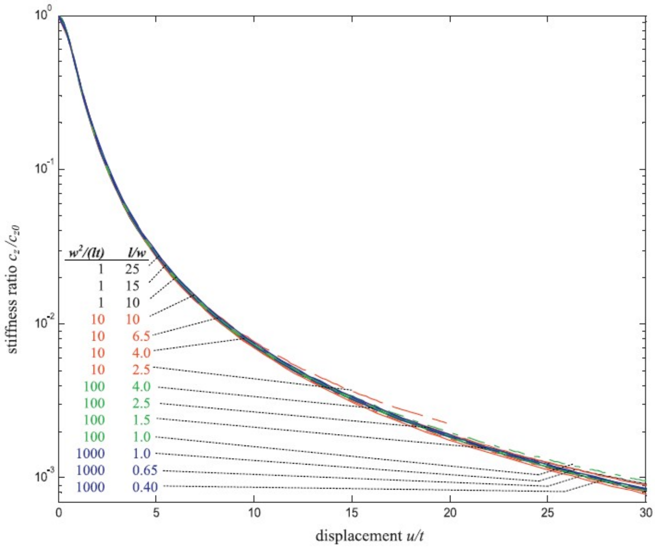


Figure 4: The dimensionless stiffness in z-direction $c_z/c_{z0}$ as a function of the dimensionless displacement u/t for various leaf-spring aspect ratios modeled by the used finite element method. The external parallel drive stiffness is zero. [1]

The stiffness in z-direction depends on the displaced position in the x-direction, the geometry of flexures, and external parallel drive stiffness due to the coupling between x- (compliance) and z- (constrained) directions.

## 0.5. MAINTAINING THE SUPPORT STIFFNESS USING PRE-CURVED FLEXURES

Mechanisms can have different sets of DOF and DOC. PLSM provides only translation motion so every other direction is a constrained direction. The out of plane motion can be mitigated by having sufficient thickness of the mechanism. Then, the longitudinal stiffness (perpendicular to the drive direction) needs to be maintained as it is in the undeformed position. The longitudinal stiffness is the highest for the perfectly flat and straight flexure. Imperfections of the size of the order of the thickness of the leaf-spring can considerably reduce its in-plane stiffness, as can deflections of the same order of magnitude [5]. So, the idea is that the flat flexure gets deformed and the pre-curved flexure gets flat, so the lost stiffness in flat flexure is compensated by stiffness gain in pre-curved flexure.

The design of a folded leaf spring with high support stiffness at large displacements using the inverse Finite Element Method (FEM) has been done by [6]. Other DOF designs, their constraint directions, and passive solutions to maintain the support stiffness are mentioned in appendix 1.3.

## 0.6. Actuators

Actuators in the precision positioning systems are commonly based on the following types:

- which works on electro-magnetic interactions like DC motor, stepper motor, induction motor, etc.
- which generates electrostatic attractive force due to the accumulation of opposite charges between two surfaces like capacitors.
- which generates strain at some applied electric potential due to its crystal structure like piezo-electric actuators
- which expands due to heating up when current is passed through it.

Piezoelectric and magnetic actuators are suitable for macroscopic nanopositioners that need to move similarly sized objects. Electrostatic and thermal devices are designed for microscopic applications. The type of actuator is based on applications in which lesser electric power consumption is desired, lesser effects due to temperature changes and smaller footprints, etc. Piezoelectric actuators generate higher force and are stiffer compared to other actuators so they have been widely used for high speed (up to some kilohertz bandwidth) and precise (up to sub-nano level) applications [7]. But the stroke is small, that is, only 0.1% of its length. So range-to-resolution ratios of piezoelectric are on the order of $10^3$. Whereas magnetic actuators have higher ratios of up to $10^7$. So if motion stages for large strokes and high force are required then using piezoelectric actuators will require an amplification mechanism.

## References


[1] D. M. Brouwer, J. P. Meijaard, and J. B. Jonker, *Elastic element showing low stiffness loss at large deflection,* in *Proceedings of the 24th Annual Meeting of the American Society of Precision Engineering, Monterey, CA* (2009) pp. 30–33.

[2] *Precision Mechanism Design, ME46015,* Lecture Notes, TU Delft, Netherlands (2018/2019).

[3] J. B. Hopkins and M. L. Culpepper, *Synthesis of multi-degree of freedom, parallel flexure system concepts via Freedom and Constraint Topology (FACT)–Part I: Principles,* Precision Engineering **34**, 259 (2010).

[4] J. Van Eijk, *On the design of plate-spring mechanisms,* (1985).

[5] J. Meijaard, *The importance of imperfections in leaf-spring flexures for the support stiffness,* Procedia IUTAM **13**, 82 (2015).

[6] J. Rommers and J. Herder, *Design of a folded leaf spring with high support stiffness at large displacements using the inverse finite element method,* in *IFToMM World Congress on Mechanism and Machine Science* (Springer, 2019) pp. 2109–2118.

[7] N. B. Hubbard, M. L. Culpepper, and L. L. Howell, *Actuators for micropositioners and nanopositioners,* (2006).

# 1

# Support Stiffness in Compliant Mechanisms

*In this chapter, the importance of support stiffness is discussed. Three performance parameters that depend on support stiffness are identified as range of motion, speed, and precision while carrying a load. The parallel leaf spring mechanism is chosen to explain the performance of 1 degree of freedom translational motion. The problems due to non-collocation in large strokes are discussed. Then the problem related to loading bearing in large strokes is discussed. Finally, the gaps in existing solutions which provide high support stiffness during large deflection are mentioned. Each gap is associated with different approaches to design which will be taken in later chapters.*

## 1.1. INTRODUCTION

Mechanical tasks like machining, positioning, measuring, imaging, or scanning at high precision with high speeds or cycles per second and overall range of motion, etc, are the growing demands in modern industries. For instance, motion of wafer stage ([1]) to manufacture billions of transistors within a $cm^2$, observing biological substances like DNA molecules which are of size in nm scale require resolution in the nm scale. Scanning electron microscope or transmission electron microscope has resolution in nm scale. [2]. Then, an atomic force microscope also requires a high speed of few kHz. The overall motion required to be achieved is on a scale of over a hundred thousand times of the resolution.

Precision mechatronic systems often have flexure guided bearings or contact-less bearings using air or magnets because they do not suffer from friction and hence don't need lubrication. In flexures, motion between two points is only due to the deflection caused by deformation in material between those two points, unlike relative motion between points in direct contact in rigid mechanisms. So, structural material has to be present between the two points. But, this eliminates friction, wear, and backlash [3]. Air and magnet-based bearings need a more controlled environment compared to a flexure guided mechanism. Whereas, flexures can be used in liquid, presence of dust, high range of pressure and temperature variations, etc. The flexure guided mechanisms are also called compliant mechanisms (CM). Apart from bearings, CMs have also been used to amplify motion from small stroke actuators. They are used in micro grippers and manipulators. They are also used as decoupling mechanisms in more than one degree of freedom stages having parallel kinematic configuration.

In all the applications of CMs, they transfers force and motion from one point to another. CMs have low load-bearing capacity due to their flexibility and less range of motion due to limited material deformation. CMs require high stiffness to support the motion in constrained motion directions and low stiffness to increase the motion range in free motion directions. In this research, the focus is on improving the support stiffness property of a CM.

## 1.2. PERFORMANCE PARAMETERS IN MECHATRONIC SYSTEMS

The performance of a mechatronic system depends a lot on its dynamics. For instance, whether it is collocated or non-collocated, how many vibration modes are observable or/and controllable, and the changing parameters such as natural frequencies and stiffness during its operation. A collocated system, ideally, does not have phase dropping below 180 degrees. Non-collocation leads to phase drop below 180 even in the ideal case, hence restricting the control bandwidth. So it is always desired to have collocation up to higher frequencies to increase bandwidth. This can be done by designing the CM in such a way that the actuator and sensor are accommodated at the same location.

A CM used for motion and force transfer to one translational direction is shown in figure 1.1. The CM provides support to the EE, orthogonal to the axis of actuation and this is required because actuators cannot take transverse loads. Such compliant mechanisms have been designed with a quasi-static deflection in mind but due to the elastic behavior, major problems are faced in the dynamic situation.

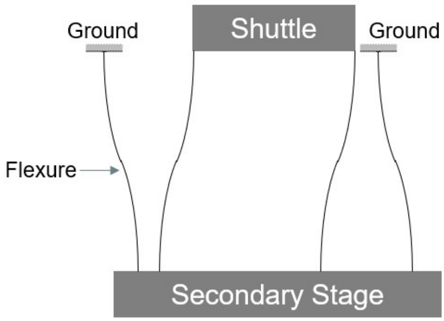


Figure 1.1: An Example of CM: Double parallel leaf spring mechanism to provide translation motion to the shuttle

**The three important** parameters in precise motion applications which are taken into account in this research are:

1. Bandwidth: The highest possible bandwidth is required both to achieve higher disturbance rejection properties and also to achieve high throughputs. The situation gets even more challenging with large displacements, as flexibility in constrained direction increases due to the loss in support stiffness. The dynamics at small displacement and the problem due to non-collocation are discussed in appendix 1.1. Here, the effects of non-collocation in large displacements will be discussed. Modes related to the support direction will appear at a reduced frequency and it is not controllable. This also reduces the ability to have a larger range of motion and so it is discussed along with the range of motion;

2. Range of motion (ROM) or stroke of CM: Larger ROM is required as discussed earlier in several applications like microscopy. It is limited due to precision or speed requirements which are also dependent on the stiffness properties. But in this research, ROM is considered to be limited due to speed requirements. Precision requirements are discussed in a separate section as mentioned below. The effect of decreasing support stiffness on bandwidth and ROM is discussed in section 1.3; and

3. Precision: The third challenge is to achieve higher precision under large deflections in any of the dynamic or quasi-static operations. Due to loss of load-bearing stiffness, the precision is not maintained in the degrees of constraint (DOC) which is a problem in applications like focusing the UV in lithography or focusing specimen in microscopy applications. Here it is discussed in terms of external forces, like gravity, changing the deformation. It is discussed in section 1.4 by taking an example of a CM carrying a load.

In this research, a 1 degree of freedom (DOF) mechanism, that is, parallel leaf spring mechanism (PLSM) as shown in figure 6, is the chosen mechanism to study problems and recommend solutions.

1

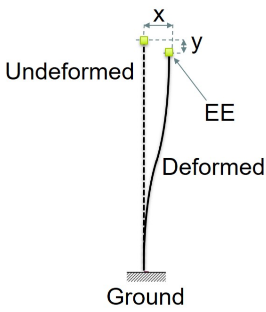


Figure 1.2: Planer flexure in undeformed and deformed configuration

The point which is required to have a certain DOF is called end effector (EE) and the point with respect to which the DOF is provided is called ground. Each flexure of the PLSM deforms equally to provide motion to EE. For any one of the constituent flexure of the PLSM, when motion is in $x$ direction there is also some motion in $y$ direction, as shown in figure 1.2).

In the next section, 1.3, we discuss how the dynamics due to loss of support stiffness during large deflections affect the bandwidth and ROM of the mechatronic system. Then in section 1.4 we discuss how it also affects precision in a quasi-static process.

## 1.3. DYNAMICS OF PLSM AT LARGE STROKES

In appendix 1.1, for quasi-static deflection of flexures, the equilibrium equations and calculation of the deformed shape using constitutive relations are discussed. Then, for the dynamics, the equations of motion and frequency response are discussed. The results of those analyses are mentioned here.

The change in stiffness corresponds to the change in drive stiffness as well as the change in support stiffness. The drive stiffness increases and there is a loss of support stiffness. Here, the focus is on support stiffness of PLSM in non collocated system.

**2 DOF motion in parallel configuration has a decoupling mechanism present between the actuator and motion stage and the sensor only senses the position of the motion stage.** An example of the XY stage shown in figure 1.3, where PLSM is the decoupling mechanism [4].

The mechanism has four pairs of flexures which are denoted by A, B, C, and D and actuators providing force $F_X$ and $F_Y$. In paper [5], the following two cases are mentioned:

- Initially, $F_X$ is applied, A and C get deformed to provide displacement in X-direction to the motion stage. The motion stage remains at the neutral position in the Y-direction. In this case, Intermediate Stage (IS) 1 and motion stage move in-phase, like rigid body mode, at frequency 18 Hz. **Second mode is when the IS1 and motion stage goes out-of-phase and it happens at a very high frequency of 1315 Hz.**

- Then, to provide displacement in Y-direction, $F_Y$ is applied. So D and B get deformed and they lose support stiffness. This can also be imagined as spring mass

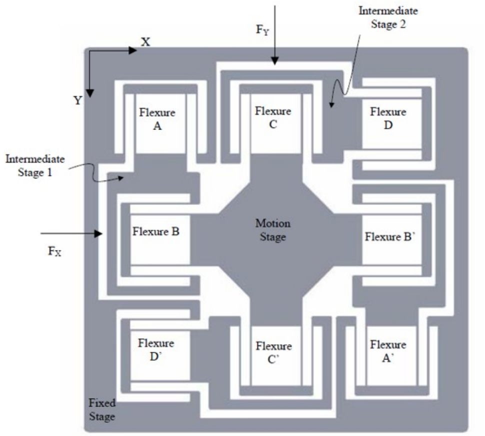


Figure 1.3: Decoupled XY Positioning of MS using CM [4]

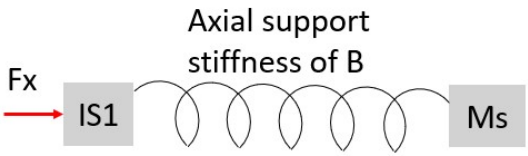


Figure 1.4: Equivalent model for fixed (non-zero) Y-direction displacement

as shown in figure 1.4. For 5 mm displacement in Y, **the frequency at which the IS1 and motion stage vibrates in out of phase drops to** 150 Hz. But there is no significant change in the first rigid body mode frequency.

So the problem is, due to non-collocation, frequency changes during dynamic operation due to loss of support stiffness. Here, the bandwidth is reduced to one-third of 150 Hz. Now, it is also important to design the controller for reduced frequency and not for the initial frequency when support stiffness was higher, else, the complete system goes unstable as deflection is increased.

One of the solutions to the non-collocated system is to have a collocated system by using more sensors and actuators which also leads to distributed mechatronics. Another way is to redesign the system using a new approach that removes the non-collocated mode while having the number of actuators equal to the number of degrees of freedom. Such a design of the XY stage is made in chapter 4.

## 1.4. PRECISION IN TERMS OF THE LOAD-CARRYING CAPACITY OF FLEXURE (LCC)

In many applications such as microscopy, the stage is in a vertical position such that gravity is acting downwards. In the case PLSM is used, due to the mass of the shuttle,

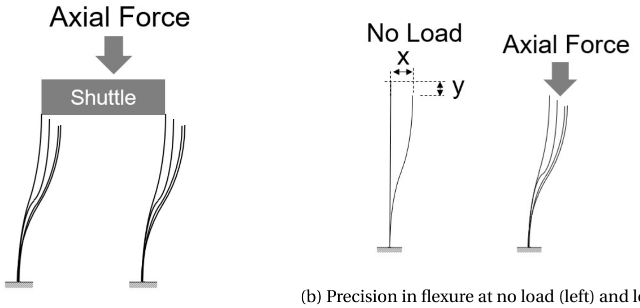


(a) Precision in PLSM

(b) Precision in flexure at no load (left) and loaded conditions

Figure 1.5: Error in position due to reduced longitudinal stiffness

there is undesired motion in the longitudinal direction when the stiffness changes during larger strokes. **Improving the load-carrying capacity of flexure (LCC), by maintaining high support stiffness while reducing drive stiffness, can also increase the ROM and increase the higher resonant frequencies.** LCC can also be defined in terms of material failure, vibration, control, actuator limitations, error in position or several other ways. Here, the LCC is defined as the maximum mass for which the mechanism has given precision. High support stiffness improves the LCC and further improves the performance of CM. So, in two different flexures having the same load, ROM and drive stiffness, support stiffness can be compared to choose the better flexure in terms of LCC.

As shown in figure 1.5, when no force is applied in the longitudinal direction, each flexure has certain deformation but when varying loads are applied, it has different deformation for each load case. So, the flexures are not robust for carrying different loads as their precision gets affected.

A CM having a larger footprint can be designed for high LCC while maintaining the same ROM. For a smaller footprint and less bulky designs, several designs to maintain support stiffness have been made and they are mentioned in the appendix 2.1. However, certain aspects have not been explored yet and solutions do not exist.

## 1.5. PASD METHOD AND GAP

In previous sections, it has been discussed that there is a need for high support stiffness for longer ROM. But before finding the solutions for high support stiffness, a design method is discussed which will be used to amplify motion in all the solution designs. This method is called providing actuation from the support direction (PASD) method. The method is proposed and four types of designs using this method are made in the next chapter 2. One of these designs is used as an example for amplifying motion in mechanisms maintaining high support stiffness using the passive approach. Two of the designs are used as examples in the two active approaches taken later.

Even if the support stiffness is maintained using the existing passive solutions, there is also a need for an actuator that can provide the required stroke and bandwidth while maintaining high resolution. For instance, piezoelectric actuators are commonly used for high-speed nanopositioning applications but their stroke requires amplification for the longer stroke. In the existing amplification mechanisms, the control stiffness in drive direction reduces along with the amplification but the force and stiffness of piezoelectric actuators are high enough to meet the requirement. The existing amplification mechanisms are also CM which has the characteristic of losing support stiffness during large strokes. There is no existing design which gives amplification along with the high support stiffness. So, a mechanism providing amplification (using PASD method) as well as maintaining support stiffness is made in chapter 2.

To reach high bandwidth, it is required to suppress higher modes of vibration. It can be damped by passive or active methods. The further development of active methods has become the point of interest in research at present times because the passive methods have reached their limitations [6]. In chapter 3, it will be shown how more local and active control of flexures can be more useful. The existing active damping method generally has the piezoelectric patch on top of the flexure or the piezoelectric embedded in the flexure laminates [7]. It needs a mechanical structure to accommodate the actuators having a higher force. The same actuators in its physical form can be used to provide the control stiffness along with the damping. So, in chapter 3, an active method to maintain support stiffness is explored in such a way that active damping can also be integrated. This is the second approach and the first active approach to solving the problem. The design proposed in this chapter will be based on the PASD method such that amplification can be provided. However, a design solution without using the PASD method has also been shown. The focus of the design proposed will be only on maintaining support stiffness and, later, it can be used to apply the control-damping which is not part of this project.

Another active approach is taken in chapter 4 which is further verified using experiments. An additional actuator to actively compensate for the loss of support stiffness is directly attached to the EE. Any undesired motion in support direction can be actively compensated by the additional actuator. This leads to a 2 DOF motion system. As problems in the non-collocated XY stage were discussed in this chapter, so, the proposed architecture should be such that it leads to a collocated system. Thus, the two actuators are directly connected to the EE, which gives a parallel kinematic configuration. In this design too, the PASD method is used to amplify motion. However, here also, a design solution without using the PASD method has been shown. In conclusion, the solution proposed is to develop higher DOF designs which are also collocated to actively compensate for any undesired motion at the EE location.

## REFERENCES


[1] J. W. Ryu, D.-G. Gweon, and K. S. Moon, *Optimal design of a flexure hinge based xyφ wafer stage,* Precision engineering **21**, 18 (1997).

[2] *Excellent guiding accuracy through flexure joints,* Physik Instrumente .

[3] L. L. Howell, *Compliant mechanisms* (John Wiley & Sons, 2001).

[4] S. Awtar, *Synthesis and analysis of parallel kinematic XY flexure mechanisms*, Ph.D. thesis, Massachusetts Institute of Technology (2003).

1

[5] S. Awtar and G. Parmar, *Physical and control system design challenges in large range nanopositioning,* IFAC Proceedings Volumes **43**, 152 (2010).

[6] *Metamech,* .

[7] E. F. Crawley and J. De Luis, *Use of piezoelectric actuators as elements of intelligent structures,* AIAA journal **25**, 1373 (1987).

# 2

# Method of Providing Actuation from Support Direction and its Application in Designing Amplification Mechanisms

*Compliant mechanism design needs to achieve a larger range of motion while maintaining the support stiffness. In this chapter, a new method is introduced in which the actuator stroke is such that the amplified motion is achieved by pre-curved flexure. Several designs have been made as examples of this method. One of the designs made using this method is taken to make a single DOF translation stage which also maintains the support stiffness passively. So the design provides amplified stroke as well as maintains the support stiffness. The design consists of an actuator block in which the piezoelectric stacks or an electromagnetic actuator can be assembled.*

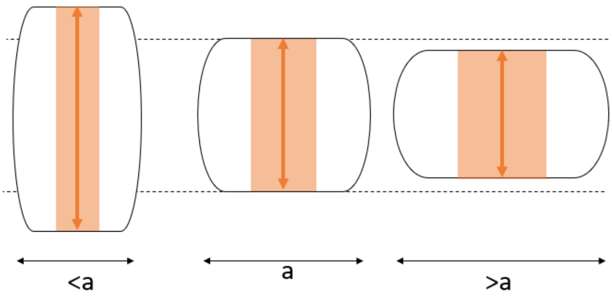


Figure 2.1: Amplification in bridge-type actuator

## 2.1. INTRODUCTION

In this chapter, the end effector (EE) of pre-curved leaf spring is actuated from the support direction of the leaf spring to provide amplification. One of the designs from this method is similar to the amplification mechanism existing in the literature and it is the bridge-type mechanism ([1]), as shown in figure 2.1. The red arrows represent the direction along which the actuator actuates. These mechanisms are commonly used with piezoelectric actuators because piezoelectric actuators have a stroke of only 0.1% of their length which is not sufficient for larger ROM.

In the conventional case, the actuator usually actuates the flexure directly in its drive direction. Here, the actuator could be fixed to the ground and apply force on the EE directly or through a mechanism. In this research, a new method is introduced which is called providing actuation from support direction (PASD). In this method, since the support stiffness decreases post deformation of flexure, the idea is to actuate the flexures from their support direction to provide the motion in the drive direction. There are several designs possible with this method and two of the designs are as shown on the left side in figure 2.2. In this case, **the actuator has to move along with the tip of the flexure, in the drive direction, to continuously actuate from the support direction.** So this is shown by a sliding roller joint, but, it is required to have a compliant mechanism. **A parallelly opposite flexure is required to move the other end of the actuator along with the primary end effector** as shown on the right side of figure 2.2. In this way, the two ends of the actuator, that are, the slider (or more commonly referred to as mover) and the stator, are directly connected to the two end effectors, one of primary flexure and the other of secondary parallelly opposite flexure. Equal and opposite force is applied by the actuator which drives both the flexures.

The first design is called "cross" because of two flexures like cross pivot flexures and the second design is called "long" because of the longer form factor. The other two designs are shown in appendix 2.2.

### 2.1.1. PRE-CURVED FLEXURES

To utilize the decreased support stiffness of deformed flexure in the PASD method, precurved flexures are made. Since a straight flexure deforms and takes shape according

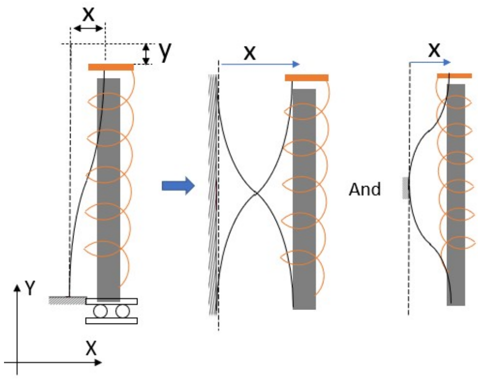


Figure 2.2: Two of the designs using PASD Method: actuation in Y-direction gives X-direction motion

to the principle of minimum potential energy, therefore pre-curved flexure has a curve that has minimum potential energy. As shown in figure 2.3, initially, flexure with 10 mm deformation and tip to tip longitudinal length of 55 mm in the curved state is drawn using 4 control vertices (CV). Then, the CV spline is converted to an interpolation spline to further change its fit method to minimize energy.

## 2.2. Passively Maintaining Support Stiffness while providing Amplified Stroke in 1 DOF Translation Motion

A passive method is present in literature (mentioned in appendix 2.1) and it is about using two pre-curved flexures in pair such that one of the flexures deforms further and the other un-deforms to maintain the support stiffness during the entire stroke. But the designs made to maintain the support stiffness using any passive method do not have amplification in strokes. Here, the second design (called "long"), shown at the left side in figure 2.2, is further developed into the translation stage with amplification in strokes.

The end effectors of two parallel pre-curved leaf springs are connected to two other parallel pre-curved leaf springs such that one of the set always maintains the support stiffness passively. The translation stage developed from "long" design is shown in figure 2.4. On the left side, a schematic outline is shown. Initially, 4 sets of "long" designs are connected and the left and right ends are fixed to the ground. The green arrow marks the point that is having X-direction motion. The red arrows represent the actuator and its stroke. The bottom figure shows the second deformed state. The center point has support stiffness maintained, as when one of the sets of flexure deforms then others get straightened. However, the center point and the tips of flexure also have rotational DOF. So, in the next step, additional sets of flexure are proposed to be connected. The connection points are shown by black arrows. Finally, the 3D model is shown on the right side. There are additional stiffeners in the middle inside where actuators can be placed. The stiffeners align the two relatively moving parts of the actuator by constraining relative

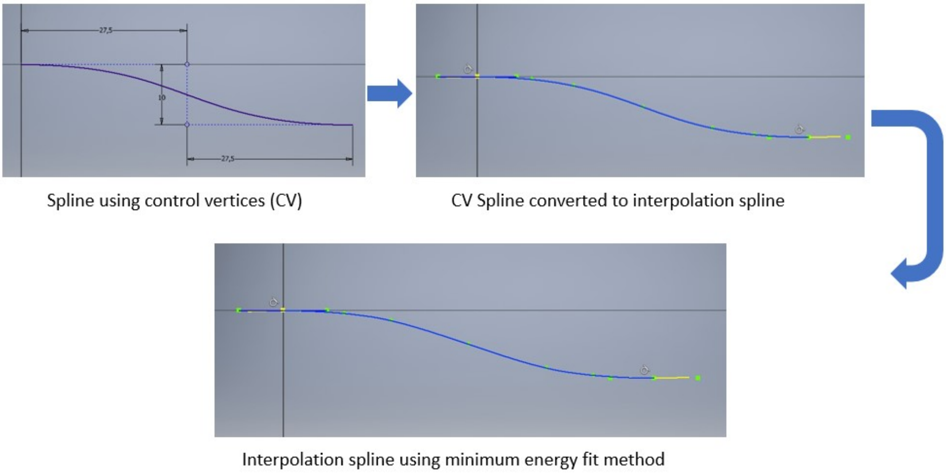


Figure 2.3: Drawing pre-curved flexures using spline

X-direction between its top and bottom parts.

The single DOF can be used to make 2 DOF XY stage. The parallel kinematic configuration is inspired from the figure 2.5. The concept mechanism outline is shown in figure 2.6. The blue arrows represent the X and Y direction motion. The blue bar represents rigid connection between its end points. The mechanism is also used to decouple the cross-axis motion. The EE is shown to be at the center point.

## REFERENCES


[1] F. Barillot, F. Claeyssen, and R. Le Letty, *Piezoactive actuator with dampened amplified movement,* (2005), uS Patent 6,927,528.

[2] S. Awtar, *Synthesis and analysis of parallel kinematic XY flexure mechanisms*, Ph.D. thesis, Massachusetts Institute of Technology (2003).

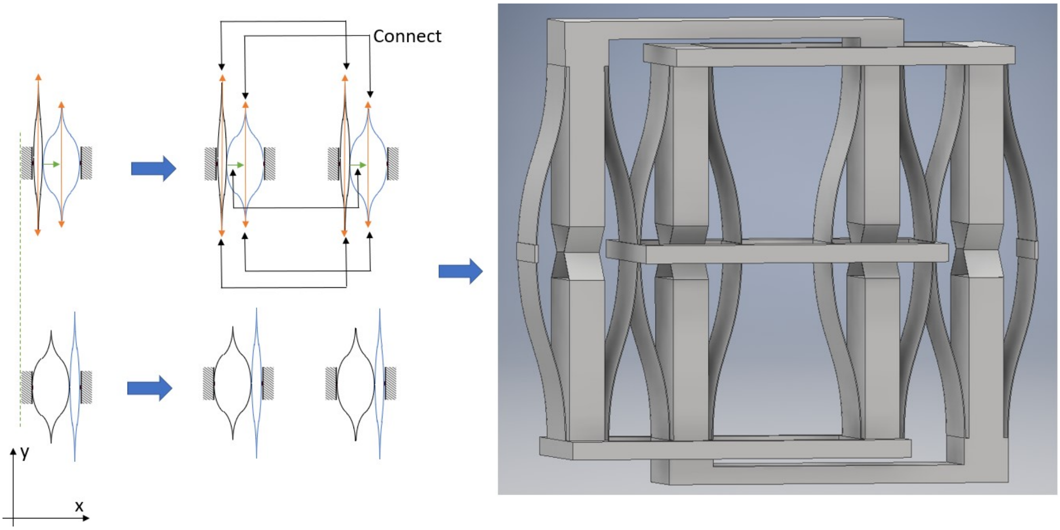


Figure 2.4: Single DOF translation stage while maintaining support stiffness passively

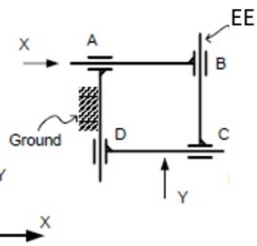


Figure 2.5: XY stage schematic for decoupled motion from [2]

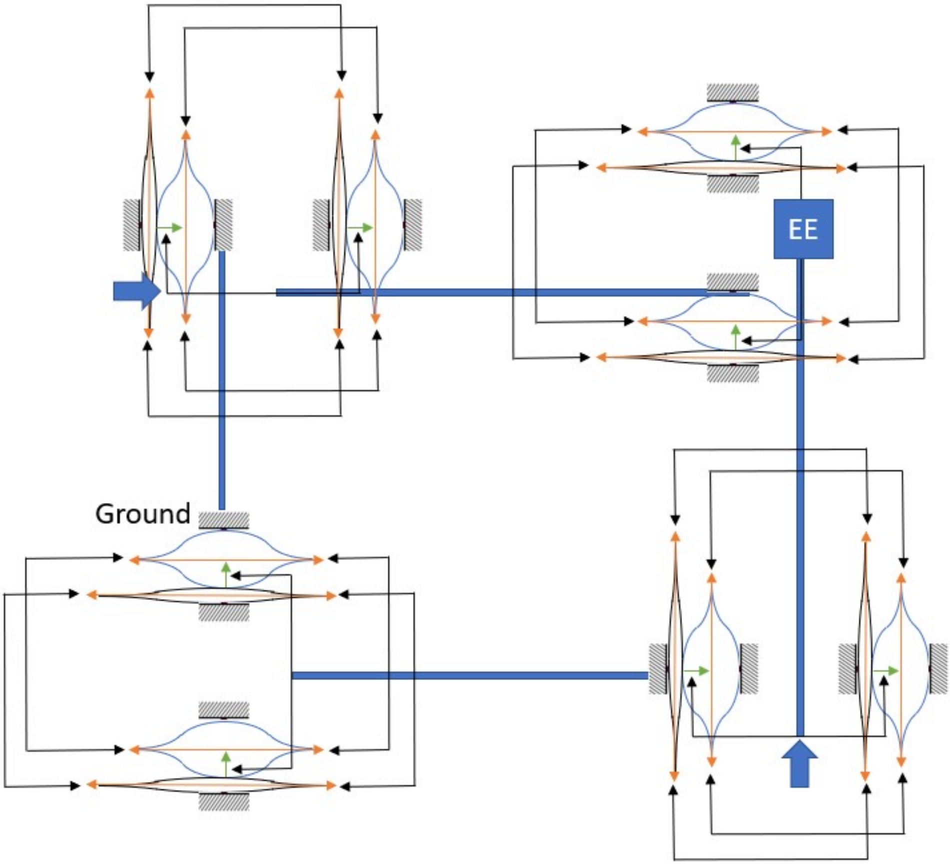


Figure 2.6: XY stage while maintaining support stiffness passively

# 3

# Distributed Mechatronics to Maintain Support Stiffness: First Active Approach

*In this chapter, it is proposed that the support stiffness of compliant mechanisms is maintained using high control stiffness of actuators due to coupling between the orthogonal directions. A leaf spring type flexure is segmented along the longitudinal direction and each segment consists of one cell. The segmented part of the leaf spring in each cell is also a leaf spring flexure. PASD method is used to make the cell design of flexure in which the actuators can be accommodated. Each cell has an actuator to actuate that segment and control its motion in the drive direction.*

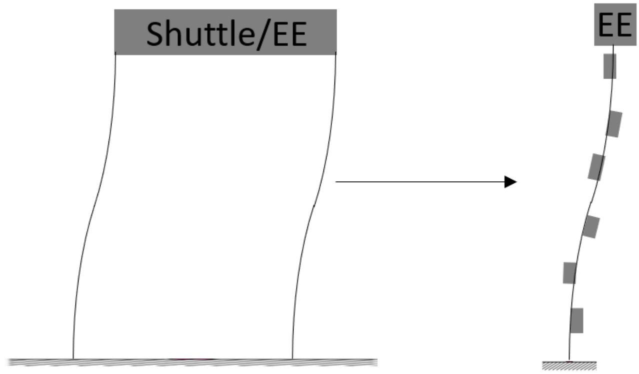


Figure 3.1: Assumed solution combining high support stiffness, controlled drive stiffness and local control using distributed mechatronics

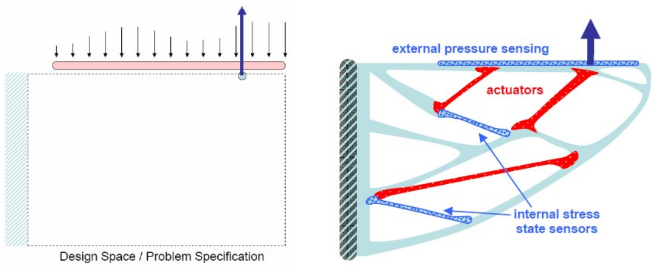


Figure 3.2: Artistic Vision of an Internalized and Adaptive Compliant System [4]

## 3.1. INTRODUCTION

Problems due to non-collocation and reduced support stiffness at large deformation have been discussed in the first chapter. In this chapter, the focus is on maintaining the support stiffness. A novel flexure beam module with low stiffness loss has been developed by increasing stiffness in some parts of the flexure in [1]. To maintain the support stiffness, more local shape control using distributed mechatronics is briefly explored in this chapter. An example of local control using several piezoelectric patches is shown in figure 3.1. **The conventional PLSM is replaced by smart flexure which has in-built actuation.** In this chapter, a cell design is made in which the actuators work within a mechanism to provide required actuator force and amplification.

Compliant mechatronic systems with high numbers of individual transducer elements could be useful for various complex distributed sensing and/or actuation tasks [2]. In CM too, actuators can be placed within the mechanism. For example, linear actuator as links, whose length is controlled. Saggere, Trease, Milojevic have take optimization-based approach to place the actuators embedded within the CM [3] [4] [5].

As shown in figure 3.2, in 2D optimization, the links cannot pass through each other. Force and displacement of the EE lie in the same plane. The next step to the 2D optimization is 3D optimization, but here, designing- based on techniques, experience, and intuition is taken in this project. The logic is basically to build up from studying the deformation of flexures.

Now, one of the flexure design has to be chosen for which the cellular structure will be made. Some types of flexures are discussed in appendix 2.1 which provide different DOFs. Here, the focus is on 1 DOF translation motion. However, each cell may have a translation or a different type of motion to provide an overall translation. So it is not necessary to use the flexures which can provide translation in cell design.

3

## 3.2. FLEXURE CHOICE

Materials are not stretched uni-axially to provide the translation motion in CM. The compliance is in the transverse direction. For rotation, only one compliant axis is required, whereas, for translation, two axes of rotations are required. For the pure translation, half of the flexure can be assumed to be analogous to quarter rotation in one direction and the other half as another quarter rotation in the counter direction as shown in figure 3.3b. So, to analyze, the flexure can be assumed to be split into these two parts and each part gives a single DOF of rotation.

Two flexure hinges can also be used to provide the 2DOF together. Examples of only translation is shown in figure 3.4. Any longitudinal load can further rotate both the flexure hinges and so together it gives a further translation. **These designs are bulkier than single leaf spring due to additional mass between the two hinges.** But, if the EE is directly actuated from actuator, the translation is constrained by the stiffness of actuator. This can be used to solve the problem of reducing support stiffness but it is not used **because the stress concentration at both the hinges become very high**. It may also not be used when maximum mass is constrained. An inspiration from light weight aircraft structure is taken here. Large aircraft structures requires high stiffness to mass ratio, the shape is controlled actively using external forces applied by actuators.

The leaf spring has constant cross-section throughout its length. So, infinitely many compliant axes between ground and EE are present and each axis provides one DOF rotation locally. So, leaf spring can be segmented into some parts where each part contributes to the overall motion of the EE of the complete leaf spring. They are segmented into as many parts as the number of rotations. Suppose more local rotations are actuated then stress increases. The shape of flexure when locally actuated is shown in figure 3.5. Points that are actuated are marked by the red arrow. The arrows do not show the direction of the force but only where force has been applied - to deform the flexure in shown shape.

## 3.3. REASON TO ACTUATE LOCALLY

The actuator is directly connected to the shuttle such that the actuator provides certain control stiffness in the drive direction. The loss in support stiffness at different control stiffness is shown in figure 3.6. There is a considerable decrease in the support stiffness when the control stiffness is negligible. But the support stiffness is maintained more when the control stiffness is high. For high control stiffness, the flexure deforms as shown in figure 3.7.

If active solutions that can locally and actively provide high control stiffness at more

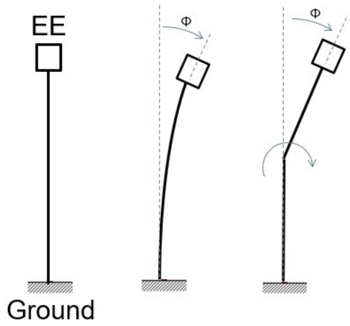


(a) 2 DOF flexure (left) under rotation only (center) its analogous rigid-body (right)

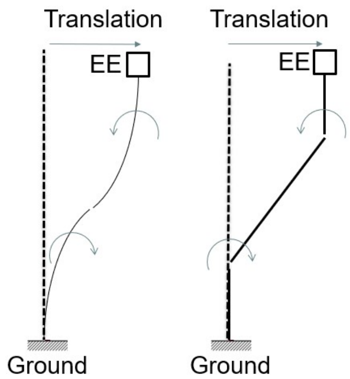


(b) 2 DOF flexure under translation only (left) its analogous rigid-body (right)

Figure 3.3: Examples of 2 DOF planer flexure

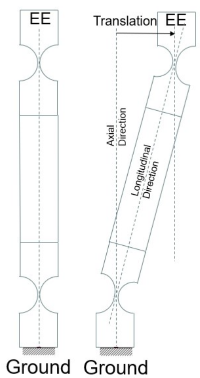


(a) Using notch flexure

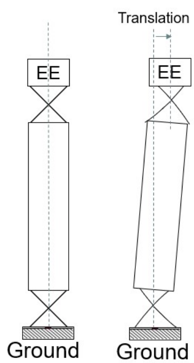


(b) Using Cross-spring flexure pivot

Figure 3.4: Example of two-axis flexure using two flexure hinges under translation

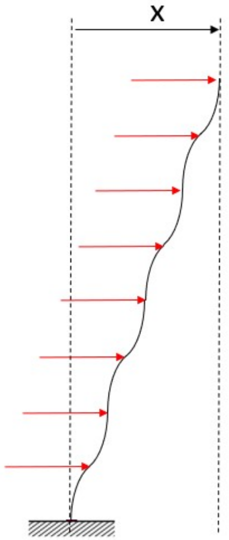


Figure 3.5: More local actuation of leaf spring flexure directly in drive direction shown at 8 points by red arrow

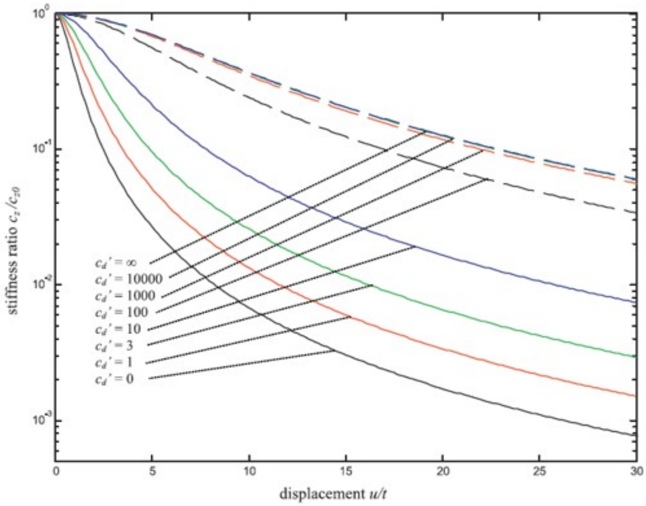


Figure 3.6: The dimensionless stiffness in z-direction $c_z/c_{z0}$ as a function of the dimensionless external parallel drive stiffness $c'_d = c_d/c_{x0}$ for leaf spring with relatively small $w^2/(lt)$ ratios and relatively small $u/l$ displacements. [6]

Figure 3.7: Longitudinal deformation of pre-curved leaf spring flexure at infinite drive stiffness

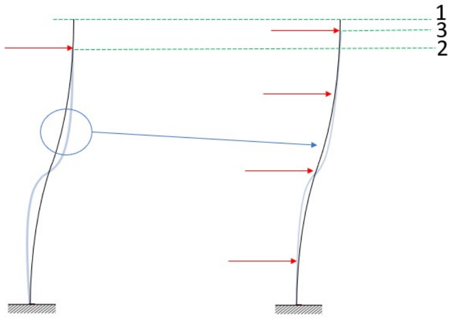


Figure 3.8: Locally actuating a flexure and shaping the material

points on flexure, then the longitudinal stiffness is maintained better. The difference between one actuator and four actuators on the shape of flexure is shown in figure 3.8. Point 1 corresponds to the tip of the flexure when there is no longitudinal load, point 2 corresponds to the case when flexure is controlled by one actuator, and point 3 when more actuators are used. Here the number of actuators shown is four. However, **such active solutions do not exist.**

When the shape of flexure is controlled by actuating at more local points then the stress between those points will also increase when compared to single point actuation in leaf springs. But for the same deflection, the stress in this mechanism will be less than the mechanism having two single DOF rotation flexures.

As shown in figure 3.9, three double parallel leaf spring mechanism are assembled such that each mechanism and its actuator form a cellular design. Each actuator directly actuates the EE of its cell to give overall motion to the EE on top most cell. **The actuator controls the position of each local EE in drive direction which also maintains the position in support direction due to the coupling between both the directions. However, in such small scale mechanism design, it would be useful if the actuators are integrated**

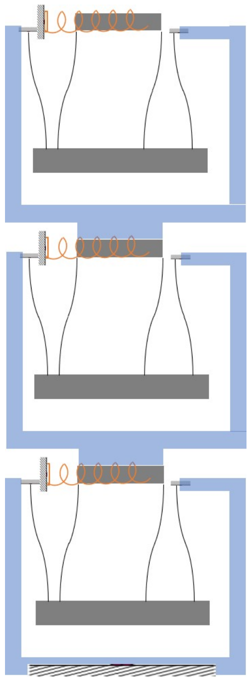

Figure 3.9: Actuators require parallel compensation mechanism because they cannot tolerate the longitudinal parasitic motion in PLSM



**into the mechanism in such a way that it can provide amplified motion.**

It is required that the actuators provide the required stiffness and stroke. This is different from active damping using piezoelectric patches, because, for the case considered in this project, the actuators also provide force during quasi-static operation. When designing for stiffness, the flexures can be imagined in the quasi-static situation for better intuition. A case study of locally controlling structures and some information on piezoelectric actuators are in the appendix 3.1.

## 3.4. MECHANISM DESIGN TO AMPLIFY STROKES USING HIGH ACTUATOR FORCE

The goal is to transfer force and motion to an end effector supported by a mechanism like a parallel leaf spring mechanism. Another requirement is to use more actuators to actively maintain the support stiffness. If actuators that provide strain are added on a flexure as shown in figure 3.1, then required actuator force and stroke is not be obtained. So, **a mechanism in which the applied force has transverse component will be more efficient.** For this, many smaller length scale mechanisms with small actuators- that can work on that length scale are made and assembled to provide the overall one DOF translation motion.

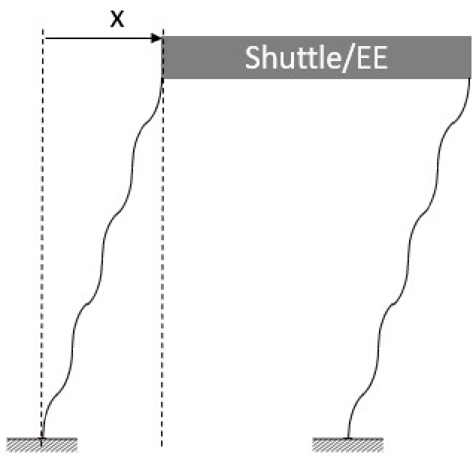


Figure 3.10: Scope for active damping higher modes of vibration using more local actuation

## Mechanism Design

Arranging bridge-type mechanism in the form, as shown in part (a) of figure 3.11, is not useful as it will not provide any motion in the required drive direction. Here, the red arrows represent the direction along which the actuator actuates. So another design is developed using the PASD method. The ends of the actuator are cross-connected by leaf spring as shown in part (b) of the figure. The leaf springs are on a different plane now. Only half of the mechanism is required. When the EE moves towards or away from each other in a vertical direction then it gives amplified motion in the horizontal direction as shown in part (c) of the figure. However, the moving part of (c) is now fixed and the actuator part moves in the horizontal direction as shown in part (d) of the figure. **This mechanism amplifies motion as a lesser stroke of the actuator is required in the support direction than the required stroke directly in the drive direction.**

For a parallel leaf spring mechanism, an embedded mechanism with an actuator is initially conceptualized to look like the one as shown in figure 3.12. Each actuator would control the motion of the leaf spring segment in the drive direction. However, it has certain flaws. **It is required to constrain any relative motion between the pair of flexures other than the actuation direction in the actuator.** So in each cell, both the end effectors (of two flexures) have to move only towards or away from each other along the axis of actuation. They should not rotate as shown in figure 3.13a and they should not translate in the transverse direction relative to each other as shown in figure 3.13b. The blue and black color of flexure represents the out of phase motion between them. The endpoints on the mechanism should move towards or away from each other in a straight line to move linearly move the straight line in its perpendicular direction. So cell designs are made as mentioned in the appendix 3.2.

Even if the EEs are constrained, they can rotate like cross pivot flexure as shown in the top left side of figure 3.14. The actuator will not be able to control the rotation so it needs to be constrained as shown in the bottom left side of figure 3.14. This results in

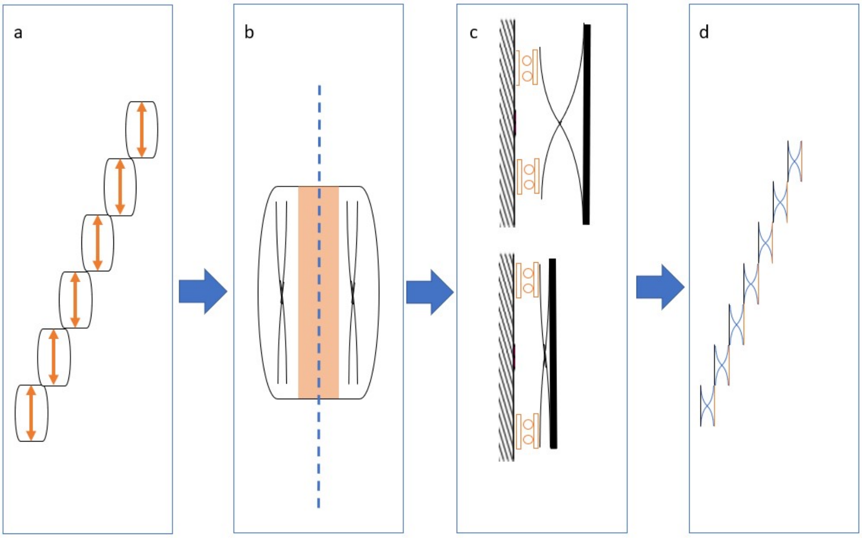


Figure 3.11: Amplification in design obtained by PASD method is same as that in bridge type actuator

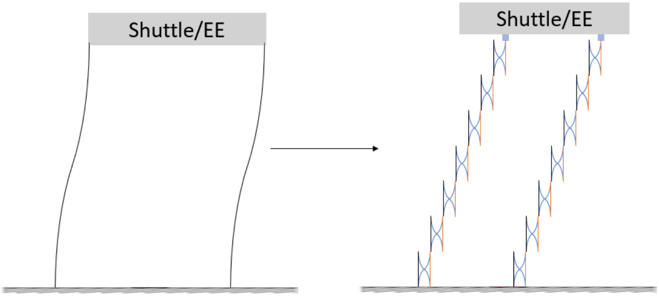


Figure 3.12: Initial concept of distributed mechatronics on each flexure of parallel leaf spring mechanism

(a) Rotation between two EEs

(b) Translation between two EEs

Figure 3.13: Relative motions between the two EEs should be constrained

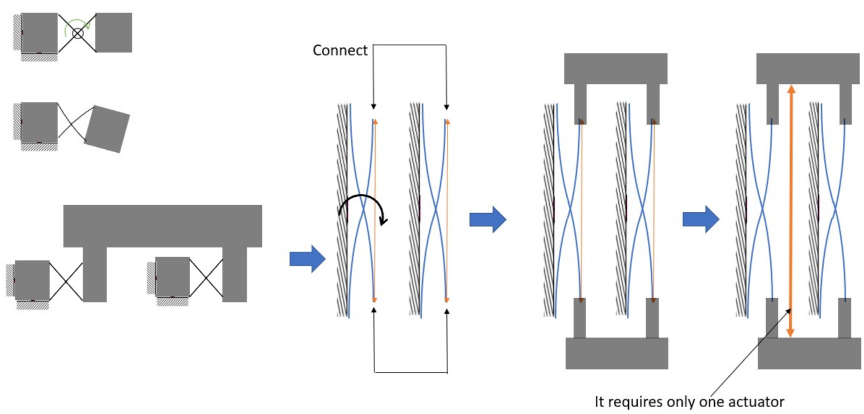


Figure 3.14: Constraining rotation using additional set of flexures parallelly

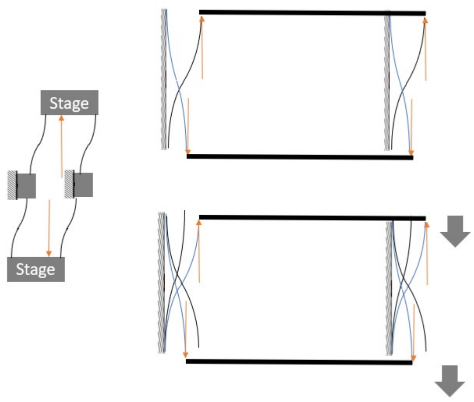


Figure 3.15: Relative translation motion between two stages after constraining rotation

the cell design shown on the right side of the same figure. There are other possible ways to constrain the rotation which are mentioned in the appendix 3.2.

The relative translation is shown in figure 3.15 and the motion is not constrained yet. In the shown case, both the secondary stages go downwards. This means that the longitudinal direction stiffness reduces when the stiffness for the relative translation motion in transverse direction decreases. For this purpose, two opposite EEs needs to be connected by a **stiffening mechanism which constrains relative motion between the end effectors in the drive direction.** This mechanism allows the motion of EEs towards and away from each other but constrains the motion in the transverse direction. It is shown in the final design. The final cell design and a complete flexure embedded with these cells are shown in figure 3.16.

There are 2 more designs like this mentioned in the appendix 3.2. Those designs are more complex than the one presented here, but their performance has not been com-

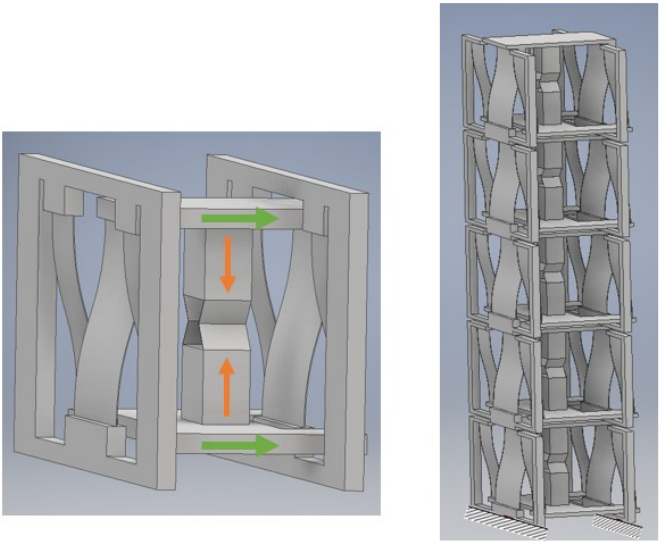

Figure 3.16: Final cell design (left) and flexure containing five cells (right)

pared and proposed for future work.

## 3.5. CONCLUSION

The goal is to locally actuate the longer flexible parts of CM so that higher modes do not appear. The conceptualized design can be further analyzed to optimize dimensions for better maintaining the support stiffness.

## REFERENCES


[1] H. Malaeke and H. Moeenfard, *A novel flexure beam module with low stiffness loss in compliant mechanisms,* Precision Engineering **48**, 216 (2017).

[2] *Distributed mechatronics,* .

[3] L. Saggere and S. Kota, *Static shape control of smart structures using compliant mechanisms,* AIAA journal **37**, 572 (1999).

[4] B. Trease and S. Kota, *Design of adaptive and controllable compliant systems with embedded actuators and sensors,* Journal of Mechanical Design **131**, 111001 (2009).

[5] A. P. Milojević and N. D. Pavlović, *Development of a new adaptive shape morphing compliant structure with embedded actuators,* Journal of Intelligent Material Systems and Structures **27**, 1306 (2016).

[6] D. M. Brouwer, J. P. Meijaard, and J. B. Jonker, *Elastic element showing low stiffness loss at large deflection,* in *Proceedings of the 24th Annual Meeting of the American Society of Precision Engineering, Monterey, CA* (2009) pp. 30–33.

# 4

# Active Support Stiffness in 1 DOF Translation Stage using Additional Actuator: Second Active Approach

*In this chapter, a concept of active support stiffness is introduced which will be used to design high bandwidth and precision mechatronics systems. The idea is to add an actuator in support direction which will compensate for the motion due to loss of support stiffness. The first step is to provide the first DOF motion in the required drive direction. Then an additional actuator is added to control motion in support direction. This way, support direction becomes a direction with a DOF and now the motion in the next higher stiff direction is undesired. Controlling higher DOF mitigates the problem of undesired modes at low frequency.*

## 4.1. INTRODUCTION

Change in support stiffness while moving the EE from one point to another causes undesired motion. The motion can be different at different points due to external forces such as gravity. For instance, in figure 4.1, it is required to rotate the EE through the solid link as shown by the red arrow but gravity is vertically downwards. Problems due to structural compliance of the link and their solutions are discussed here which will lead to the concept of active support stiffness.

- In part 1, the EE is straight upwards so the link is longitudinally very stiff to support the load of EE. So there is a negligible error in precision
- In part 2, the actuator rotates the link and ideally it should be in the position as shown here (green color).
- In part 3, due to structural compliance of solid link, there is bending which deviates the EE from the desired position (red color).
- In part 4, control is implemented to reduce the error shown in step 3. A sensor can be placed on the EE and feedback control can bring the linkage to the position shown by the dotted green color. However, the orientation of the EE is wrong as shown by the red color of EE.
- In part 5, another actuator is added to re-orient the EE correctly. Now the system will require a multi-input multi-output (MIMO) control.
- In parts 6 and 7, the EE is brought back to a straight-up position. Since the compliance of the link is different at each position so the mechanism suffers parasitic motion. It will be a choice to put the mechanism at either orientation shown in part 6 or that shown in part 7.
- In part 8, an additional actuator is added to remove the error caused by the parasitic motion.
- In part 9, the architecture of the system, using MIMO control, is free from errors caused due to external forces and structural compliance. But the system has become 3 DOF system where the additional two actuators compensated for the loss in support stiffness in part 3.

This means a mechanism has to be first made for a drive direction and then the mechanism is modified to accommodate additional actuators to compensate for the loss of support stiffness. Further to make a collocated system, all the actuators should be directly connected to the EE. By designing mechanisms, that provide 1 DOF translation motion, and then adding another actuator, to control the motion in support direction which is perpendicular to the transverse direction, will lead to an XY positioning stage. Another method is to directly choose the XY positioning stage and control both X- and Y-direction motion by including the compensation for loss of support stiffness.

Now, the vibrations of EE in the X-direction, while moving in the Y-direction (or vice versa), can be actively controlled which was not possible by passive support such as rigid

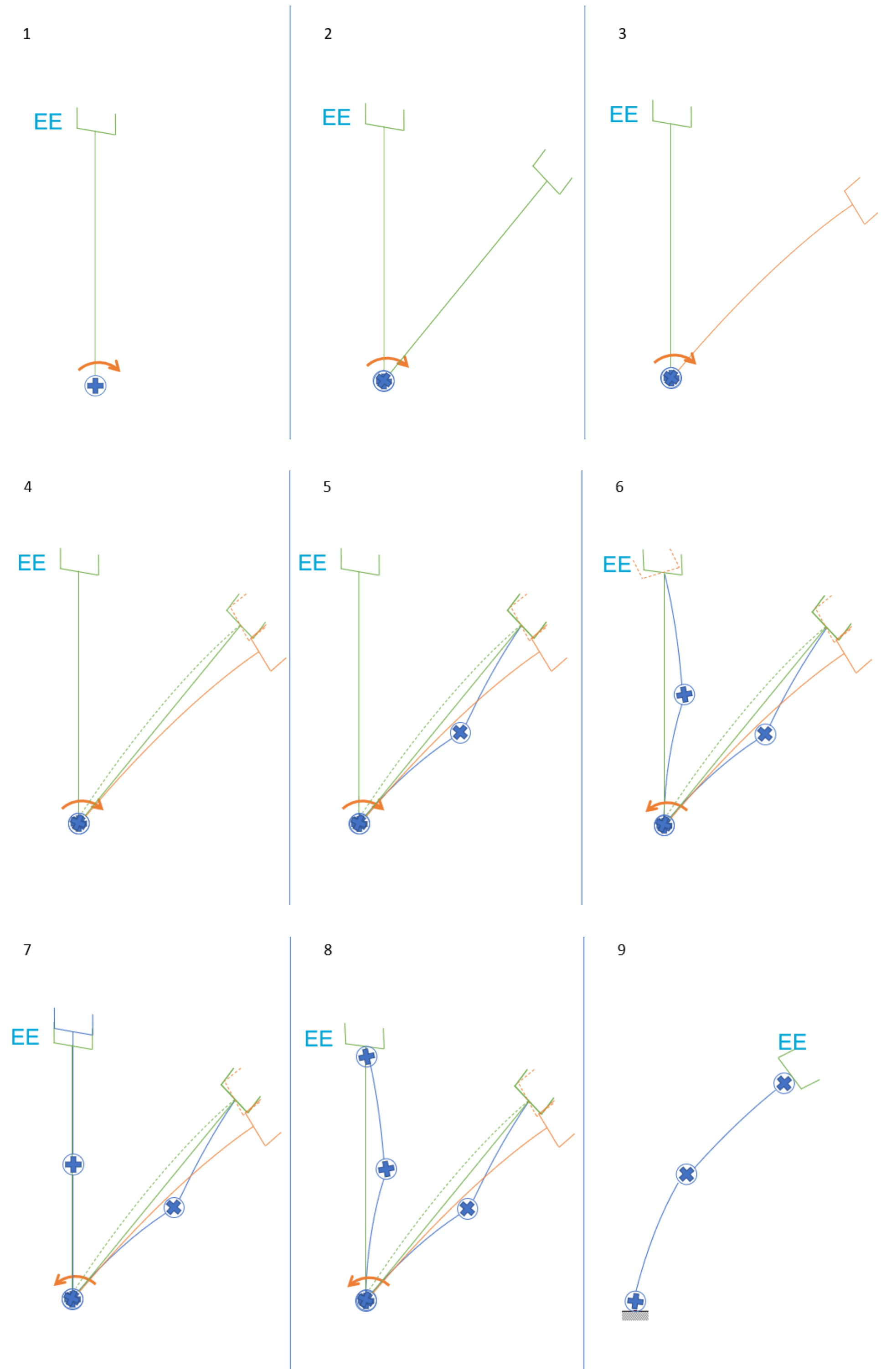


Figure 4.1: Problem due to structural compliance and its solution. Gravity is present vertically downwards.

body bearings or a compliant mechanism. Since longitudinal support direction has become a DOF, so yaw rotation becomes the new first undesired mode. Then, active support in the direction of yaw rotation will eventually lead to $XY\theta$ positioning stage and there will be motion in other directions that becomes the first undesired mode of vibration.

## 4.2. NOVEL COMPLIANT XY POSITIONING STAGE: FOR HIGH BANDWIDTH AND LARGE STROKE APPLICATIONS

(Next page)

# Novel Compliant XY Positioning Stage: for high bandwidth and large stroke applications

Mridul Gandhi

***Abstract*—In this paper, we present a novel design of an XY positioning stage for high bandwidth and precision mechatronics systems. The idea is to remove non-collocation in existing designs and have the undesired modes at higher frequencies. Firstly, a decoupling mechanism to provide 1 DOF translation motion and up to 10 times amplification is designed. Then an additional actuator is added to control another translation motion in the perpendicular direction which leads to the XY stage. This results in a range of motion of 2 cm in X-direction and 1 cm in Y-direction within the footprint of 20 cm in X-direction and 15 cm in Y-direction. The natural frequency of undesired motion such as yaw rotation does not appear up to 10 times the frequency of the desired X-direction motion. These results are also found to be in line with the simulations done in a finite element analysis software.**

## I. Introduction

Micro-/nano- positioning systems are required in a variety of applications such as microscopy, lithography, metrology, imaging, etc. Several positioning stages have been designed and each new design is pushing the previous limits of performance such as speed, range of motion (ROM), and resolution. In large range nano-positioning systems, only $20\,\mathrm{nm}$ RMS radial tracking error while traversing a $2\,\mathrm{mm}$ diameter circle at $2\,\mathrm{Hz}$ has been made possible. Here the range is $\sim 10^7$ times the resolution [1][2]. It is high time to develop these machines using a new design method that crosses the limits of performance attained by existing machines. It is possible when the new system behaves in ways where it is possible to control it at higher bandwidths and hence achieve overall higher speeds of operation.

There are two types of kinematic configurations in a mechanism, that is, serial type and parallel type. In the serial configuration, each mechanism that provides one degree of freedom (DOF) is on top of the mechanism of one other DOF. In this way, actuation of the mechanism which is directly connected to the EE can respond like the response of a collocated system, that is, one of the DOF shows pole-zero pair. But lower mechanisms will show a response like that of a non-collocated system. So, it is desired that the stage is of parallel configuration and all the motions in desired directions show collocated response.

## II. Prior Art

In parallel type XY stages, as shown in figure 1, design architecture generally consists of two actuators actuating perpendicular to each other. Also, it may or may not have an amplification mechanism. Then, there are two similar decoupling mechanisms (DM) each associated with one actuator or actuator-amplifier. Then a rectangular motion stage (MS) is

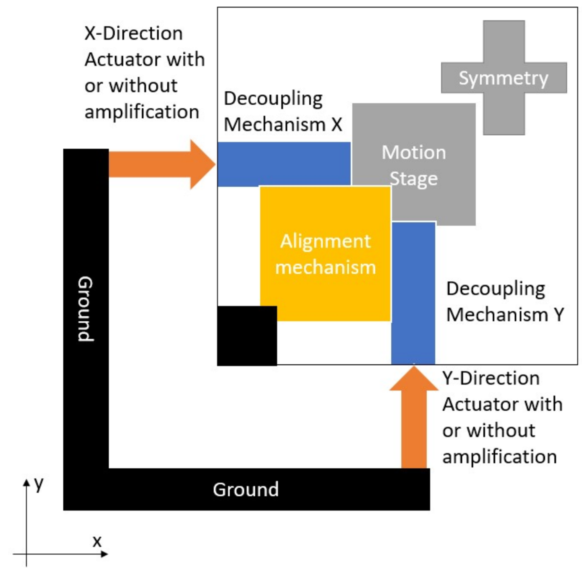


Fig. 1: Common architecture in the existing literature

connected by the DM on its perpendicular adjacent edges. Each of the other two edges of the rectangular EE also consists of similar DM to create a symmetrical design. This is required to reduce the coupling between the X- and Y-axis. Then, since there is no connection between the stator and mover of the actuator, therefore, an additional mechanism to align them is used and here it is called alignment mechanism. So, the basis of this design is that it has actuation from perpendicular directions [3] [4] [5] [6] [7] [8] [9] [10] [11] [12] [13].

While driving the motion stage in one of the axes, the drive stiffness increases because of the DM on the other axis. So it requires control that can handle the non-linearity. The DM also has support stiffness to transfer force and motion to the motion stage. But, the support stiffness along one axis reduces when the second axis actuator moves the motion stage. For small ROM, it could have been approximated as multiple SISO (single input single output) systems from the control's perspective. But, since the stiffness of the spring depends on the position in another axis, therefore a MIMO (multiple input multiple output) control or decoupling filters are used for large ROM. Even in such a scenario, the reduction of stiffness requires complex control and/or significant reduction of control bandwidth.

A novel 2-DOF large stroke flexure based positioning mechanism is designed in [14]. It has a different architecture which gives work-space-area to footprint ratio of 1/32 and undesired motion at a high frequency of 80 Hz. But the full lengths of the

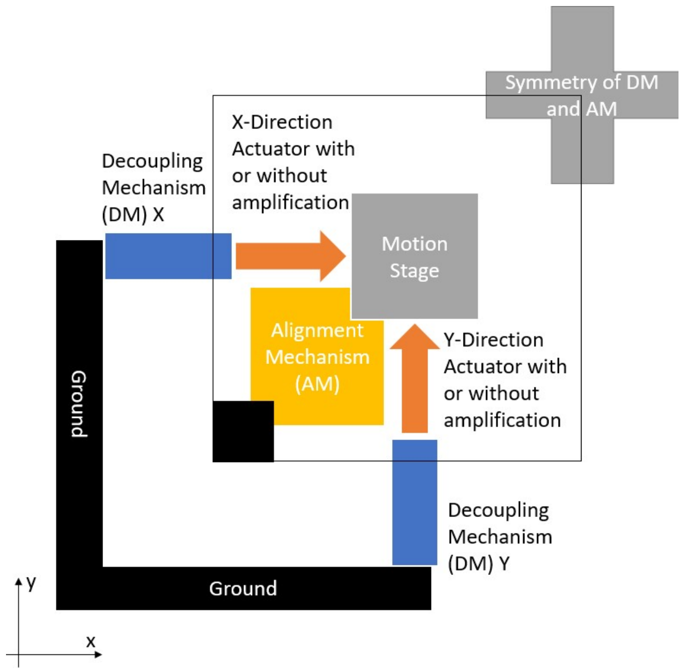


Fig. 2: An option of removing the non collocated mode due to out of phase vibration between actuator block and MS.

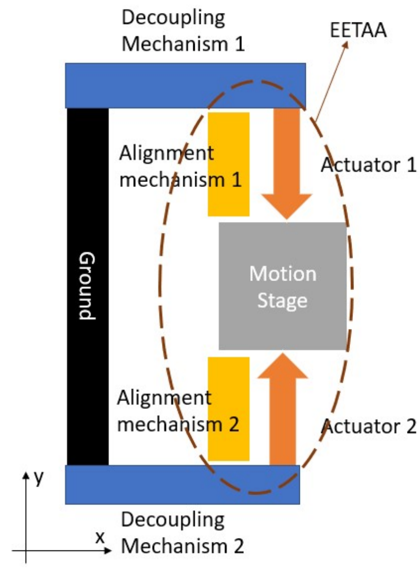


Fig. 3: New architecture using the proposed method

links are not flexible and have cross pivot flexures as hinges. In this research, the objective will also be to improve the footprint ratio so the DM will provide amplification besides decoupling, but moreover, the entire link will be flexible like leaf springs. So, the stress developed for a given stroke is reduced.

### *A. Limitations in Current XY Positioning Stages*

The dynamics and control of precision machines based on compliant designs such as XY positioning stages can be discussed in two cases. First, the out of phase vibration between the point of actuation and the MS happens at lower frequencies due to loss in support stiffness when there is a larger stroke in the other direction. This is a problem of controlling a non-collocated system and so it is required to remove the non-collocation by having both the actuators directly connected to the MS - without the DM in between. One way of doing it is to connect the DM to the ground and actuator between the DM and MS, as shown in figure 2. In this case, the alignment mechanism will have to be modified to accommodate the moving actuator in middle.

Second, even if the system is without the above non-collocated modes, then the first undesired mode is usually the yaw rotation. The desired two modes are in X- and Y-direction and they are required at lower frequencies compared to the yaw rotation. But, yaw rotation stiffness should be high to avoid its excitation. This is possible by changing the architecture of "actuation in the 2 perpendicular directions for two DOF motion". In this paper, the architecture is changed to "using differential actuation in single direction for two DOF motion".

## III. New Mechanism Design

The new architecture made using the differential actuation method is as shown in figure 3. The MS is connected on the top and bottom sides which are separately connected to the ground via alignment mechanism and DM. This forms a parallel configuration. It is chosen that the two actuators control the motion in X- and Y-direction while applying forces only in the Y-direction (positive as well as negative) such that both the actuators are uni-axial. Both the actuators need to be directly connected to the MS, so the MS is present in the middle of the actuators. The coil of the actuators are fixed to the MS and the magnets are fixed to the end-points of the DM (later it will be called secondary stages of the XY stage). The MS and the coil of both the actuators need to be driven in X-direction along with the magnets of both the actuators, so, an alignment mechanism is used. The motion stage is like a common EE for both the combinations of DM and alignment mechanism.

The alignment mechanisms, their common EE (MS), and two actuators form a sub-assembly which is called the "EE and Two Actuators Assembly" (EETAA). So, the EETAA is between the secondary stage of both the DMs.

So, the XY stage has two sub-assemblies: first is the set of two DMs and the other is the EETAA. The DMs together provide 1 DOF to the EETAA in X-direction and the EETAA provide 1 DOF to the MS in Y-direction.

### *A. 1 DOF Decoupling Mechanism with Amplification in stroke*

The translational motion provided by the two DMs together is chosen to be in X-direction. It is chosen that, when both the "secondary stages" are actuated towards or away from each other (force in opposite directions) then the DM moves EETAA in positive or negative X-direction. That is, the difference in the actuators' force determines the position of MS in X-direction.

To move the MS in positive or negative Y-direction, both the actuators will apply force on MS in the same direction. That is, the sum of forces generated by the actuators determines the position of MS in Y-direction.

Two of the possible configurations are shown in figure 4. DMs designed in the first part amplifies the motion provided from both the actuators together. In this configuration, the angle between the direction of actuation and flexures is 0 degrees. It requires higher force and pre-curved flexures to operate. Applying the longitudinal force on straight flexures leads to buckling but deflections of the order of the thickness of the leaf-spring can considerably reduce its in-plane stiffness [15]. So the pre-curve having the curvature of deformed flexure helps in reducing the required magnitude of the force which is practically possible to implement.

For the second configuration as shown in the second part of the figure, the stroke of DMs in X-direction is lesser than the stroke provided by the two actuators but the DMs require lesser force to operate. In this configuration, the angle between the direction of actuation and flexures is 90 degrees. The flexures in this configuration can also be pre-curved to tune the force and ROM. However, the first DM design is chosen to proceed as it has more amplification. It can be observed that the direction in which the actuator in EETAA is actuating is the support direction of the DM, where DM is a parallel leaf spring mechanism. Stroke is amplified when the actuator actuates from the support direction of a flexure. So, the method of designing such amplification mechanisms is called providing actuation from the support direction (PASD) method.

A DM can also be designed between the two extreme cases ($0^\circ$ and $90^\circ$) discussed above. As shown in figure 5, the EETAA is at an angle with the flexure of DM. The flexures are shown to be straight but they can also be pre-curved as discussed above. The angle can be chosen by optimizing the available actuator force and the amplification of the stroke.

*1) Stiffener:* A stiffener between the secondary stages is required for several reasons:

First, as shown on the left side of figure 6, the relative motion of the secondary stages in X-direction needs to be constrained to avoid damage to EETAA. Here the blue and black color of flexure represent the out of phase motion of the secondary stages with respect to each other. While the DMs provide X-direction motion, the force on secondary stages acts in the Y-direction such that they are in opposite directions to move the secondary stages towards or away from each other. So relative Y-direction translation should be allowed while constraining the relative X-direction motion.

Second, when the EETAA has to provide the Y-direction motion to the MS then the reaction force on secondary stages are in the same direction along Y. In the shown figure 6, when the MS is required to move in the positive Y-direction then reaction forces on both the secondary stages are acting in negative Y-direction. So, the secondary stage on top would move in positive X-direction and the secondary stage on the bottom would move in negative X-direction. This leads to both the secondary stages going in negative Y-direction and the EETAA would also go along with them in the negative Y-direction. So required Y-direction motion cannot be achieved without constraining the relative X-direction motion.

Third, when actuators apply unequal magnitudes of force, the secondary stages need a coupling so that the difference in forces is used to move to the required position in X-direction.

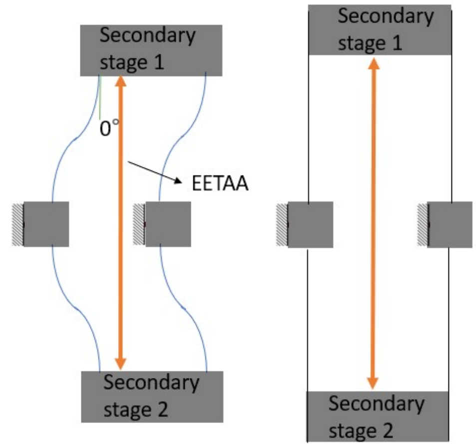


(a) DM designed using PASD method for amplification. But it requires higher force and pre-curved flexures to operate

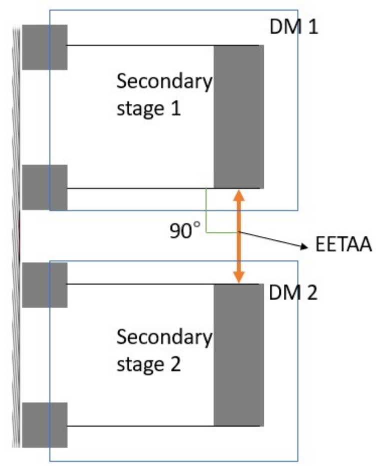


(b) DM having lesser stroke but requires lesser force to operate

Fig. 4: DM designs to provide motion perpendicular to EETAA (orange)

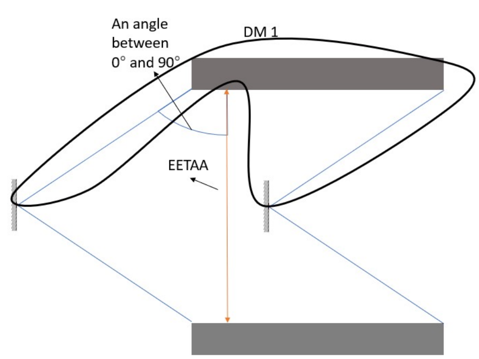


Fig. 5: Third design of DM having an angle between EETAA and the DM

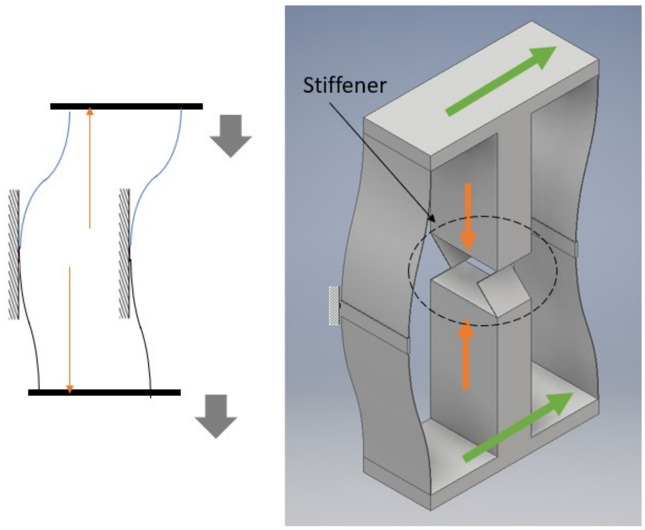


Fig. 6: (Left) problem due to relative X-direction motion, (Right) using stiffener to constrain the relative X direction motion but allow Y direction motion

For above reasons, a stiffener is made of L-shaped flexures as shown on the right side of figure 6. The stiffener allows relative Y direction motion but not in the X-direction. This is the final design of DMs and stiffener assembly which provide only 1-DOF translation motion when the two secondary stages on top and bottom are actuated. These are called secondary stages because the primary stage is designed in EETAA. The secondary stages have the parasitic motion like the parallel leaf spring mechanism but the primary stage designed in the next sub-section will not have the parasitic motion. So it is the motion stage for the complete XY stage setup.

## B. EETAA: End Effector and Two Actuator Assembly

The 3D model of EETAA and one DOF translation motion, along the Y direction is as shown in figure 7a and 7b respectively. For showing Y-direction motion, opposite ends of the EETAA are considered as fixed reference points. To move only in Y-direction, both the actuators have to apply equal force in the same direction. This way the force on the other ends of EETAA is also equal so that there is no X-direction motion.

In presence of an external force on MS in the Y-direction, both actuators apply force in the opposite direction of the external force to cancel the motion due to the external force. This way, the position or motion of the MS in Y-direction can also be controlled during the change in support stiffness of DM while moving in X-direction. This is a multiple input multiple output non-linear system.

An alignment mechanism is required to constrain relative X-direction motion between the two actuators, MS and DM. The alignment mechanism is made of the L shaped flexures as the design is based on Sarrus linkage to allow only one DOF translation motion. This is used to align the stator with

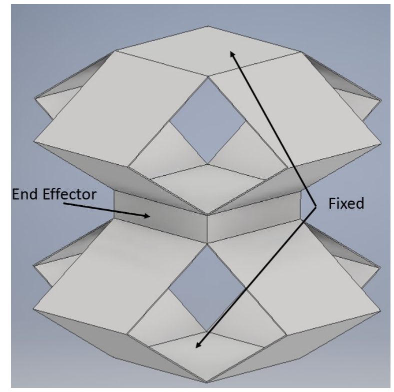


(a) 3D model of EETAA

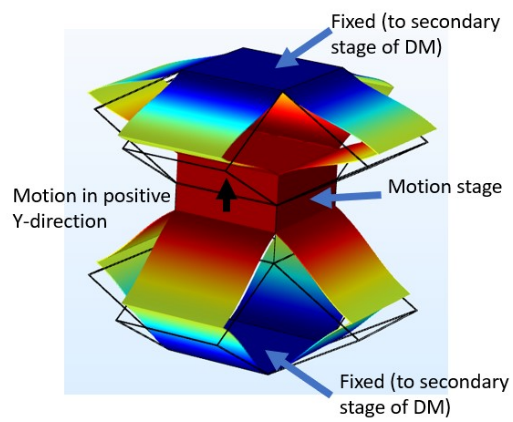


(b) Motion of EE in EETAA

the mover part. For the two actuators, there are two such mechanisms.

The opposite ends are shown to be fixed because they are fixed to the secondary stages of DMs. Both the DMs along with the stiffener does not allow any relative motion other than the translation along the Y-direction. That is, secondary stages are moving towards or away from each other only during X-direction motion. It can be assumed fixed during the Y-direction motion provided by EETAA as there is no X-direction motion.

The stiffener between two DMs also constrains the relative X-direction between top and bottom of EETAA. If the opposite ends were not constrained, then both the sets of L-shaped flexures can rotate about the Z-axis as shown in figure 8. But the connection at DM can only translate as shown on the right side of the figure and the rotation about the red dot is constrained. In the figure, each of the two sets L-shaped flexures of the EETAA are assembled within a parallel leaf spring mechanism.

The thickness of flexures in DMs constrains the out of plane motion of EETAA. Similar to the in-plane rotation, that is in the XY plane (along Z-axis), the set of L-shaped flexures could also be rotated in the out-of-plane direction (along X-axis). But, the rotation is constrained by having a sufficient thickness of the DMs in out-of-plane, which is the Z-direction.

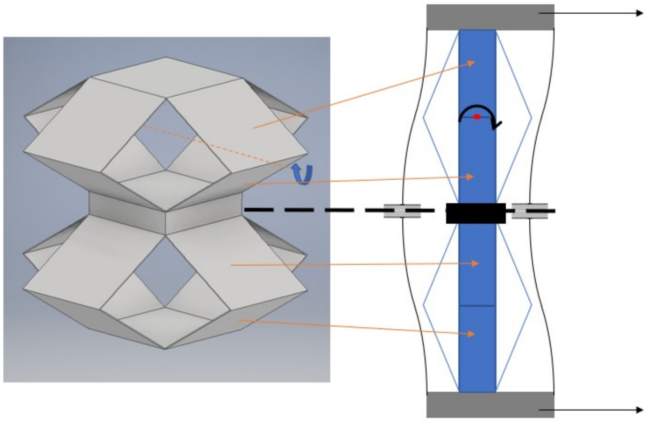

Fig. 8: Integrating EETAA into parallel leaf spring mechanism constrains rotation of L-shaped flexures in EETAA

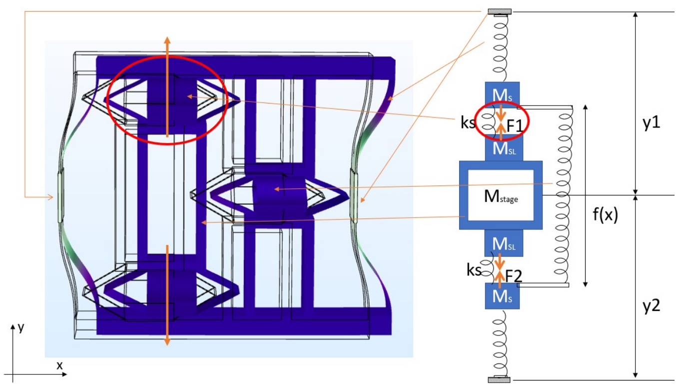


Fig. 9: Equivalent spring mass model

## IV. Modelling in equivalent Spring-Mass System

As shown in figure 9, the flexures of DM are shown as springs directly connected to the ground on top and bottom. The springs representing the alignment mechanism are shown parallel to the actuators. In the center, it is the mass of MS which is attached to the slider of both the actuators. The stiffening mechanism is shown by another spring on the right and parallel to the EETAA spring-mass. The forces due to actuators are shown in orange color arrows. $M_{ST}$ is the mass of the stator of the actuator, $M_{SL}$ is the mass of the slider of the actuator, and $M_s$ is the mass of each secondary stage added with the mass of the stator.

The existing models have the DM between the actuator and the EE. But in the proposed model, the actuator is directly connected to EE. Since the sensor is placed on EE for the feedback control, so the existing models are non-collocated and the proposed model is collocated. The difference is shown in figure 10. The derivation of the transfer function, which shows the collocated system, is in appendix A.

For a symmetric EETAA, y1 and y2 are equal when there is no external force and no net force by the actuators on the MS in Y direction. In presence of an external force like gravity in the Y-direction or net force from actuators in the Y-direction, the difference between y1 and y2 will give the position of MS in the Y-direction.

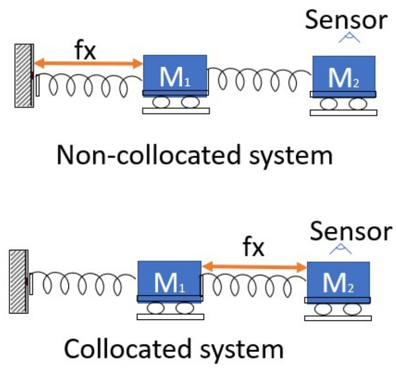


Fig. 10: (Top) non-collocated and (bottom) collocated system

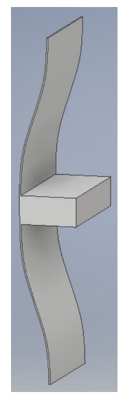

Fig. 11: 3D model of pre-curved flexures drawn using spline feature in CAD

The length of the EETAA at any value of Y is the function of X. The inverse of this function gives the position of MS in the X-direction. The length of EETAA depends on the longitudinal length of flexure in DM and this depends on the displacement of flexure in transverse which is the X direction.

## V. CAD, Simulations, and Manufacturing

### A. CAD

*1) Pre-curved flexures:* For straight flexures, any shape it achieves after deformation is governed by the principle of minimum potential energy. A curved flexure like the deformed straight flexure is required for reduced support stiffness to implement actuation from support direction. So, the pre-curved flexures are made with splines of minimum potential energy in CAD software Autodesk Inventor. The thickness is comparable to the available printing capability of making the minimum wall thickness, that is, 0.5 mm. So, the width of the flexures is chosen to be 0.5 mm. The initial deflection due to the curve is 10 mm in the flexures. The combined length of flexures such that the initial distance between the two secondary stages of DM is 55 mm.

*2) Modules of 3D prints:* Firstly, the DM, MS, and the part of the alignment mechanism of EETAA which is in the same plane is 3D printed as one piece such that the flexures are made as walls. This does not require any support material. A

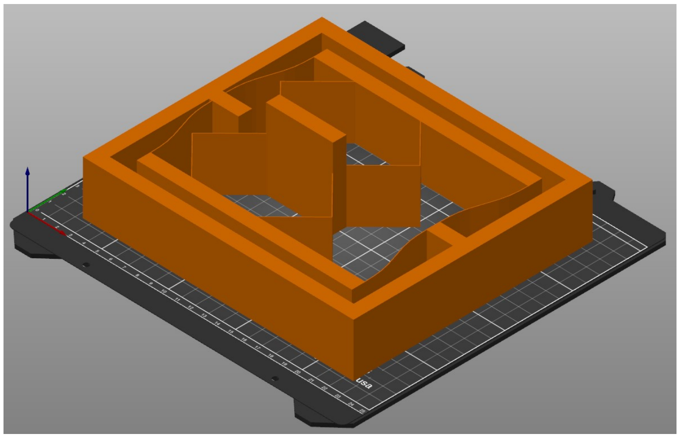

Fig. 12: 3D printing pre-curved flexures of DM and part of EETAA which is in the same plane

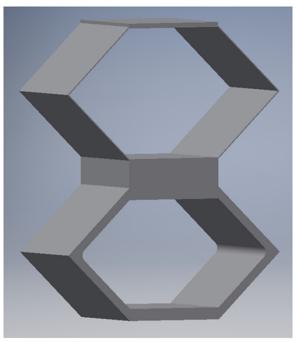

Fig. 13: 3D model of stiffener

rigid rectangular block is also made in the perimeter of the complete mechanism. It is connected to the fixed end of the DM to hold or stand the complete setup. The 3D CAD, as shown in figure 12, is kept on the horizontal printing plate.

Second, the stiffener of DM is made separately. Again it is printed in such a way that the L-shaped flexures make walls on the printer plate. The 3D model of the stiffener is as shown in figure 13. The hexagonal stiffener is made with another rigid hexagonal part for better looks.

Third and the final print is of the hexagonal actuator blocks which complete the alignment mechanism in EETAA as well as accommodates actuators. As shown in figure 14, circular slots are made on top and bottom to align the cylindrical stator and the coil.

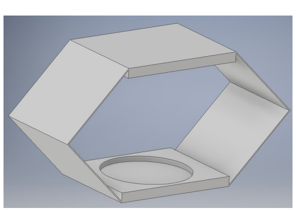

Fig. 14: 3D model of hexagonal actuator blocks

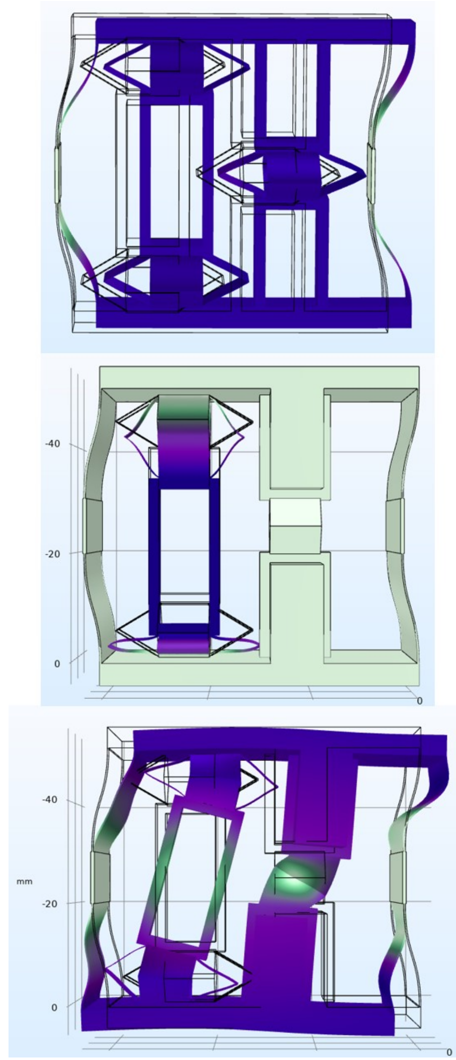


Fig. 15: Eigenmodes in X, Y, and Yaw rotation

## B. Simulations

The 3D CAD is imported in COMSOL. The material properties of steel are chosen to proceed with simulations. The fixed parts of the mechanism are fixed and then the eigenfrequency analysis is done. The first three eigenfrequencies are 103.22 Hz, 524.85 Hz, and 1005.6 Hz. The first frequency corresponds to the translation in the X-direction, the second frequency corresponds to the translation in Y-direction, and the third frequency corresponds to the yaw rotation.

## C. Manufacturing

The DM, its stiffener, and the 2 actuator blocks are 3D Printed separately. This way printer did not require any support material but smooth flexures can be printed. Voice Coil Actuators (VCA) are bought in the form of a subwoofer. The subwoofer is dis-assembled to separate the coil and the stator. Slots were made in the hexagonal actuator blocks to align the stator and the coil in the same axis. Then both coil and stator are fixed in the alignment mechanism with super glue. Similarly, the second actuator is assembled. The hexagonal

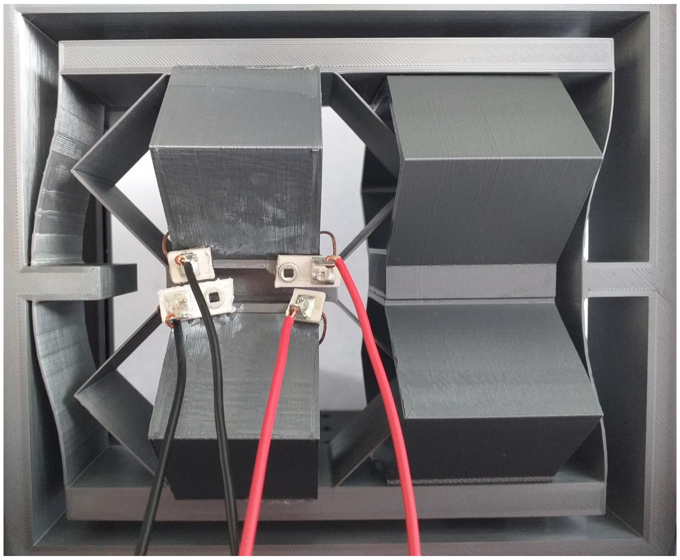

Fig. 16: Final mechanism

actuator blocks and the stiffener are then inserted in the DM and the final mechanism is as shown in figure 16.

The stiffeners are made larger than the available distance between secondary stages so that additional stress is used as a force to stick the stiffeners in CM using superglue or double tape.

## VI. Experimental Setup and Results

The mechanism made has a range of motion of up to 2 cm in X-direction and 1 cm in Y-direction within the footprint of 20 cm in X-direction and 15 cm in Y-direction.

The sensor block consists of a laser triangulation sensor. The sampling frequency is 10 kHz. The complete mechanism and sensor block is fixed on Thorlabs 30x30 cm optical breadboard. NI CompactRIO is used for real-time control and programmed with LabView. The sensor values are taken through the analog input module chirp signal is given from the analog output module to an amplifier that powers the VCA.

The frequency response function of the mechanism was obtained in both the X and Y directions by applying a chirp actuating signal. The X-direction resonance is around 8 Hz as seen in figure 17 and Y-direction resonance is around 40 Hz as seen in figure 18. The ratio of these frequencies is similar to the ratio obtained in COMSOL simulations. The Y-direction frequency is about 5 times the X-direction. However, yaw rotation is not clearly observed in the experimental results due to the limited resolution of the sensor. However, there are no other resonance peaks up to 70-80 Hz. This means that the undesired modes do not occur up to approximately 10 times the X-direction resonance frequency. The phase drop observed from 40 Hz is verified to be due to the low-pass filter characteristics of the sensor.

In figure 18, The X-direction appears as zero-pole pair. The X-direction mode can be observed because of the non-symmetrical nature of the VCA. Indeed, there is also coupling between the X-direction and Y-direction. At lower frequencies

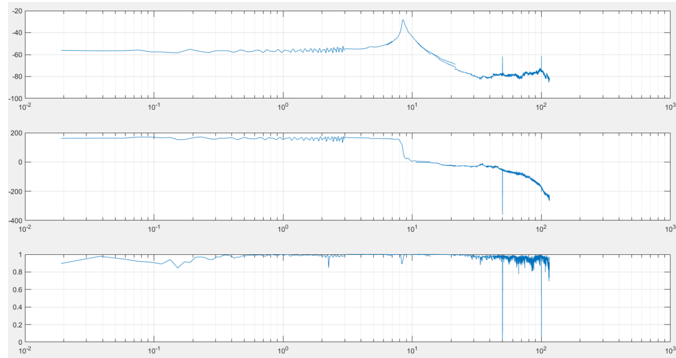

Fig. 17: Bode Plot when sensor is measuring position in X-direction and Both the actuators are driving EE in X-direction

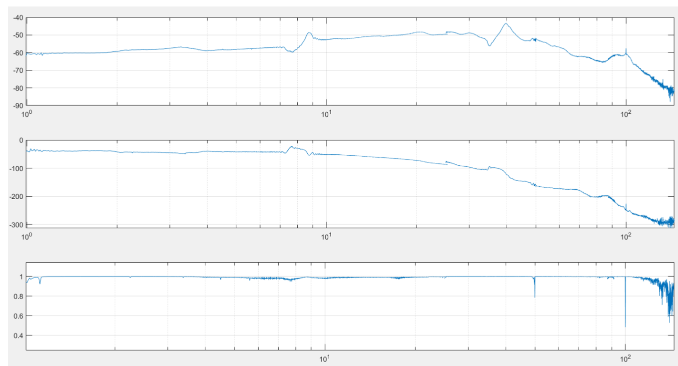

Fig. 18: Bode Plot when sensor is measuring position in Y-direction and Both the actuators are driving EE in Y-direction

the X-direction motion dominates and after the X-direction mode, Y-direction motion dominates.

## VII. Conclusion and Future Work

A novel design of the XY positioning stage for high-speed precision mechatronic systems is made. It has a high frequency for undesired motion which is the yaw rotation. A comparison table is shown in appendix B. The other stages also have the yaw rotation as the first undesired mode.

The actuators are directly connected to the motion stage so there is no out-of-phase motion between the two. Thus the non-collocation due to DM is removed. This feature along with high frequencies of undesired modes helps in increasing the bandwidth of the overall system.

Several factors in architecture also reduce the footprint of the entire mechanism. First, the DM provides amplification besides the 1 DOF motion so additional amplification mechanism is not required. Second, both the actuators are within the alignment mechanism so they don't occupy additional volume outside the mechanism. Third, the EETAA is within the DM so the volume within DM is utilized, and further symmetricity of quarter of the mechanism is not required which increases the yaw rotation stiffness and cross-axis coupling in existing stages. While footprint decreases, amplification in DM helps to achieve larger workspace in X-direction. High actuator force can also be used to further deform the mechanism and achieve higher ROM.

The Y-direction motion has higher stiffness but it can be reduced by changing the thickness, length, and angle of L-shaped flexures. Further material and different manufacturing processes can be explored. For instance, EDM of the different modules which were printed separately and assembling them.

The mechanism can be further optimized for better work-space-area to footprint ratio, stress developed to the range of motion, and actuator force to amplification in DM, etc. To provide more DOF such as translation in Z-direction or rotation in the XY plane, it is required to produce the designs where the additional actuator is/are connected directly to the motion stage.

## References


[1] S. Awtar and G. Parmar, "Design of a large range xy nanopositioning system," *Journal of Mechanisms and Robotics*, vol. 5, no. 2, 2013.

[2] G. K. Parmar, "Dynamics and control of flexure-based large range nanopositioning systems." Ph.D. dissertation, 2014.

[3] K.-q. Qi, Y.-l. Ding, Y. Xiang, C. Fang, and Y. Zhang, "A novel 2-dof compound compliant parallel guiding mechanism," *Mechanism and Machine Theory*, vol. 117, pp. 21–34, 2017.

[4] J. Shang, Y. Tian, Z. Li, F. Wang, and K. Cai, "A novel voice coil motor-driven compliant micropositioning stage based on flexure mechanism," *Review of Scientific Instruments*, vol. 86, no. 9, p. 095001, 2015.

[5] Z. Liu, Z. Zhang, and Y. Peng, "A self-adjusting stiffness center design for large stroke compliant xy nanomanipulators," *Mechanical Sciences*, vol. 9, no. 1, p. 41, 2018.

[6] S. Wan and Q. Xu, "Design and analysis of a new compliant xy micropositioning stage based on roberts mechanism," *Mechanism and Machine Theory*, vol. 95, pp. 125–139, 2016.

[7] Y. Li and Q. Xu, "Design and analysis of a totally decoupled flexure-based xy parallel micromanipulator," *IEEE transactions on robotics*, vol. 25, no. 3, pp. 645–657, 2009.

[8] L.-J. Lai, G.-Y. Gu, and L.-M. Zhu, "Design and control of a decoupled two degree of freedom translational parallel micro-positioning stage," *Review of Scientific Instruments*, vol. 83, no. 4, p. 045105, 2012.

[9] Q. Xu, "Design and development of a compact flexure-based $xy$ precision positioning system with centimeter range," *IEEE Transactions on Industrial Electronics*, vol. 61, no. 2, pp. 893–903, 2013.

[10] H. Liu, S. Fan, X. Xie, Z. Zhang, and D. Fan, "Design and modeling of a novel monolithic parallel xy stage with centimeters travel range," *Advances in Mechanical Engineering*, vol. 9, no. 11, p. 1687814017729624, 2017.

[11] Z. Wu, Y. Li, and M. Hu, "Design and optimization of full decoupled micro/nano-positioning stage based on mathematical calculation," *Mechanical sciences*, 2018.

[12] Z. Zhang, B. Liu, P. Wang, and P. Yan, "Design of an additive manufactured xy compliant manipulator with spatial redundant constraints," in *2016 35th Chinese Control Conference (CCC)*. IEEE, 2016, pp. 9149–9154.

[13] Q. Zhang, J. Zhao, X. Shen, Q. Xiao, J. Huang, and Y. Wang, "Design, modeling, and testing of a novel xy piezo-actuated compliant micro-positioning stage," *Micromachines*, vol. 10, no. 9, p. 581, 2019.

[14] K. Folkersma, S. Boer, D. Brouwer, J. Herder, and H. Soemers, "A 2-dof large stroke flexure based positioning mechanism," in *International Design Engineering Technical Conferences and Computers and Information in Engineering Conference*, vol. 45035. American Society of Mechanical Engineers, 2012, pp. 221–228.

[15] J. Meijaard, "The importance of imperfections in leaf-spring flexures for the support stiffness," *Procedia IUTAM*, vol. 13, pp. 82–89, 2015.

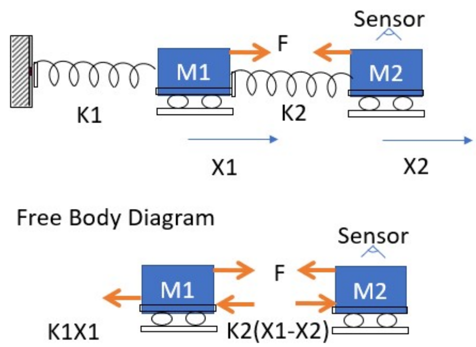


Fig. 19: Model and Free Body Digram

## Appendix A
## Derivation of transfer function

As shown in figure 19
Equations of motion after laplace transformation:

$$\begin{aligned} M_1X_1s^2 + K_1X_1 + K_2(X_1 - X_2) = F \\ \implies (M_1s^2 + K_1 + K_2)X_1 - K_2X_2 = F \end{aligned} \tag{1}$$

$$\begin{aligned} M_2X_2s^2 - K_2(X_1 - X_2) = -F \\ \implies (M_2s^2 + K_2)X_2 - K_2X_1 = -F \end{aligned} \tag{2}$$

From equation 1

$$X_2 = \frac{(M_1s^2 + K_1 + K_2)X_1 - F}{K_2} \tag{3}$$

Putting in equation 2

$$\begin{aligned} (M_2s^2 + K_2)\frac{(M_1s^2 + K_1 + K_2)X_1 - F}{K_2} - K_2X_1 = -F \\ (M_2s^2 + K_2)(M_1s^2 + K_1 + K_2)X_1 - F(M_2s^2 + K_2) - K_2^2X_1 = -FK_2 \\ ((M_1M_2)s^4 + (M_1K_2 + M_2K_1 + M_2K_2)s^2 + K_1K_2)X_1 = F(M_2s^2) \\ \frac{M_2s^2}{(M_1M_2)s^4 + (M_1K_2 + M_2K_1 + M_2K_2)s^2 + K_1K_2} = \frac{X_1}{F} \end{aligned} \tag{4}$$

putting back in equation 3

$$\begin{aligned} X_2 &= \frac{(M_1s^2 + K_1 + K_2)(M_2s^2)F - F((M_1M_2)s^4 + (M_1K_2 + M_2K_1 + M_2K_2)s^2 + K_1K_2)}{K_2((M_1M_2)s^4 + (M_1K_2 + M_2K_1 + M_2K_2)s^2 + K_1K_2)} \\ \frac{X_2}{F} &= \frac{(M_1M_2)s^4 + (M_2K_1 + M_2K_2)s^2 - (M_1M_2)s^4 - (M_2K_1 + M_2K_2)s^2 - M_1K_2s^2 - K_1K_2}{K2((M_1M_2)s^4 + (M_1K_2 + M_2K_1 + M_2K_2)s^2 + K_1K_2)} \\ \frac{X_2}{F} &= \frac{K_2(-M_1s^2 - K_1)}{K2((M_1M_2)s^4 + (M_1K_2 + M_2K_1 + M_2K_2)s^2 + K_1K_2)} \\ \frac{X_2}{F} &= \frac{-M_1s^2 - K_1}{(M_1M_2)s^4 + (M_1K_2 + M_2K_1 + M_2K_2)s^2 + K_1K_2} \end{aligned} \tag{5}$$

## Appendix B
## Comparison Table

Following is the comparison with eigen-frequencies few existing XY stages. All these frequencies were calculated by finite element simulations by the respective authors.

| | Proposed Design | [3] | [4] | [5] | [6] | [7] | [8] | [9] | [10] | [11] | [12] | [13] |
|---|---|---|---|---|---|---|---|---|---|---|---|---|
| X | 103.22 | 51.953 | 48.05 | 44.38 | 33.332 | 101.4 | 396 | 59.9 | 34.471 | 354.209 | 26.7 | 44.234 |
| Y | 524.85 | 52.009 | 48.28 | 44.47 | 33.527 | 101.6 | 396 | 60.5 | 34.300 | 355.319 | 26.8 | 44.335 |
| Yaw | 1005.6 | 106.135 | 2.74 | 75.88 | 58.758 | 101.8 | 842 | 128.5 | 54.356 | 179.992 | 62.8 | 88.232 |

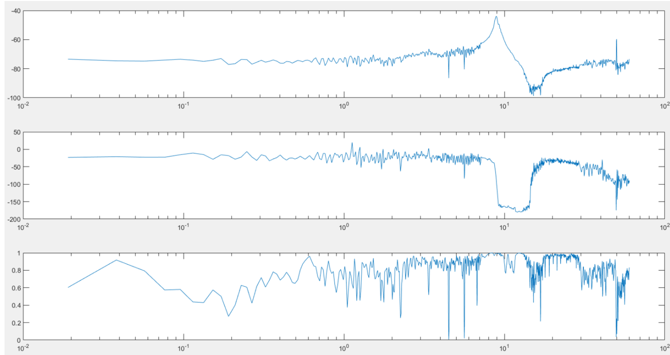

Fig. 20: Bode Plot when sensor is measuring position in Y-direction and Both the actuators are driving EE in X-direction

## APPENDIX C
## BODE PLOT

In this plot, the peak and zero of X-direction motion while sensing in Y direction can be seen.

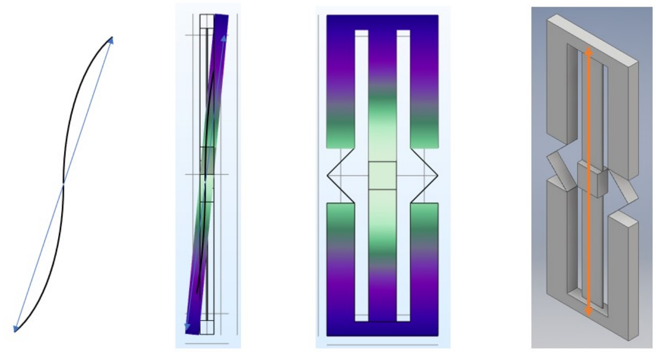

Fig. 21: Actuation in radial direction to drive theta rotation

## Appendix D
## R$\theta$ Stage

Using the PASD method, designs of mechanism for translation of EE of a leaf spring has been made. Since, a leaf spring has two drive directions, that are, translation and rotation. So, another design for the rotational DOF of leaf spring using the same PASD to move in rotational DOF is conceptualized. This design is also driven by linear actuation in the same radial direction. The additional feature of controlling motion in support direction can also be added to the rotation mechanism to obtain a total of 2 DOF of $R\theta$ motion. The radial direction is the direction of actuation for both actuators. The two actuators can deferentially operate to control motion in angular and radial directions.

# 5

# CONCLUSION

In this research, two novel active approaches to solve the problem of reducing support stiffness in 1 DOF translation motion stage is taken. Both the designs are based on the method of providing actuation from support direction which is used to amplify the stroke of actuator. The active designs without this method but solving the problem using same approaches are also shown. The PASD method was explained using an example which led to design of a 1 DOF translation motion stage which also maintains support stiffness passively.

For first active approach, a distributed mechatronics which is embedded in the flexure is proposed in chapter 3. It is used to locally control the shape of flexure so that the vibration modes are pushed to higher frequencies. The individual cell is designed for shaping the flexure at the location of cell. Designs of flexure were studied to bring the change in how they are physically integrated with actuators. Here 1 DOF translation was chosen as a starting point and later designs can be made for different DOFs and higher DOF. The design can be analysed and tested for its stiffness properties in future.

The second active approach led to the conclusion that active compensation of loss in support stiffness can be done using an additional actuator which will be driving the EE in support direction. This leads to the idea of making an XY stage. For this, a change in the existing architecture of XY stages is suggested to remove the first non-collocated mode. The first non collocated mode is from out of phase motion of motion stage and actuator. This is removed when actuators are directly connected to the motion stage. Further, another complete novel architecture is proposed to increase the yaw rotation stiffness. This is possible when the stage has both the actuators along common axis. In this case they have to deferentially actuate to drive in X and Y directions. The decoupling mechanism of new architecture can be made such that driving force and amplification of actuator stroke can be optimized. The proposed design of decoupling mechanism is based on PASD method to achieve amplified strokes. The alignment mechanism of the new architecture consists of actuators and the motion stage inside itself which also gives a more compact design of XY stage.

In XY stage cross axis coupling is still present, that is, the force and motion in Y-direction is affected by additional force applied or motion in X-direction and vice versa. In future, the design needs to be optimized and a controller is required. The aim will be that these designs be used to achieve larger range of motion of up to a cm range, 1-10 nm accuracy, and 1-5 kilo Hz in precision machines.

5

# APPENDIX 1.1

## EARLY FLEXURE DESIGNS

Bearings have been used to provide support to moving parts. Flexure guided bearings have been used for precision applications. Eastman reported drive stiffness and maximum angle of rotation for allowable stress developed in flexure pivot (figure 1a) under compression, tension, and no-load conditions. To support higher compressive or tensile loads, more number of flexures are suggested [1]. Two of the flat plate flexure pivots, aligned at an angle was studied experimentally by Young [2], theoretically by Wittrick [3] and Haringx [4]. The crossed pivot flexures (figure 1b) maintains higher stiffness perpendicular to its EE. Flexures have also been called springs due to its elasticity in the DOF directions. The parallel (leaf) spring mechanism (PLSM) was developed by R V Jones for rectilinear motion. In pairs, the compound mechanism (figure 1c) had perfect parallelism theoretically [5]. Then, for modeling the support stiffnesses and the drive force of this mechanism, approximations have been provided by van Eijk [6]. Term "compliance" is newer when compared to elastic or flexible, but is more suitable so is commonly used in the research [7]. Paros and Weisbord designed circular flexure "hinges" (figure 1d) which has one DOF of rotation like the revolute joints. [8]. So the hinges can also be called as compliant revolute joints.

## SYNTHESIS OF FLEXURE DESIGN

Some of the design synthesis techniques are:

- Constraint Based Design (CBD): was discussed in the Preliminaries chapter.
- Freedom and Constraint Topology (FACT): Synthesis of multi-degree of freedom, parallel flexure system concepts via FACT has been given by [9] [10].
- Optimization based approach: An optimization-based numerical method for the topological synthesis of compliant mechanisms based on the force-deflection relationship has also been presented in [11]. Many algorithms and techniques have been used for several applications with different constraints.

## ANALYSIS OF FLEXURE DESIGN

The theories to perform analysis are discussed here. Using these, the displacement and stiffness in a flexure can be found at their different deformed states. Then it is checked if the displacement and stiffness are within the required range. Dimensions are also be optimized as per requirements. If they are not within the required range, the flexures are redesigned with new initial dimensions or type synthesized in a completely new way.

First, the following can be assumed:

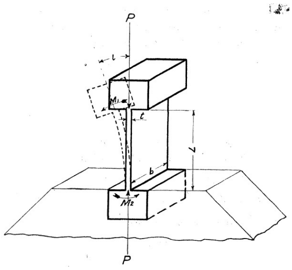


(a) Eastman's flexure pivot to replace knife edges for supporting rotation

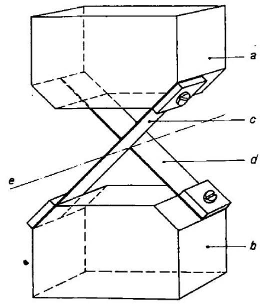


(b) Cross-spring pivot adapted from [4]

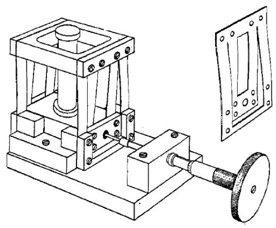

(c) Jone's folded compound parallel spring mechanism

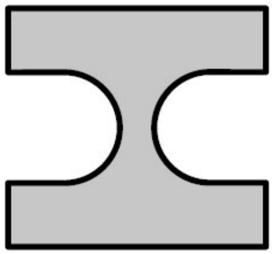

(d) Circular flexure adapted from [7]

Figure 1: Early Design of Flexures

- conservative mechanical system,
- ignoring thermal properties and changes due to them,
- homogeneous, isotropic, and linear elastic material

Analysis of the design of the flexure gives the relation between applied force and displacement. External forces develop stress in the material which causes the deformations and then deformations give the displacement. Any mechanical analysis requires the following three steps: [12] [13]

- Geometric equilibrium or geometric compatibility relationships: Deflection-Deformation or Displacement-Deformation Equations. This is also known as the kinematic equation.
- Constitutive relationships: Stress-Strain Equations. This is given by the constitutive equation.
- Force equilibrium or force compatibility relationships: External Force-Stress Equations: This relationship is obtained by the equilibrium equation.

Initially, **dimensions of the flexure are heuristically chosen and then the type of deformation (and its corresponding type of stress developed) in material between any two points of the flexure is predicted.** The three types of deformations (and corresponding stress) are:

- Elongation (tensile stress)
- Compression (compressive stress)
- Shear (shear stress)

Bending and torsion may also be assumed to be a combination of the three deformations. Other effects like the Poisson effect, anticlastic curving, and warping can also be assumed to be due to one or more of the three types of deformation. For flexures like a slender beam, the shear is neglected and only elongation and compression type of deformation are considered. The curvature of slender beams at each point is then given by the geometric relationship. Based on the type of calculation required, the curvature is either calculated linearly or non-linearly:

- When deformation is assumed to be small to easily solve the equations in later steps. But it is not valid in case of large deformation of flexure. It is governed by small displacement theory or infinitesimal strain theory: for example, the curvature of the beam is approximated to:

$$\frac{1}{\rho} = \frac{d^2 w}{dx^2} \tag{1}$$

  where $\rho$ is the radius of curvature and $w$ is the beam's deflection. Figure 2.

- When the deformation is large and cannot be approximated. It is governed by large displacement theory or finite strain theory: for example, the curvature of the beam in its exact form is:

$$\frac{1}{\rho} = \frac{\frac{d^2 w}{dx^2}}{\left[1 + \left(\frac{dw}{dx}\right)^2\right]^{\frac{3}{2}}} \tag{2}$$

After predicting the type of deformation (which also means that the type of stress developed is also predicted), the deformed shape (and the corresponding values of stress) is required to be calculated. The shape also gives the displacement (and stress values gives the force). To calculate the values, energy as a function of the unknown shape (and stress values) is formulated and solved using fundamental principles like thermodynamic laws. While solving the equation, the relationship between deformation and displacement is the same as the relationship between stress and external force.

Deformation is a physical phenomenon, so, the constitutive relationships are derived using the phenomenological approach or using physics on the lower length scale. Like the geometric relationship, the constitutive relationship can also be of two types:

- Linear: The relationship between stress and deformation is considered linear, that is, stiffness remains constant when the deformations are small as well as material is linear. But, such an assumption is not valid in our interest because flexure has large deformation and so its stiffness changes with the deformation as mentioned in the non-linear case below.

- Non-Linear: The relationship between stress and deformation is considered non-linear when the deformations are large or the material is non-linear or both. In this chapter, the emphasis is on changes in stiffness during large deflections and so material non-linearity is not generally taken into account. This means properties of material do not change (remains constant) due to deformations but overall stiffness in the motion of EE may change with large deflections. The material nonlinearity is also called physical non-linearity and the non-linearity due to the changing shape is called geometric non-linearity. [14]

Some of the constitutive relationships like Hooke's Law, Euler–Bernoulli beam theory are discussed below:

- Hooke's Law: According to it, the uniaxial relationship between stress and strain is constant for the linear elastic materials. It is valid for small deformations only because of non-linearity in the material during large deformations. But, for the flexure undergoing large deformations and having only the geometrical non-linearity, the law can be used to find the deformed shape because the material remains in its linear regime. The uniaxial stress($\sigma$)-strain($\epsilon$) relation is given as:

$$\sigma = E\epsilon \tag{3}$$

  Here, E is the slope of the linear part of the stress-strain curve and is called Young's modulus or the modulus of elasticity.

  This is the uniaxial relationship between stress and strain but for the transverse load on a structure like bending a cantilever beam, the deformed shape at each point is given by the curvature discussed in equations 1 and 2. The moment to curvature relationship is given by the beam theory.

- Euler–Bernoulli beam theory: For a beam, undergoing bending, there exists a neutral axis and, at one side of it, the material gets compressed and at the other side of it, the material gets elongated. In figure 2, 0-0 is the neutral axis. It is only valid for the long slender beam because it does not consider shear but only the elongation and compression parallel to the neutral axis. This means that the length of the neutral axis does not change. Later Timoshenko also included the effects of shear in the bending and formulated a more general beam. [15]

  The theory states that the curvature, $\frac{1}{\rho}$ (equation 2), is proportional to the bending moment:

$$\begin{aligned} M &\propto \frac{1}{\rho} \\ M &= \frac{EI}{\rho} \end{aligned} \tag{4}$$

  EI is the flexural rigidity of the beam, E is Young's modulus (in Pa), I is the second moment of area (in $m^4$).

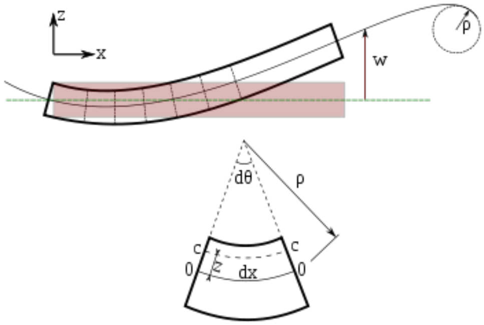


Figure 2: Euler–Bernoulli beam theory from [16]

So, theories predicting the type of deformation (and its corresponding type of stress developed) for different types of flexures are available in the literature. But values are required to be calculated. Generally, the external force is applied at certain points (which is known) and displacements of any of the points on flexure are required to be calculated. It is generally not the case that, the displacement at all the points is given and the forces at certain points would be required to calculate. So, first, equilibrium equations are derived, then the value of known applied external forces is inserted in it, then it is solved for values of displacement, and finally, the stiffness is calculated.

So initially, only the geometric relationship, like equations 1 and 2 and the constitutive relationship, like equations 3 and 4, are known. Then using fundamental principles, for instance, it is mentioned above that using thermodynamics, the equilibrium equation is derived.

Generally, flexures have been designed with a quasi-static deflection in mind by designers. Later, the designs are improved or/and new sub-systems are made to solve problems faced due to dynamics. In this section, for quasi-static deflection of flexures, inertia terms have been ignored while calculating the deformed configuration. The equations of motion, in the case of dynamics, is discussed later. Here, the derivation of the equilibrium equation is discussed:

- Newton's Laws of Motion: In the case of statics, for any point to be in equilibrium, the sum of all forces at that point is equal to zero. So an external force at a point on a flexure has equal and opposite reaction due to the developed stress. The stress depends on deformed shape and stiffness and it is given by the constitutive relationship discussed below. But, before that, other methods to obtain the equilibrium equation are discussed because its easier than Newton's laws of motion. Newton's laws of motion require the calculation of reaction forces for putting them in equilibrium equations. But if energy and work methods are used, reaction forces do not do any work and so these methods do not require such calculation.

- Balance Principles: The principles which are used to solve the flexure system are conservation of mass, momentum, and energy. These are used to formulate variational principles which comes in the next step.

- Variational Principles: Balance Principles are written in form of variational principles which are laws in the form of minimizing or maximizing certain quantities. These quantities depend on some functions, and so, by minimizing or maximizing those quantities, these functions are found. For instance, quantities such as

  - work done due to external loads or internal stresses on flexure during deformation
  - potential energy stored in the flexure in its deformed state

  depends on functions like

  - the deformed or undeformed shape of the flexure, and,
  - the stiffness

  So, the principle is used to obtain the virtual work principle or the minimum potential energy equations. These equations also have an important role in developing finite element methods as, usually, the flexure is discretized and each element is solved. [17].

  The principle of virtual work is a general principle in the variational principle's form.

- Principle of Virtual Work (PVW): Path taken by particle to move from point A to point B due to certain forces is such that work done due to the forces along the path is minimum. A flexure undergoing deformation is assumed to be a quasi-static process and so it develops stress against the external loads such that it is always in equilibrium. So, the virtual work done by external loads and virtual work done by internal stress are equal [18]. PVW gives the equilibrium equations as well as the geometric equations as discussed above. It is non-linear for large deformations due to nonlinearity in constitutive equations.

$$\delta W_i = \delta W_e \quad \text{for all admissible virtual displacements,} \tag{5}$$

  Internal work is due to stress and strain. External work is due to external forces and displacements.

  Within, PVW, minimum potential energy theorem is a special case that is valid only for the conservative system.

- Minimum of Potential Energy (MPE): MPE is only valid for a conservative system and generally the flexure in solid mechanics is assumed to be a conservative system. In the quasi-static process, flexure is always in the state of equilibrium and the shape of flexure is such that the PE is always minimum. Minimizing the PE also gives the equilibrium equations, as given by PVW.

  To minimize the potential energy, the potential energy needs to be calculated and so, like the internal work in PVW, MPE also requires the calculation of stress.

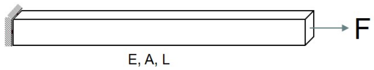


Figure 3: Example of solid bar for which the stiffness at the tip is calculated

PVW and MPE give the relationship between external forces and stress which is used along with stress-deformation and deformation-displacement relationships to calculate displacements and stiffness. The equilibrium equation also consists of dimensions and initial position terms which are optimized for the required value of EE displacement and stiffness.

- Solving for elongation or compression in a solid bar: For example, stiffness at the tip of the rod for the displacement along the direction of force (F) depends on the material property, that is Young's modulus (E), and geometrical properties, that are the length of the rod (L) and area of cross-section (A). It is important to note that due to physical linearity, E remains constant but due to geometric non-linearity, L and A changes with deformation. Generally, the iterative method is used for calculating large deformation. In the shown figure 3, stiffness (K) for shown L and A is initially calculated for small deformation. Due to the small deformation, the displacement of the tip is given as $\delta L$. For further deformation, L and A are updated from the previous deformation and new stiffness is calculated.

$$
\begin{aligned}
\frac{F}{A} &= \sigma \\
\sigma &= E\epsilon \\
\epsilon &= \frac{\delta L}{L} \\
K &= \frac{F}{\delta L} \\
\implies K &= E \times A/L
\end{aligned} \tag{6}
$$

- Solving for large deflection in beam bending: Equation 2 and 4 may be solved either through a classical method using elliptic integrals [19] or numerically [20] [21]. Howell and Midha have used the analytical approach and the loop-closure method for developing a pseudo-rigid body model [22] [23]. Two simpler methods, one numerical method called non-linear shooting and another semi-analytical method known as Adomian decomposition to obtain large deflection of a cantilever beam including geometric non-linearity have also been proposed [24]. Further, the end tip of the beam subjected to forces and moment acting in opposite directions is also modeled in [25].

## DYNAMICS

In statics, the deformed shape of the flexure is calculated and the stiffness is found. In dynamics, the shape of the flexure changes with respect to time due to external load which may or may not be changing with time. The given external load is called as input to the system and the motion behavior at the sensor is the response of the system to the input. The response is calculated from solving the equation of motion (EOM). EOM can be derived from laws such as Newton's Laws of Motion and the variational methods. Now, inertia terms are also included while deriving the EOM. In EOM, displacement, velocity, and acceleration of material are related to the external forces. Three characteristics of flexure in each direction, which includes translational as well as rotational are

- Inertial terms: They are included in the coefficient of acceleration and is represented by matrix M
- Stiffness in each direction due to displacement in that and every other direction: It is included in the coefficient of displacement and is represented by matrix K.
- Damping: It is represented by matrix C.

All external forces including body forces, traction, and point loads are included in a matrix denoted by F.

$$M\ddot{x} + C\dot{x} + Kx = F(t) \tag{7}$$

To obtain this equation, there are several methods, few of the methods are [26]:

- Newton's laws of motion.
- D'Alambert Principle which is based on the principle of virtual work.
- Hamilton's Principle which is based on the conservation of energy
- Lagrange Equations which is also based on the conservation of energy but more suitable for dealing with individual masses and stiffness elements.

The superposition principle holds for small deformations, which is used to combine the response of the system at different frequencies.

Superposition principle: The deformation at any point in an elastic body under the action of a load system is equal to the sum of deformations produced by each load when acting separately. But this is valid only when stiffness for any deformation has not changed due to the deformation at the other point. So, it is also valid, only, for small deformations which are geometrically as well as physically linear. [7]

Equilibrium is the undeformed configuration when parallel leaf springs are perpendicular to the ground and the shuttle. The EOM is linearized around the equilibrium and so it is only valid for small deformations. Small deformations in different patterns of shapes are obtained at different frequencies of the external force. Each pattern of the deformed shape is mode shape. For each mode shape, modal mass is calculated to make the M matrix and the stiffness values associated with the mode shape are calculated to make the K matrix. The stiffness is calculated using statics as discussed above. Then, the eigenfrequency can be calculated from the M and K matrices. The stiffness of each mode is a constant value due to the assumed linear behavior. This analysis method is modal analysis.

The mode shapes and eigenfrequencies for the mechanism shown in figure 4 are obtained from COMSOL and are shown in figure 5.

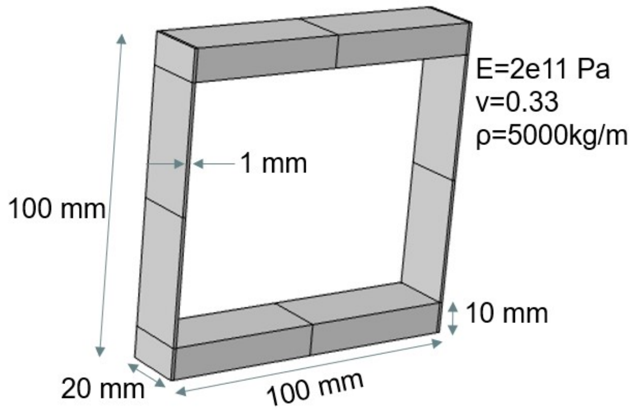


Figure 4: Undeformed parallel leaf spring and dimensions

Frequency response from EOM is found using fourier transformation. It gives steady-state response of the system for a given frequency of excitation. From equation 7, taking laplace transformation:

$$
\begin{aligned}
&Ms^2x(s) + Csx(s) + Kx(s) = F(s) \\
&\text{where,} \\
&s = j\omega \\
&\omega \text{ is frequency in radians per second}
\end{aligned}
\tag{8}
$$

For each mode shape, having modal mass $M_i$, damping coefficient $C_i$, and stiffness $K_i$,

$$\frac{x_i(s)}{F_i(s)} = \frac{1}{M_i s^2 + C_i s + K_i} \tag{9}$$

Equation 9 is used to plot the graph of $\frac{x_i(s)}{F_i(s)}$ versus frequency $\omega$ for each mode shape. The peak is obtained at frequencies at which the system tends to vibrate due to its characteristics. Using the superposition principle, the response at each mode shape can be added to find the required frequency response function (FRF).

The details of geometry and material in the undeformed configuration is given in figure 6. The modal mass corresponding to each eigenfrequency is calculated in COMSOL and then both; the modal mass and the eigenfrequency are imported in MATLAB to generate a bode plot of FRF. The code was adapted from the third assignment of the predictive modelling course [27] and mentioned in appendix 1.2. Certain damping is also assumed to be present in the system.

In figure 7, the node at which the actuator is located is denoted by A and the node at which the sensor is located is denoted by S. When A and S are the same points, that is, in the collocated system, controlling is not a problem. But many times sensors cannot

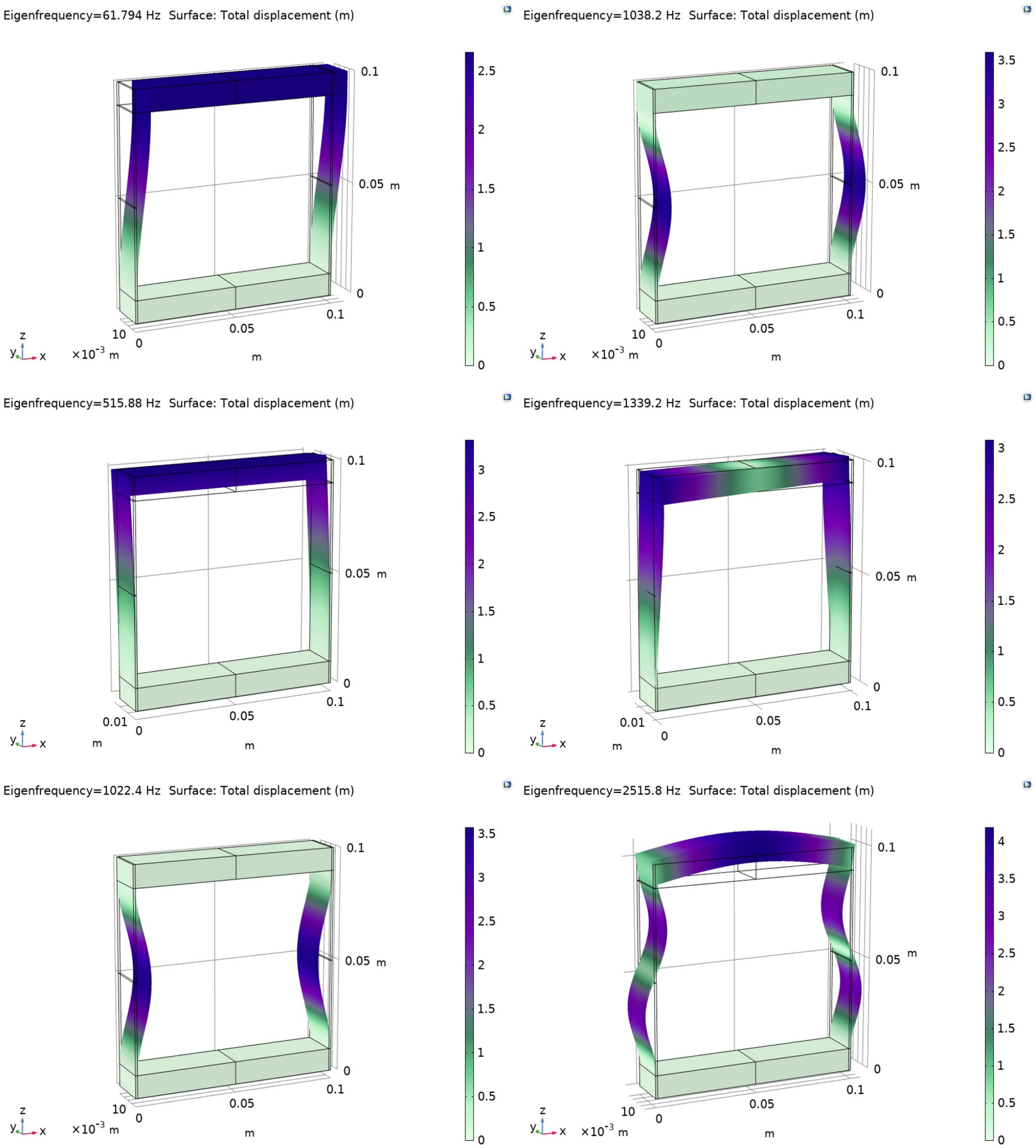


Figure 5: Mode shapes of parallel leaf spring

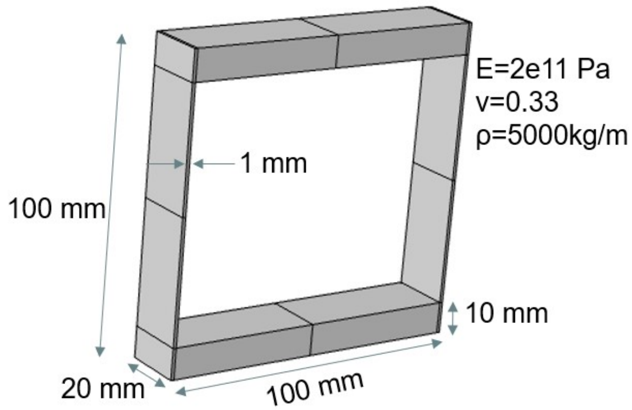


Figure 6: Undeformed PLSM and dimensions

be placed at the point where the external force is applied. So when the A remains at the same node but the sensor is moved to S', that is a non-collocated system, then controlling it becomes a problem. Note that, the actuation and sensing, both are in the x-direction.

For a collocated system, when the sensor and actuator are at the same point, the response of the system around equilibrium is shown in a bode plot.

The bode plot of each FRF, as shown in figure 8a, is obtained. Combining them using the superposition principle, bode plot, as shown in figure 8b, is obtained. Each pole is accompanied by a zero. The phase does not go below 180°.

But, when the actuator and sensor are at different nodes, the phase goes below 180°. **The system is non-collocated and so the modes destabilize the system. It has become a challenge to control even when the deformation is small.** For the non-collocated system, the bode plot is as shown in figure 9b.

In the FRF shown in figure 10, the second peak is high to cross the 0dB line. To control, the second peak needs to be pushed below the 0dB. To further increase the bandwidth, it needs to be pushed further away from the initial 0dB crossing as, using the rule of thumb, the bandwidth is at the $1/3^{rd}$ frequency of the frequency at which the second peak is observed.

## STATICS OF PLSM AT LARGE DEFLECTION

A basic embodiment of parallel leaf-spring flexures from [29] is shown in figure 11. Both the leaf springs have the same EE and ground and undergo the translation along the x-direction. A proper parallel guiding keeps the rotation $\phi$ equal to zero irrespective of the driving force $F_x$. So, $F_x$ should pass through both the center of gravity and the center of compliance for a free-of-tilt suspension of the shuttle. In the center of compliance, the compliance matrix has the smallest coupling between directions of compliance. The most appropriate position for the point of application of force F is when the line of action for F goes through the middle of the springs [30]. So, the stiffness is considered at this

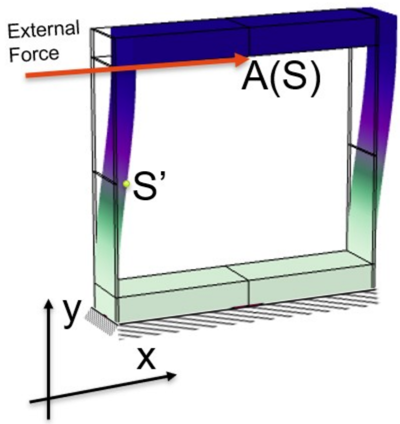


Figure 7: Actuator (A) and senor(S) nodes in PLSM

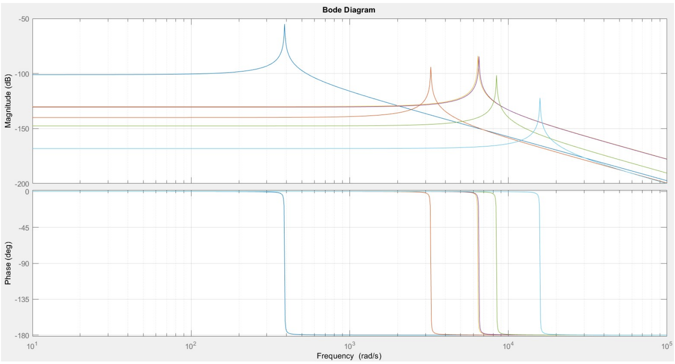


(a) Bode plot of each mode shape separately

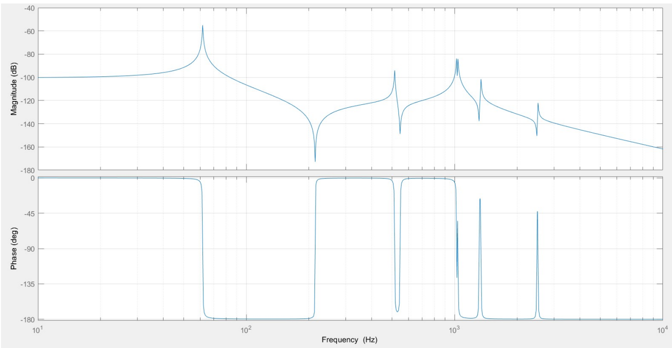


(b) Bode plot of combined transfer function

Figure 8: Bode plot of parallel leaf spring mechanism when actuator and sensor are at same point

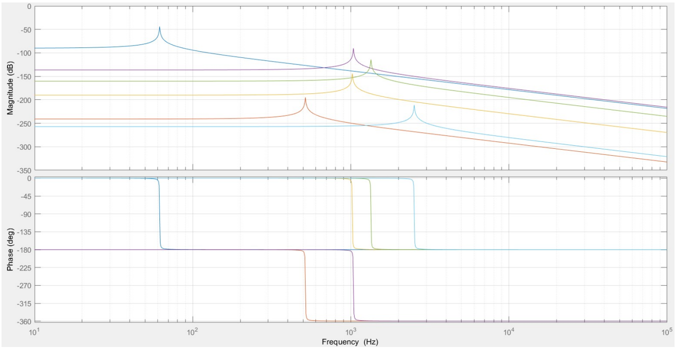


(a) Bode plot of each mode shape separately in non collocated system

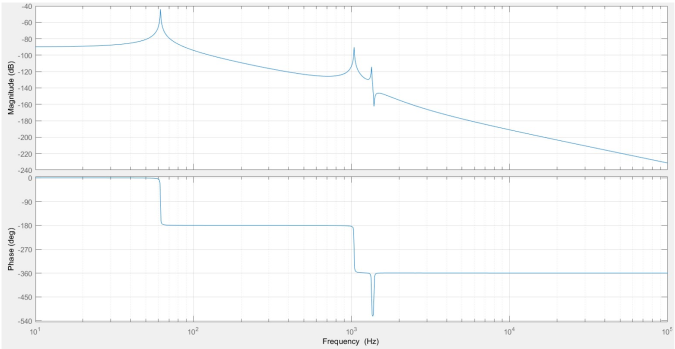


(b) Bode plot of combined transfer function

Figure 9: Bode plot of PLSM when actuator is at point A and sensor is at point S'

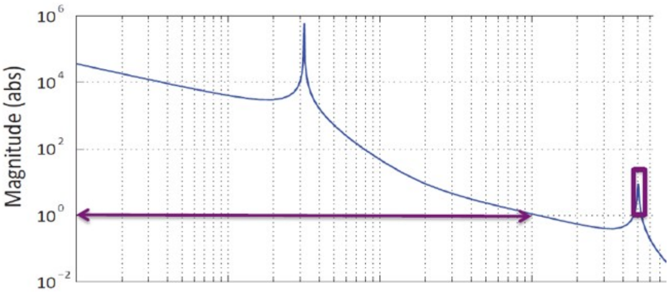


Figure 10: Challenge during control of non collocated system, figure from [28]

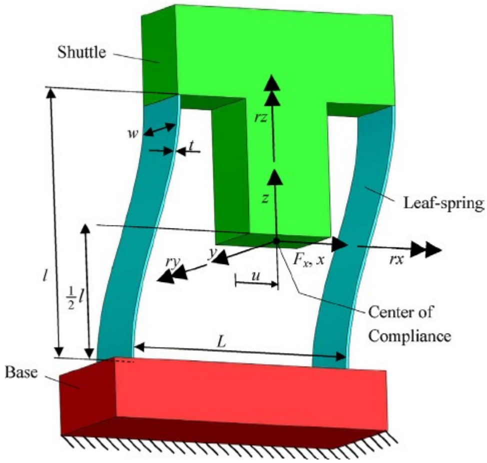


Figure 11: Basic embodiment of parallel leaf-spring flexures in [29]

point in the shuttle. Therefore the parasitic error motion in RY-direction will not occur during loading in the X-direction. The compliance matrix at the center of compliance is diagonal with complete decoupling of directions.

The results of this research paper are mentioned because it is found to be the most precise and has more refined analytic formulas that take into account shearing, finite external parallel drive stiffness, constrained warping, anticlastic curving, and constrained anticlastic curving effects. However, not driving collinear with the center of compliance will cause longitudinal stress in the leaf-springs. This will cause extra non-linearity in the relation between the driving force and the displacement which is not considered in the paper [29].

The driving force and stiffness in the x-direction are influenced by the actuator position in the z-direction. But when the driving force is collinear with the center of compliance, the motion of EE is precisely known during its motion in the x-z plane. So, for the given position in the x-direction, the position in the z-direction is known and vice versa.

The change in drive force, $F_x$, according to the extensible elastica model for a certain displacement, $u$, from the linear beam deflection formulas is given by a factor $\delta$ as

$$F_x = \delta \frac{24EI}{l^3} u \tag{10}$$

The change in $\delta$ is increasing with normalized displacement $u/l$ as shown in figure 12. Thus $F_x$ also increases which suggests that drive stiffness increases. Generally, it is desired to have free motion along the compliant direction for which the flexure was designed to provide the DOF.

The X-direction stiffness increases while the Z-direction stiffness decreases. The Z-direction stiffness is given by:

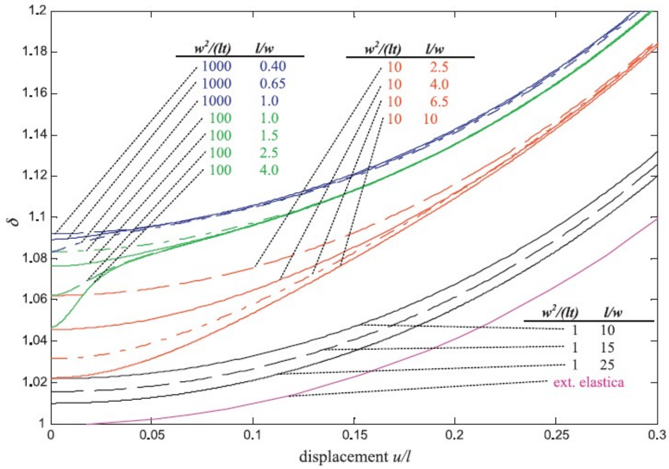


Figure 12: The deviation $\delta$ of the drive force of the linear beam deflection formulas from the extensible elastica model and the finite element model for relatively large deflections. [29]

$$\frac{c_z}{c_{z0}} = \left(1 + \frac{\left(\frac{51}{35}\right) + \left(\frac{3}{175}\right) c'_d}{1 + c'_d} . \left(\frac{u_l}{t}\right)^2\right)^{-1} \tag{11}$$

where,

- $c_z$ is the scaled translational stiffness in z direction.
- $c_{z0}$ is the translational stiffness in z direction at no deflection.
- $c'_d = \frac{c_d}{c_{x0}}$ is the dimensionless external parallel drive stiffness, where
  - $c_d$ is the external parallel drive stiffness.
  - $c_{x0}$ is the translational stiffness in x direction at no deflection.
- $\frac{u_l}{t}$ is the normalized displacement, where
  - $u_l$ is the EE displacement.
  - $t$ is the thickness of leaf springs.

# REFERENCES


[1] F. S. Eastman, *The design of flexure pivots,* Journal of the aeronautical sciences **5**, 16 (1937).

[2] W. Young, *An investigation of the cross-spring pivot,* ASME J. Appl. Mech **11**, 113 (1944).

[3] W. Wittrick, *The theory of symmetrical crossed flexure pivots,* Australian Journal of Chemistry **1**, 121 (1948).

[4] J. Haringx, *The cross-spring pivot as a constructional element,* Flow, Turbulence and Combustion **1**, 313 (1949).

[5] R. Jones, *Parallel and rectilinear spring movements,* Journal of Scientific Instruments **28**, 38 (1951).

[6] J. Van Eijk, *On the design of plate-spring mechanisms,* (1985).

[7] N. Lobontiu, *Compliant mechanisms: design of flexure hinges* (CRC press, 2002).

[8] L. Weisbord and J. Paros, *How to design flexure hinges,* Machine Design **27**, 151 (1965).

[9] J. B. Hopkins and M. L. Culpepper, *Synthesis of multi-degree of freedom, parallel flexure system concepts via Freedom and Constraint Topology (FACT)–Part I: Principles,* Precision Engineering **34**, 259 (2010).

[10] J. B. Hopkins and M. L. Culpepper, *Synthesis of multi-degree of freedom, parallel flexure system concepts via freedom and constraint topology (FACT)–Part II: Practice,* Precision Engineering **34**, 271 (2010).

[11] M. I. Frecker, G. Ananthasuresh, S. Nishiwaki, N. Kikuchi, and S. Kota, *Topological synthesis of compliant mechanisms using multi-criteria optimization,* (1997).

[12] R. R. Archer, S. H. Crandall, N. C. Dahl, T. J. Lardner, and M. S. Sivakumar, *An introduction to Mechanics of Solids* (Tata McGraw-Hill Education, 2012).

[13] S. Awtar, *Synthesis and analysis of parallel kinematic XY flexure mechanisms*, Ph.D. thesis, Massachusetts Institute of Technology (2003).

[14] H. C. Martin, *Large deflection and stability analysis by the direct stiffness method,* (1966).

[15] S. P. Timoshenko and J. M. Gere, *Theory of elastic stability* (Courier Corporation, 2009).

[16] *Beam theory image,* .

[17] G. A. Holzapfel, *Nonlinear solid mechanics: a continuum approach for engineering science,* Meccanica **37**, 489 (2002).

[18] *Non-Linear Mechanics, ME46000,* Lecture Notes, TU Delft, Netherlands (2018/2019).

[19] K. Bisshopp and D. Drucker, *Large deflection of cantilever beams,* Quarterly of Applied Mathematics **3**, 272 (1945).

[20] A. Saxena and S. Kramer, *A simple and accurate method for determining large deflections in compliant mechanisms subjected to end forces and moments,* (1998).

[21] T. Beléndez, C. Neipp, and A. Beléndez, *Large and small deflections of a cantilever beam,* European journal of physics **23**, 371 (2002).

[22] L. L. Howell and A. Midha, *Parametric deflection approximations for end-loaded, large-deflection beams in compliant mechanisms,* (1995).

[23] L. L. Howell and A. Midha, *A loop-closure theory for the analysis and synthesis of compliant mechanisms,* (1996).

[24] A. Banerjee, B. Bhattacharya, and A. Mallik, *Large deflection of cantilever beams with geometric non-linearity: Analytical and numerical approaches,* International Journal of Non-Linear Mechanics **43**, 366 (2008).

[25] C. Kimball and L.-W. Tsai, *Modeling of flexural beams subjected to arbitrary end loads,* Transactions-american Society of Mechanical Engineers Journal of Mechanical Design **124**, 223 (2002).

[26] *Engineering Dynamics, ME46055,* Lecture Notes, TU Delft, Netherlands (2018/2019).

[27] *Predictive Modelling, ME46090,* Lecture Notes, TU Delft, Netherlands (2018/2019).

[28] *Mechatronic Systems Design, ME46085,* Lecture Notes, TU Delft, Netherlands (2018/2019).

[29] D. M. Brouwer, J. P. Meijaard, and J. B. Jonker, *Elastic element showing low stiffness loss at large deflection,* in *Proceedings of the 24th Annual Meeting of the American Society of Precision Engineering, Monterey, CA* (2009) pp. 30–33.

[30] H. Soemers, *Design Principles for precision mechanisms* (T-Pointprint, 2011).

# Appendix 1.2

## Matlab code for collocated system

```
clear all; close all; clc
% This file will load the modal data from the COMSOL model. It will then
% plot the tranfer from the actuator location to one of the nodes on the
% sensor block

%% load modal data
% These text files contain the modal data as extracted from the COMSOL
% model. The first column of these matrices contains to modal
% frequencies (in Hz).
load ModalMassesC.txt

%%
n = size(ModalMassesC,1);          % number of modes
f = ModalMassesC(:,1);             % eigen frequencies
m = ModalMassesC(:,2);             % modal masses
k = m.*(f*2*pi).^2;               % modal stiffnesses
Q = 2e2;                          % quality factor of resonances
c = sqrt(m.*k)/Q;                 % damping

%% calculate modal masses
for i = 1:n
        M(i) = tf(1,[m(i) c(i) k(i)]);
end
%% Plot tranfer
close all
P = tf(0,1);                  % initiate total transfer
f1 = figure();
for i = 1:n
    bodeplot(M(i));           % plot modal transfer
    hold on;
    P = P+M(i);               % add modal transfer to total transfer
end

f2 = figure();
```

```
bodeplot(P);
```

## MATLAB CODE FOR NON-COLLOCATED SYSTEM

```
clear all; close all; clc
% This file will load the modal data from the COMSOL model. It will then
% plot the transfer from the actuator location to one of the nodes on the
% sensor block

%% load modal data
% These text files contain the modal data as extracted from the COMSOL
% model. The first column of these matrices contains to modal
% frequencies (in Hz).
load ModalMassesNonC.txt
load dispXactuator.txt
load dispXsensor.txt

%%
n = size(ModalMassesNonC,1);          % number of modes
f = ModalMassesNonC(:,1);             % eigen frequencies
m = ModalMassesNonC(:,2);             % modal masses
k = m.*(f*2*pi).^2;                   % modal stiffnesses
Q = 2e2;                              % quality factor of resonances
c = sqrt(m.*k)/Q;                     % damping

% displacement in X of actuator node
Xa = dispXactuator(:,2);

% displacement in X of measurement node
Xs = dispXsensor(:,2);

% calculate effective masses and stiffnesses. These can become negative due
% to the movement of the actuator and sensor point being out of phase.
m_eff = m./(Xa.*Xs);                  % effective modal mass
k_eff = k./(Xa.*Xs);                  % effective modal stiffness
c_eff = c./(Xa.*Xs);                  % effective damping

%% calculate modal masses
for i = 1:n
        M(i) = tf(Xa(i).*Xs(i),[m(i) c(i) k(i)]);
end
```

```
%% Plot tranfer
close all
P = tf(0,1);                    % initiate total transfer
f1 = figure();
for i = 1:n
    b1 = bodeplot(M(i));         % plot modal transfer
    hold on; grid on
    p1 = getoptions(b1);
    p1.FreqUnits = 'Hz';
    setoptions(b1,p1);
    P = P+M(i);                  % add modal transfer to total
        transfer
end
ht1 = title('All considered modes');

f2 = figure();
    b2 = bodeplot(P); grid on
    p2 = getoptions(b2);
    p2.FreqUnits = 'Hz';
    setoptions(b2,p2);
    ht2 = title('Modal using all considered modes');
```

# Appendix 2.1

## Introduction

It gets difficult to control a non-collocated system due to reduced undesired higher-order resonant frequencies. To overcome this, several passive solutions which maintain high support stiffness have been reviewed. In this appendix, initially, the type of flexures are discussed and a conclusion on what support direction is required to be maintained. Then solutions to maintain that support direction are mentioned.

## Types of flexures

The flexures have been classified based on their DOF in spatial dimensions:

### 2 Dimensional (2D) or Planer

The flexures have the following sets of DOF:

- 1 DOF planer flexure: Only One Rotation, represented as $\phi$: Flexure hinge is supposed to be compliant only about one axis - along which there is the relative rotation between the EE and ground. The rotation is the result of the combination of the types of deformations (elongation, compression, and shear). The compliant axis (also called sensitive axis) lies in the cross-section having minimum material, where maximum bending compliance is present and is perpendicular to the plane formed by the longitudinal and transverse axes.

  Rotation also causes translation as shown in figure 19c. So only one among "rotation $\phi$", "translation $x$" and "translation $y$" can be called the DOF. Generally, the rotation is mentioned as the one DOF. An example of notch flexure is shown in figure 13. It rotates about the center where it has minimum cross-section. It is called a flexure hinge.

  Like the 2D circular flexure design by Paros and Weisbord, elliptic flexure (figure 14) was introduced by Smith et al., then the parabolic, hyperbolic and flexures were introduced by Lobontiu et al [2]. All these flexure hinges are the single axis and therefore are designed to cover planer CM applications.

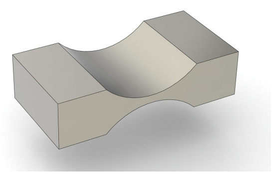

Figure 13: Notch flexure [1]

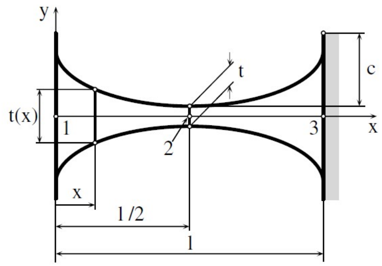


Figure 14: Elliptical flexure adapted from [2]

Usually, the flexures have high stiffness in its longitudinal direction due to the presence of material uniaxially between the EE and the ground. So it provides the DOC along this direction. The longitudinal direction changes along with the rotation of EE about the compliant axis. It is required to maintain the stiffness in the longitudinal direction for the 1 DOF flexure hinges. Any longitudinal direction load can further rotate the flexure hinge because of the rotational DOF but rotation can be controlled by the control stiffness of the actuator. However, stiffness in the longitudinal direction is not controlled by the actuator. Therefore, designs are made keeping in mind that stiffness in the longitudinal direction remains high.

Maximum stress is developed in the region of the minimum cross-sectional area where the compliant axis lies. So designs are made to avoid it. For example, the cross-spring flexure pivot provides 1 DOF rotation as shown in figure 1b. Here, each flexible part has a constant cross-section, so stress developed for the same displacement of EE is lesser compared to the notch flexure.

- 2 DOF planer flexure: One Rotation and One Translation, represented as $x$ and $\phi$: Two DOFs are provided to the EE as shown in figure 15. One is rotation like the flexure hinge and the other is the translation along the transverse direction. The 1 DOF of rotation is due to the deflection of the blade flexure like the bending of the cantilever beam due to the transverse load. So, the instantaneous axis of rotation will become the compliant axis. An analogous rigid body linkage can be assumed to be rotating about this instantaneous axis of rotation.

  For the load along the longitudinal direction of the flexure, both the segments of one DOF rotation will experience the same load longitudinally, as shown in the free body diagram in figure 16. Here, the reaction force C is equal to the external force. The reaction force A is equal and opposite to the reaction force B. Symmetrically, both the segments are identical and experience identical external force. So both the segments can be analyzed as individual flexures with single DOF rotation.

  The longitudinal stiffness is the highest for the perfectly flat and straight flexure. Imperfections of the size of the order of the thickness of the leaf-spring can considerably reduce its in-plane stiffness, as can deflections of the same order of magnitude [3].

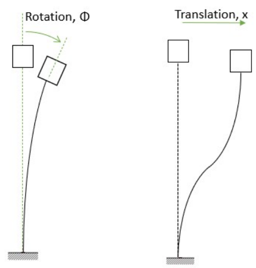


Figure 15: Rotation and translation provided by leaf spring

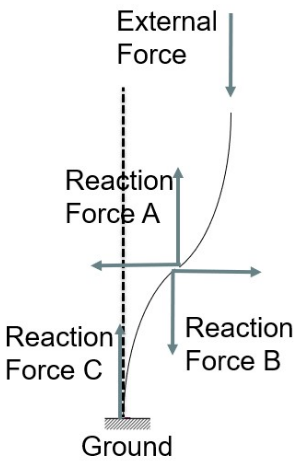


Figure 16: Action-Reaction Pairs

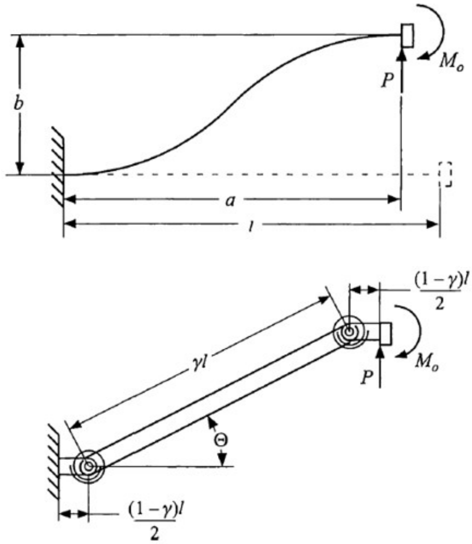


Figure 17: Pseudo-rigid body model of 2 DOF planer flexure, figure from [4]

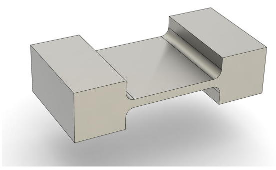

(a) Blade Flexure [5]

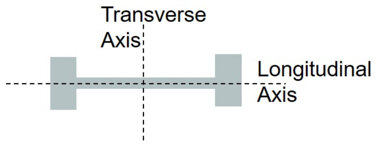


(b) Longitudinal and transverse axis [2]

Figure 18: An example of 2 DOF planer flexure: Blade flexure

For combined translation and rotation, each part, now, has the unequal counter rotations to give the combined results. All the segments are analyzed separately for their single DOF of rotation. For example, using the pseudo-rigid body model, the location of each axis and required stiffness of each rotation is analyzed as shown in figure 17.

More than two axes are generally not required because planer flexures do not have more than 2 DOF. An example is blade flexure as shown in figure 18a. Its longitudinal and transverse axis is also shown in figure 18b. The flexure constraints translation along its longitudinal direction.

### 3 DIMENSIONAL (3D)

The flexure is supposed to be compliant in two or more axes which are not parallel. Two-axis flexure, for instance, enable bending and the resulting relative rotation about two mutually perpendicular compliant axes generally at different spring rates. An example of two-axis flexure is small width blade flexure as shown in figure 19a. For other flexure configurations that have rotational symmetry (they are revolute), bending is non-specifically possible about any axis that is perpendicular to the axial direction. An example of multi-axis flexure is the pin flexure shown in figure 19b.

#### SHELL FLEXURES AND CYLINDRICAL FLEXURES

As shown in figure 20, other shapes of flexures are also designed for different applications which are not discussed in this chapter.

- The transverse axis is curved: [7] In figure 20a, the tension side and the compression side are relatively far apart causing a high second moment of inertia. Whereas the flattened cross-section has a less second moment of inertia.

- The longitudinal axis is curved: [8] In figure 20b, the flexure has a curvature in its undeformed configuration and so the stress is zero. Whereas, if the straight beam is bent to have the same curvature then it is in its deformed configuration and it has stress. So, the pre-curved and the bent beam have the same geometry but different stresses. Due to different stresses, they have different stiffness.

Both the above types of flexures can also be combined to form longitudinal as well as the transverse axis is curved type flexures. Further, hollow flexures like the pipe, bellow, etc can also be found in the literature but they are not discussed here.

### CONCLUSION ON TYPE OF FLEXURES

In planer flexures, the following two cases are possible to consider for solving the problem of reducing support stiffness:

- Maintaining the stiffness along the changing longitudinal direction in 1 DOF rotation flexures

- Maintaining the stiffness along the longitudinal direction in 1 DOF translation flexures or parallel leaf springs

Whereas, in 3D, stiffness may also be required to be maintained in torsional direction.

## PASSIVE SOLUTIONS

In planer flexures, the in-plane support stiffness and in 3D situations torsional stiffness is required to be maintained. By the end of this section, solutions have also been classified in these three types of support stiffness cases. A combination of the designs can also be used to achieve the required performance.

### USING NEGATIVE STIFFNESS

Larger support stiffness in comparison to drive stiffness is required. If drive stiffness is too large it can be decreased by fitting a mechanism with negative stiffness parallel to the elastic element. Negative spring stiffness can be obtained at the buckling state of a leaf spring [9]. An example of the mechanisms having negative stiffness is shown in figure 21

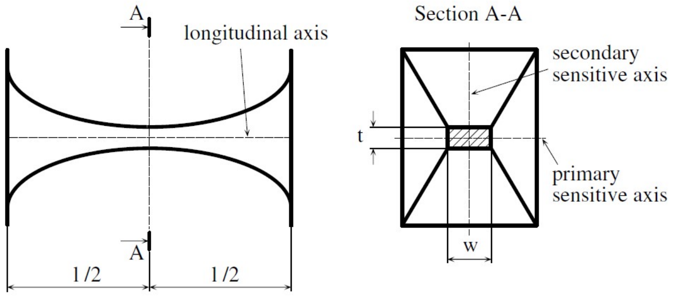


(a) 2-axis 3D flexure: Rectangular flexure [2]

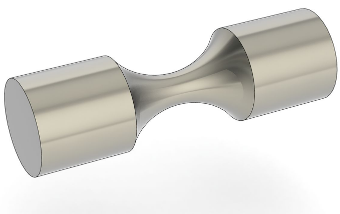

(b) Multi-axis 3D flexure: Pin flexure [6]

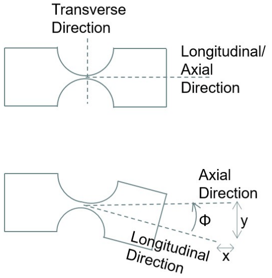


(c) Rotation as one DOF

Figure 19: Examples of 3D flexures

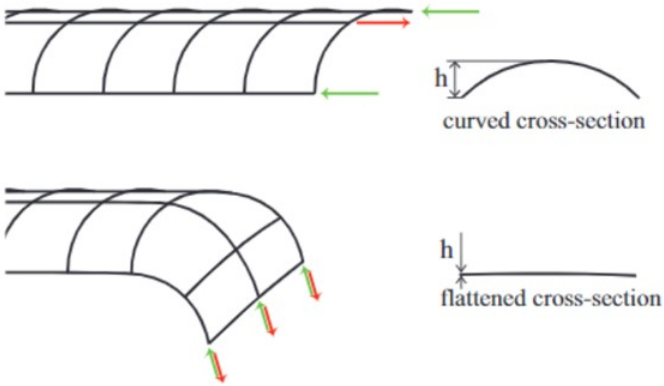


(a) Transverse axis curved [7]

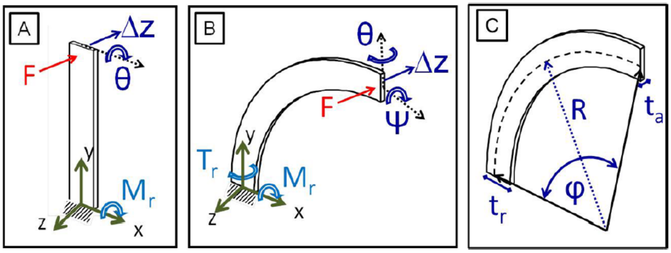


**Figure 2.** **(A)** Straight-beam mechanics, $F$ is the load on the beam, $M_r$ is the resulting bending moment, $\Delta z$ is the displacement along the z-axis, and $\theta$ is the parasitic rotation about the x-axis. **(B)** Curved-beam mechanics, highlighting the added twist, $\psi$, and torque, $T_r$ and **(C)** Curved-beam parameters. $R$ represents the radius of curvature, $\phi$ is the sweep angle, $t_r$ is the thickness of the beam in the radial direction, and $t_a$ is the thickness in the axial direction.

(b) Longitudinal axis is curved, screenshot from [8]

Figure 20: Examples of pre-curved flexures

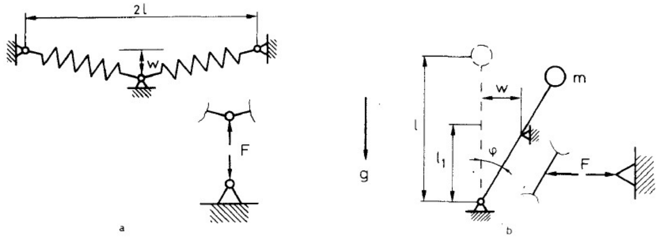


**Figure 1.** Mechanisms with negative stiffness
(a) Composed of two compression helical springs.
(b) Composed of an unstable pendulum.

Figure 21: Example of mechanisms deflected $w$ and having negative stiffness from [9]

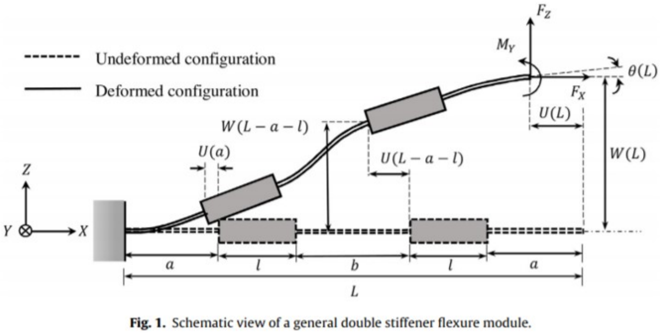


(a) Thicker crossection for stiffening from [10]

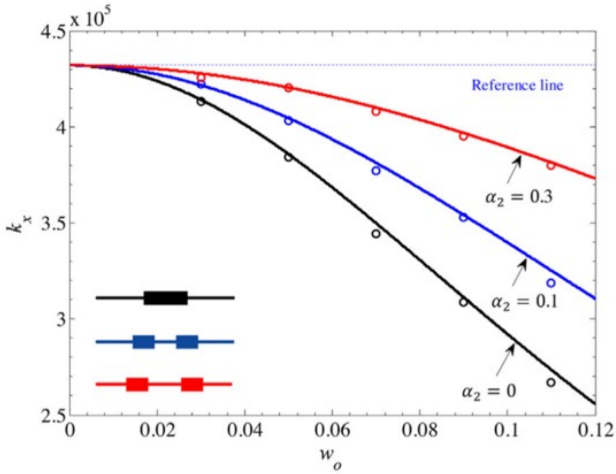


(b) Variation of axial stiffness with DOF displacement for different beam topologies

Figure 22: Passive stiffening modules from [10]

## USING LOCALLY STIFFENING MODULES

A novel flexure beam module with low stiffness loss is developed by increasing stiffness in some parts of the flexure [10]. Each of these modules can be called passive stiffening modules(PSM). $\alpha_2 = b/L$ is taken, where $b$ and $L$ are as shown in figure 22a. In figure 22b, for different values of $\alpha_2$, change in longitudinal support stiffness with deflection is plotted. **However, by decreasing the flexible portion in flexure increases stress developed while achieving equivalent ROM.** This method is similar to using two 1 DOF rotation flexures to make hinge joints of 2 DOF rotation and translation motion.

## USING PRE-CURVED FLEXURES

### FOR TRANSLATIONAL DOF

Design of a Folded Leaf Spring (FLS) with high support stiffness at large displacements using the inverse Finite Element Method (FEM) is shown in figure 23 and 24 [11]. In

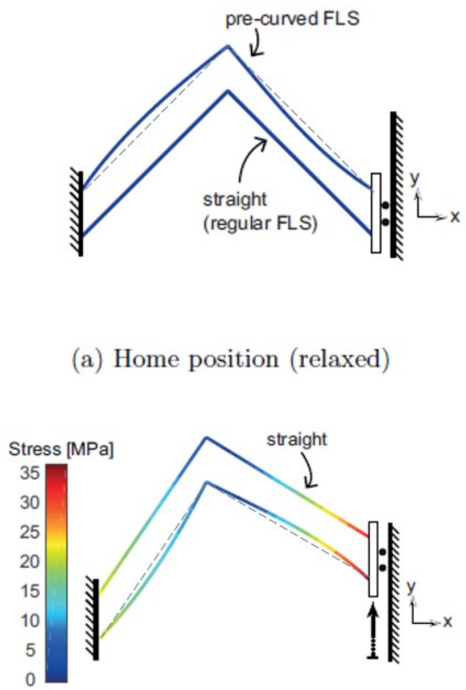


(a) Home position (relaxed)



(b) Actuated state (loaded)

Figure 23: Pairs of straight and pre-curved flexure leaf springs from [11]

inverse FEM, the required deformed shape for the given external force is known and the undeformed shape is calculated. Generally, in FEM, undeformed shape and external forces are given and deformed shape is calculated. Here, at certain deformation a flexure becomes flat, that is, initially it was curved. The initial curvature can be found using inverse FEM. The other flexure that is flat initially gets deformed and the deformed shape can be calculated by FEM.

The longitudinal stiffness is the highest for the perfectly flat and straight flexure. Imperfections of the size of the order of the thickness of the leaf-spring can considerably reduce its in-plane stiffness, as can deflections of the same order of magnitude [3]. As shown in 23, the flat flexure gets deformed and the pre-curved flexure gets flat, so the lost stiffness in flat flexure is compensated by stiffness gain in pre-curved flexure. The performance of the combined flexure is shown in red in the graph shown in 25.

### FOR ROTATIONAL DOF

Elastic element showing low stiffness loss at large deflection is shown in figure 26. [12]. Initially, the curved hinge flexure consists of two curved leaf-springs. In this state, both the leaf-springs contribute together to the longitudinal stiffness. The elastic element deforms such that it provides rotation. Note that, here the longitudinal axis is changing

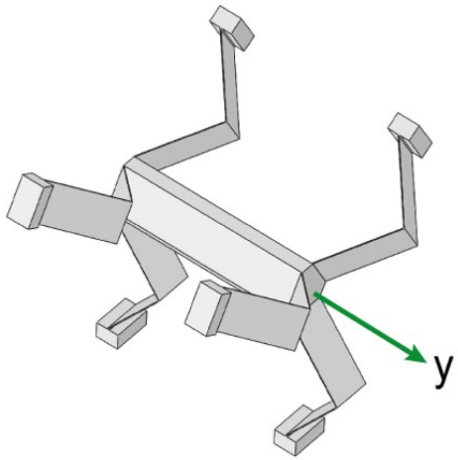


Figure 24: Translational DOF with high support stiffness from [11]

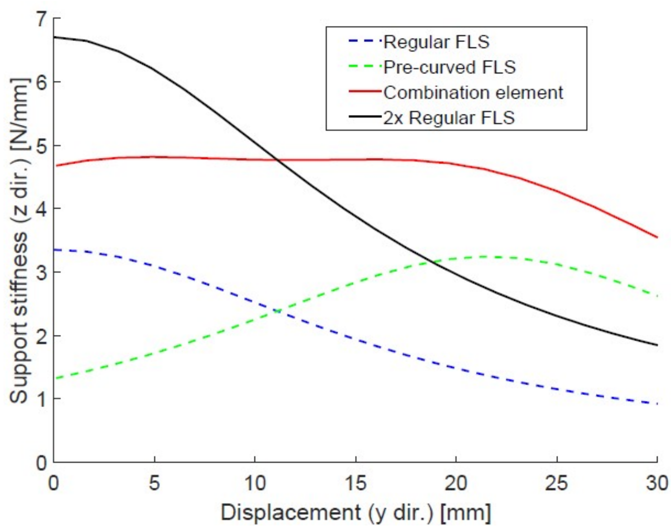


Figure 25: Support stiffness of the combination element compared to the case with two regular, straight flexures (black)

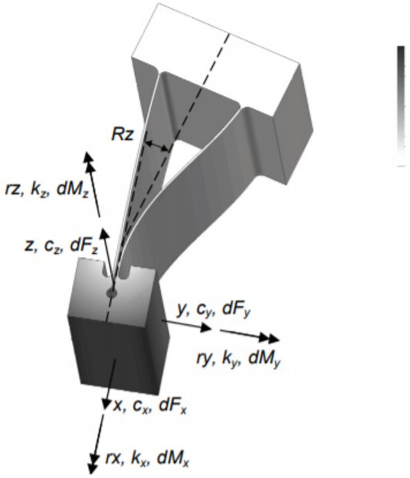


Figure 26: Two curved leaf-springs from [12]

direction while rotation. So, stiffness cannot be maintained along the initial longitudinal direction else it would not allow the rotation.

## USING REINFORCEMENTS

### CONSTRAINING TORSION WHILE 1-DOF ROTATION

In 3D, at large deflections, the torsional stiffness also decreases and so the first unwanted natural frequency is for the rotation about the axis which is perpendicular to the desired axis of rotation. Since it is perpendicular to the plane having motion, so the torsion stiffness is called out of plane stiffness. For example, in figures 27b and 27d, the desired rotation is about x-axis but at large deflection, rotations about y- and z- axes become compliant. The following designs are present in literature which were designed using some tricks like "switch-back" to improve the performance.

- Solid-flexure cross Hinge (SFCH) as shown in figure 27b
- Three-flexure cross hinge (TFCH) as shown in figure 27d
- Butterfly flexure hinge (BFH) as shown in figure 27c
- Curved hinge flexure (CHF)
- Cross revolute hinge (CRH)
- Torsionally Reinforced LeafSpring (TRLS)

To further improve torsional stiffness, the above designs have been optimized and a new design called as Torsionally Reinforced Leaf Spring (TRLS) or $\infty$ -Flexure Hinge ($\infty$-FH) has been introduced by Wiersma et al. The $\infty$ -flexure hinge is found to have the highest second natural frequency as shown in the plot in 28. The comparison is done

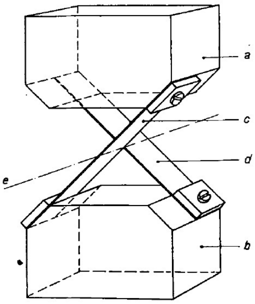


(a) Cross-spring pivot adapted from [13]

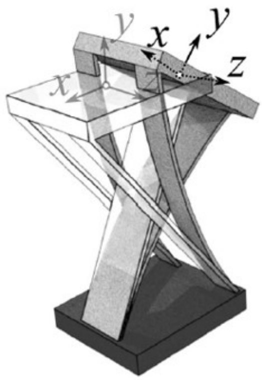


(b) TFCH adapted from [14]

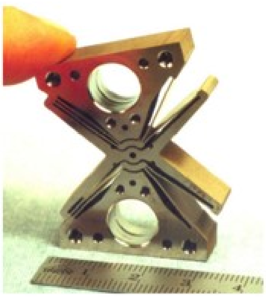

(c) BFH adapted from [15] supports 1.2 Kg payload mass

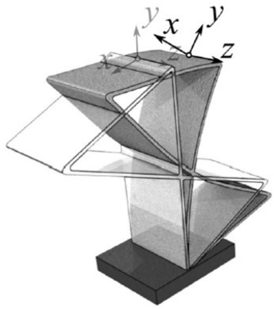


(d) Two sets of triangular reinforcements on one flexure from [16]

Figure 27: Reinforcing of Flexures

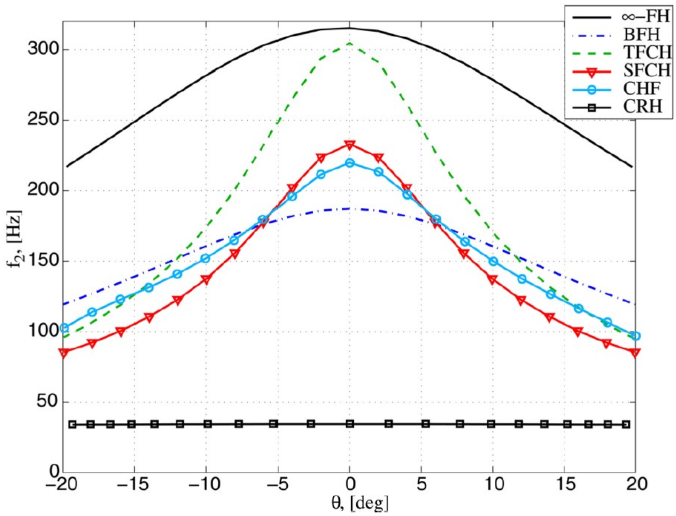


Figure 28: Second eigenfrequency as a function of the angle of deflection for the optimal solutions, determined with the FE method

using the same constraints such as maximum stress developed, actuation moment and deflection angle, height along the axis of rotation, and same material properties [14].

### HIGH SUPPORT SPHERICAL FLEXURE JOINT

As shown in figure 19b, the pin joint provides 3 DOF rotational motion like a ball joint. The construction of higher support stiffness of the spherical joint is discussed here. Three compliant folded leaf springs with the folding axis meeting at point P as shown in figure 29a. Then, three more compliant folded leaf springs with the folding axis meeting at the same point P are shown in figure 29b. One of the ends of each folded leaf spring is connected to a common ground as shown. Top and bottom frames are connected to the free ends of the three bottom and the three top folded leaf springs respectively as shown in figure 29c. Then deflected state about one of the three-axis of the spherical joint is shown in figure 29d.[17]

The spherical joint provides 30° tip-tilt and 10° pan motion. It maintains a support stiffness of over 200 N/mm and a load capacity of almost 300 N at the maximum deflection.

## CONCLUSION ON PASSIVE METHODS TO MAINTAIN SUPPORT STIFFNESS

The existing solutions:

- provide longitudinal stiffness while translational DOF
- provide longitudinal stiffness which is changing direction while rotational DOF
- provide torsional stiffness while rotational DOF

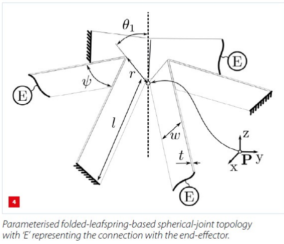


(a) Three compliant folded leaf springs

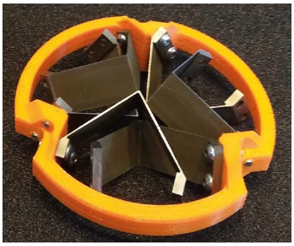

(b) Three more compliant folded leaf springs

(c) Top frame and bottom frame connected

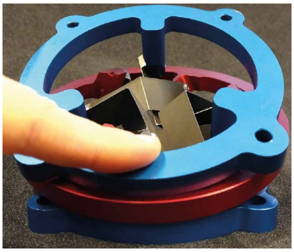

(d) Deflected state

Figure 29: Spherical Flexure Joint from [17]

Variation of support stiffness or eigenfrequency (which also depends on the support stiffness) with the deflection has been plotted in the above cases. More ideas can also be generated by combining designs such as:

- Using locally stiffening modules along with leaf flexures in other designs
- Using triangular reinforcements along with pre-curved flexures in the case of translational and rotational DOF
- Using pre-curved flexures along with torsionally constrained rotation

All the designs in literature and their combinations suggested above are the passive solutions. More designs based on the passive maintenance of support stiffness are made in chapter 2.

## REFERENCES

[1] *Notch flexure image,* .

[2] N. Lobontiu, *Compliant mechanisms: design of flexure hinges* (CRC press, 2002).

[3] J. Meijaard, *The importance of imperfections in leaf-spring flexures for the support stiffness,* Procedia IUTAM **13**, 82 (2015).

[4] *Compliant Mechanisms, ME46115,* Lecture Notes, TU Delft, Netherlands (2018/2019).

[5] *Blade flexure image,* .

[6] *Pin flexure image,* .

[7] G. Radaelli and J. Herder, *Gravity balanced compliant shell mechanisms,* International Journal of Solids and Structures **118**, 78 (2017).

[8] M. Telleria and M. Culpepper, *Understanding the drivers for the development of design rules for the synthesis of cylindrical flexures,* (2012).

[9] J. van Eijk and J. F. Dijksman, *Plate spring mechanism with constant negative stiffness,* Mechanism and Machine Theory **14**, 1 (1979).

[10] H. Malaeke and H. Moeenfard, *A novel flexure beam module with low stiffness loss in compliant mechanisms,* Precision Engineering **48**, 216 (2017).

[11] J. Rommers and J. Herder, *Design of a folded leaf spring with high support stiffness at large displacements using the inverse finite element method,* in *IFToMM World Congress on Mechanism and Machine Science* (Springer, 2019) pp. 2109–2118.

[12] D. M. Brouwer, J. P. Meijaard, and J. B. Jonker, *Elastic element showing low stiffness loss at large deflection,* in *Proceedings of the 24th Annual Meeting of the American Society of Precision Engineering, Monterey, CA* (2009) pp. 30–33.

[13] J. Haringx, *The cross-spring pivot as a constructional element,* Flow, Turbulence and Combustion **1**, 313 (1949).

[14] D. Wiersma, S. Boer, R. G. Aarts, and D. M. Brouwer, *Design and performance optimization of large stroke spatial flexures,* Journal of computational and nonlinear dynamics **9**, 011016 (2014).

[15] S. Henein, P. Spanoudakis, S. Droz, L. I. Myklebust, and E. Onillon, *Flexure pivot for aerospace mechanisms,* in *10th European Space Mechanisms and Tribology Symposium, San Sebastian, Spain* (2003) pp. 285–288.

[16] M. Naves, D. M. Brouwer, and R. G. Aarts, *Building block-based spatial topology synthesis method for large-stroke flexure hinges,* Journal of mechanisms and robotics **9**, 041006 (2017).

[17] M. Naves, R. Aarts, and D. M. Brouwer, *Maintaining high support stiffness: Large-stroke spherical flexure joint,* Mikroniek **59**, 17 (2019).

# Appendix 2.2

## Designs

The passive method of maintaining support stiffness in the 3rd 1 DOF translation motion design is discussed here. The third design is more similar to the long design. The fourth design is modified version of third design in which longer actuator can be implemented.

The design steps are similar to steps taken in appendix 3.2. So figures are marked with references to analogous figures of the appendix. Third design is taken further to develop into 1DOF translation motion stage.

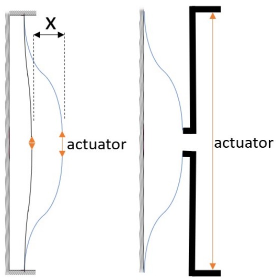


Figure 30: Third (left) and fourth (right) design by PASD method

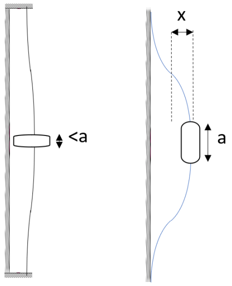


(a) Mechanism outline (47)

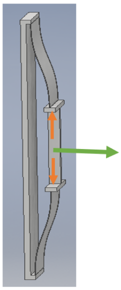

(b) 3D model of the mechanism in which actuator is represented by a rod in center (48)

Figure 31: Providing actuation from support direction to two pre-curved flexures for amplified motion

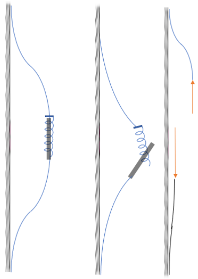

Figure 32: Problem of relative motions between the two EEs. It should be constrained (60)

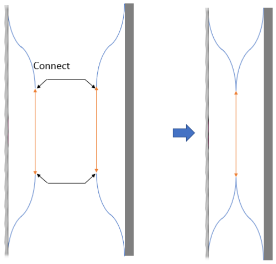


Figure 33: Solution of step 5 (61)

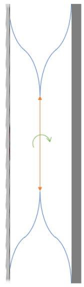

Figure 34: Problem of step 4 (57)

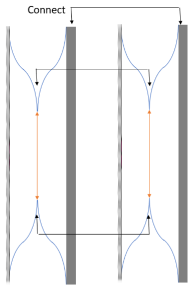


Figure 35: Solution of step 4 (62)

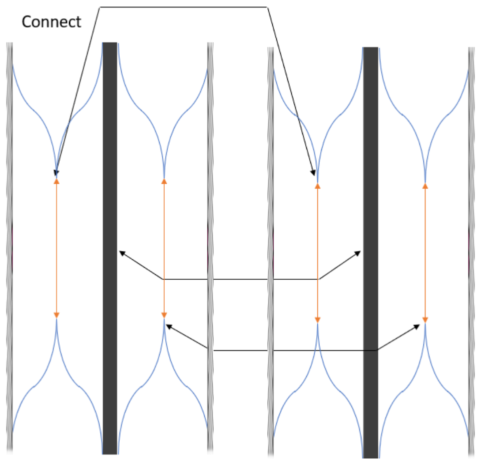


Figure 36: Second mechanism with zero parasitic motion and passive maintenance of support stiffness (64)

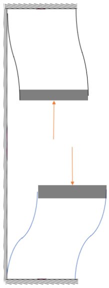

Figure 37: Problem of step 6 remains: relative translation motion in transverse direction (65)

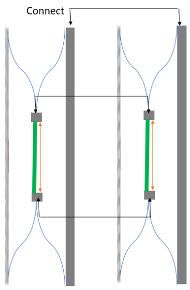


(a) First design

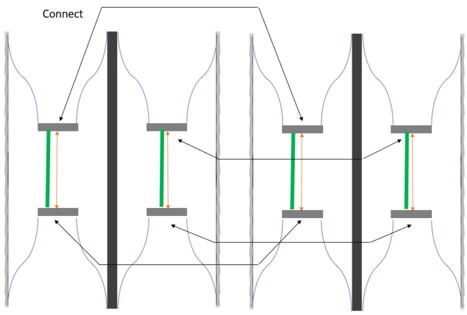


(b) Second design

Figure 38: Solution in step 6: solving the problem of relative translation (66)

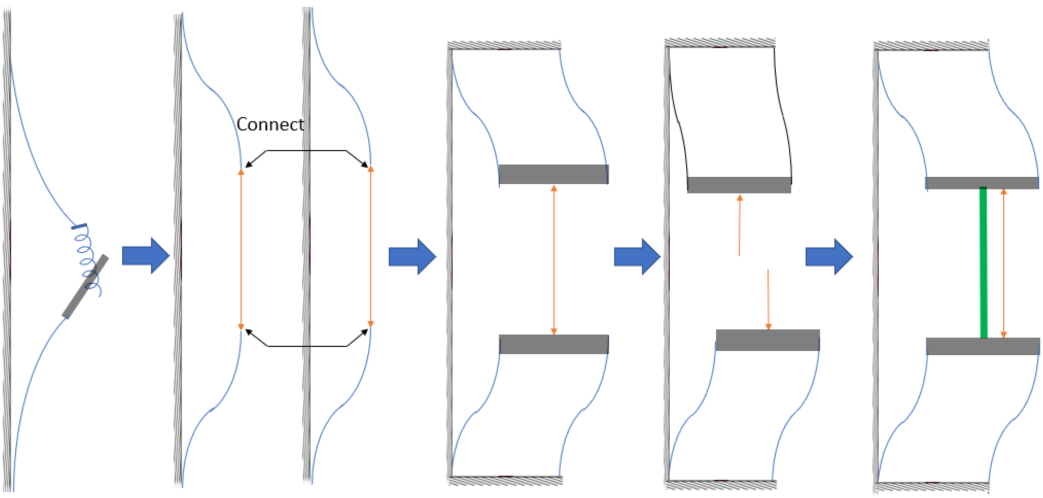


Figure 39: Third design (67)

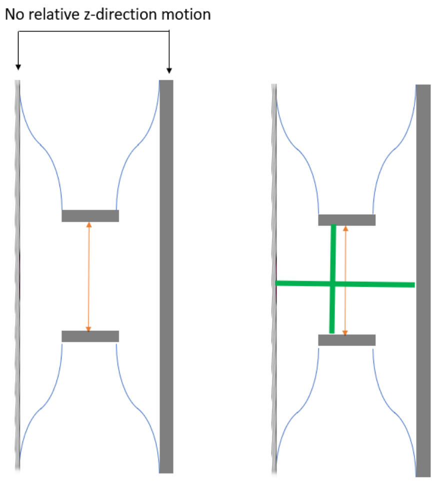


Figure 40: Fourth design (68)

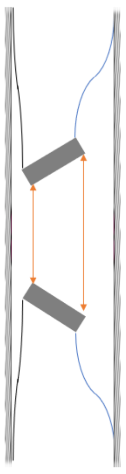

Figure 41: Rotational DOF design (69)

# Appendix 3.1

## Distributed Mechatronics

Precision positioning machines have been characterized by their performance criteria such as range of motion, speed, repeatability, and resolution. The aim is to generate an innovative design method that can be used later to design the mechanical subsystems which improve the performance of the precision machine. Mechanical systems without active elements, that is, only having passive properties has limited performance. These systems with the help of control engineering can cross the performance limits which were not possible before. Electronics, actuators, and manufacturing of all these have enabled us to implement better control algorithms.

For instance, consider the task of rotating a light weight rod, as shown on left side in figure 42. A rotary actuator is used to rotate the rod as shown on the right side.

In presence of gravity which is vertically downwards, the rod deforms as shown in next figure 43.

A solution to improve the precision is to implement a controller which rotates the rod to desired position as shown in figure 44.

But, there still exists undesired orientation of EE as shown by the blue arrow. It cannot be controlled by the actuator. So, to reduce the structural compliance, a thicker rod can be used which increases mass, or an active method like piezoelectric patches can be used, as shown in figure 45.

In case of additional vibrations, the same actuators can be used to damp them, as shown in figure 46

If required stroke and force can be achieved by distributed actuation then unlike having conventional transducers, entire mechatronic systems can be realized by etching each transducer and components into a monolithic 'smart' material substrate [1].

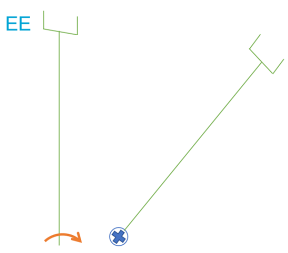


Figure 42: A rotary actuator is used to rotate the rod

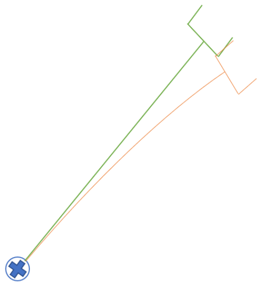

Figure 43: Reduced precision due to structural compliance

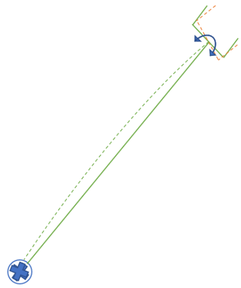

Figure 44: A partial solution of implementing control to reduce the error

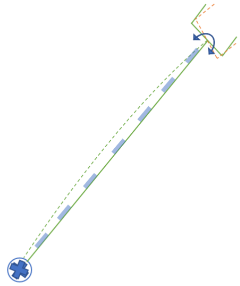

Figure 45: A solution to mitigate the error

Figure 46: Damp vibrations actively

## Piezoelectric Actuators

(The following information about piezoelectric literature is taken from The NanoPositioning Book, by Thomas R Hicks, Paul D Atherton. [2])

Naturally occurring minerals have lower intensity of the piezoelectric effect, but by the certain manufacturing processes of ceramics, the higher piezoelectric effect is obtained. Most of the ceramics are based on lead zirconate titanate and also known as PZT ceramics (from Pb, Zr, Ti). It produces strains of up to 0.1% so 100 µm of displacement can be obtained from 100 mm long piezoelectric.

The advantages of piezo actuators are:

- the motion is smooth and continuous - no stick-slip (the expansion is an atomic process). In practice, the smallest step size is limited by the noise level of the controller.
- Piezo actuators are very stiff: practical actuators have over 20% of the stiffness as the equivalent made out of solid stainless steel. They can thus generate a lot of force.
- The response to an electrical signal is very quick.
- They require less electrical power. Typical power dissipation: moving, a few milliwatts; static, a few microwatts.

Piezo actuators have their problems too:

- The nonlinear behavior such as hysteresis and long term drift.
- They are not very good at pulling (though they will do it) so require pre-loading.

The piezo actuators are used in a closed-loop system to overcome the non-linear effects. For exciting vibrations and controlling them, distributed actuation and sensing can improve controllability which is not possible with the small number of sensors and actuators. The piezo actuators are placed at, for example, the parts of materials which undergo maximum strain. Also, the phase in which it operates is taken into consideration. [3].

The following manufacturing technique and problems associated with each technique is adapted from [3].

The piezoelectric actuator can be surface-bonded or embedded in the structure. Surface bonding can be done on an aluminum beam and embedding is done using glass/epoxy and graphite/epoxy laminates.

For surface bonding, manufacturing difficulties were mentioned by Crawley et al.:

- making electrical contact with both sides of the piezoelectrics;
- the electrical contact has to be prevented from short-circuiting;
- the bonding layer thickness should remain uniform to match experimental data with the analytical one.

In embedded assembly, the nominal thickness of the leads attached to piezoceramic is equal to the thickness of the laminates. Holes equal to the dimensions of the piezoceramics along with the leads are cut in the laminate to fit the piezo sub-assembly. Teflon is wrapped around the leads outside the laminate to prevent any excess epoxy that might flow during the curing process from bonding to the leads. The problem with embedding piezoelectrics inside a graphite/epoxy beam is that the graphite fibers electrically short-circuit the piezoelectric by making contact with the electrodes or the bonded leads.

## REFERENCES

[1] *Distributed mechatronics,* .

[2] T. R. Hicks, P. D. Atherton, Y. Xu, and M. McConnell, *The nanopositioning book* (Queensgate Instruments Torquay, Torbay, UK, 1997).

[3] E. F. Crawley and J. De Luis, *Use of piezoelectric actuators as elements of intelligent structures,* AIAA journal **25**, 1373 (1987).

# APPENDIX 3.2

## STEPS TO DESIGN CELLS TO LOCALLY ACTUATE FLEXURES

The design procedure to realize the design in 47 is as follows:

- In 3D, the model would look like that shown in figure 48.
- But, during actuation, certain moment on the flexures will act like that shown in figure 49.
- So, to balance one of the flexure, other side is symmetrically made as shown in figure 50
- Yet, the flexures on sides are not balanced and their reaction moment can break the actuators as shown in figure 51.
- A method to prevent damage to actuator is to connect the ends which will cancel the moment as shown in figure 52.
- It can be done in two ways:

  One is to connect them in-plane as shown in figure 53. The-in plane connection does not allow cells to stack up on top of each other.

  The second is to connect them out-of-plane by making a bridge, as shown in figure 54. In this case, only one actuator is only required which will be actuating the two EE from out of the plane of flexures. The actuator is in a different plane than the flexures.
- To operate manually for demonstration purposes, additional flexures are conceptualized as shown on the left side of figure 55. A 3D model of the cell with the earlier

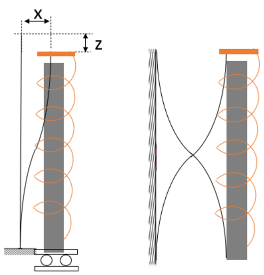


Figure 47: Step 1: Mechanism outline

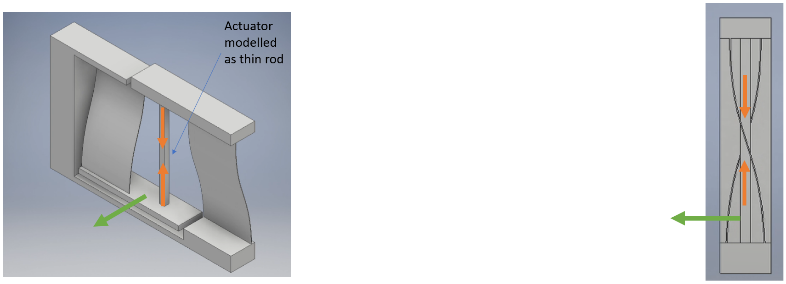


(a)

(b)

Figure 48: Step 1: 3D model of the mechanism

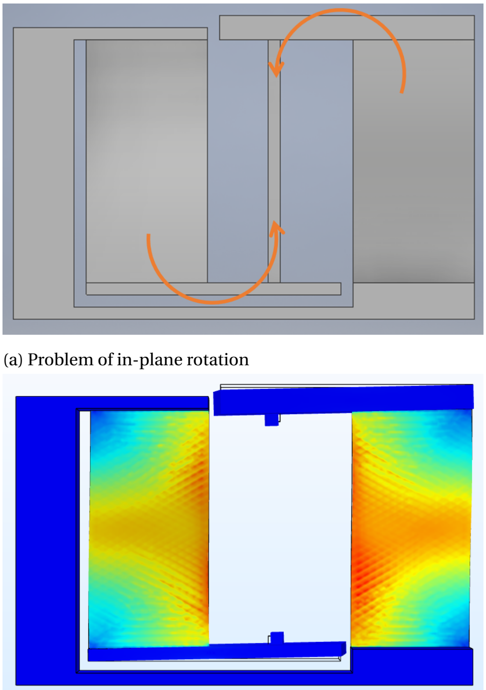

(a) Problem of in-plane rotation

(b) Deformation simulation in COSMOL

Figure 49: Problem in Step 1

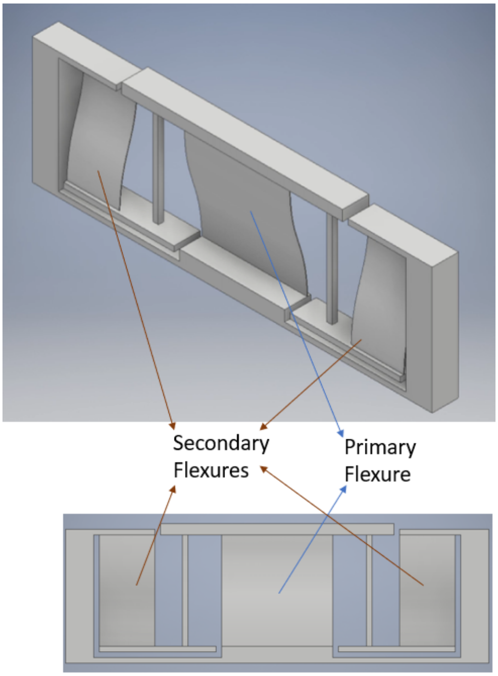


Figure 50: Step 2: Balancing primary flexure

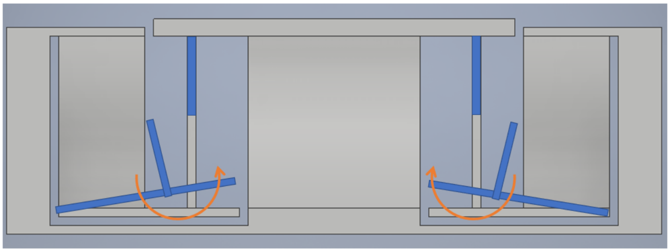

(a) Problem of in-plane rotation remains partially in step 2

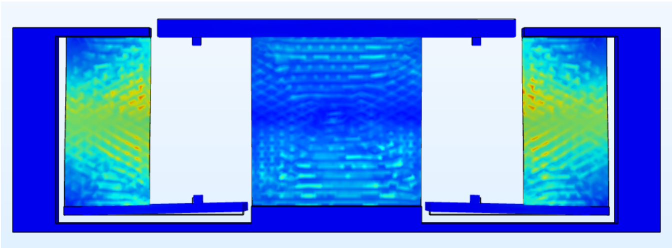

(b) Deformation simulation in COMSOL

Figure 51: Problem in step 2

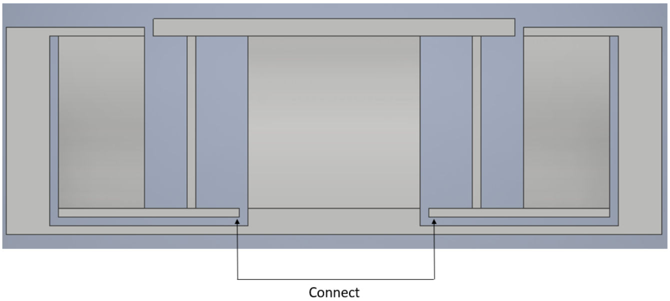


Figure 52: Step 3: Solving problem in step 2

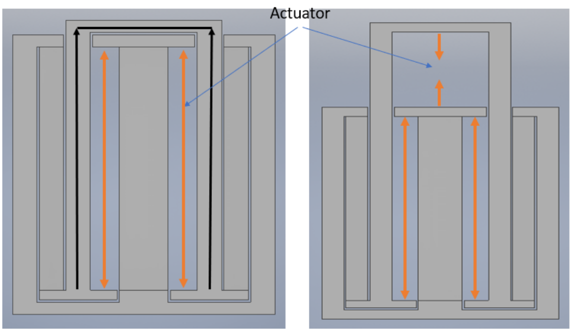


(a) In-plane connection

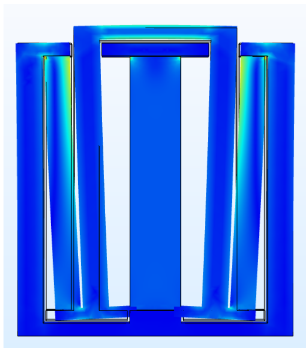

(b) Deformation simulation: Deformation only when there is deformation in the rigid connection

Figure 53: Step 3: wrong approach: Solving problem in step 2 by in-plane connection

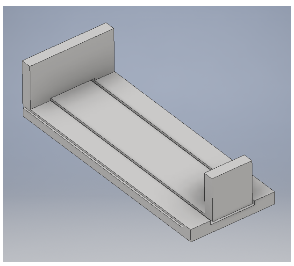

(a) CAD model showing no deformation

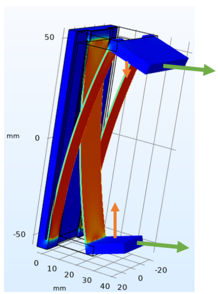


(b) After deformation

Figure 54: Step 3: Correct approach: Solving problem in step 2 by out of plane connection

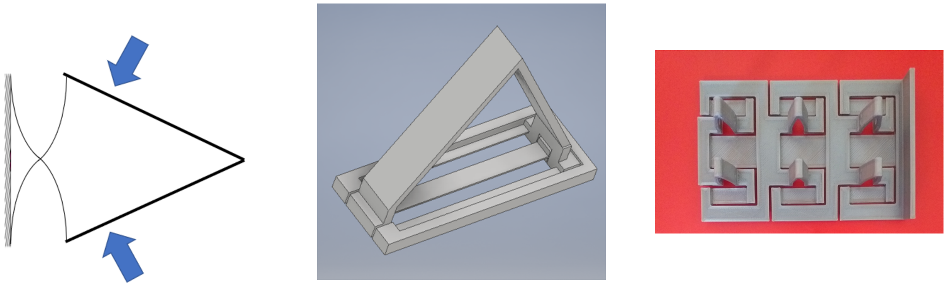

Figure 55: Additional triangular flexures to actuate manually

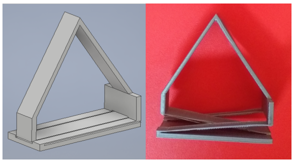

Figure 56: Compact cell design with out-of-plane connection between side flexures

proposed out of plane connection is shown in the middle of the figure. A physical model of flexure with 3 embedded cells is as shown on the right side of the figure. Here, the cells are without the proposed out-of-plane connections since there is no actuator.

- A more compact cell can also be designed, as shown in figure 56. It has the out-of-plane connection and is used to demonstrate the mechanism manually.
- The assembly of two main flexures of the mechanism is similar to the cross pivot flexures. So it can rotate as shown in figure 57a. Rotation is prevented by assembling additional mechanisms as shown in figure 57b. This is analogous to PLSM constraining rotation in single leaf spring to give only translational motion.

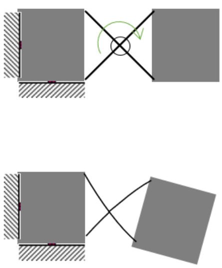

(a) Rotation in cross-pivot flexure

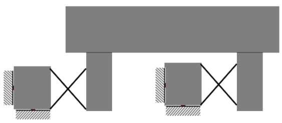

(b) Constraining rotation by joining additional set of mechanism

Figure 57: Step 4: problem: rotation like that in cross pivot flexure

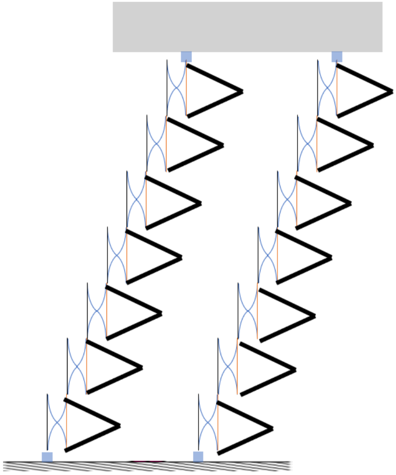

Figure 58: Step 4: wrong approach: The design of CM equivalent to PLSM made from wrong flexure design

- So, it is thought that two such flexures with the cells designed in the previous step need to be connected parallelly to provide only translational DOF. The concept is represented by the image shown in figure 58. But during analysis, the first 6 mode shapes of the design are obtained as shown in figure 59. This shows that there is no constraint on rotation between two cells as middle cells do not have the constraint.

- It is also observed that the flexures have deformation such that the two EE provide rotation figure 54b or have the relative translation as shown in the right side of the figure 60. Both rotation and translation can damage the actuator as shown in the figure.

- Firstly, to prevent the damage to the actuator, additional flexures are added to counter the moment as shown in figure 61a. A 3D model of the cell is shown in figure 61b. The EE of the complete mechanism does not have parasitic motion as marked in the figure.

- But due to rotation (like that in cross pivot flexures shown in figure 62a) not being able to be under control, the two rotations, as shown in figure 62b, needs to be constrained. It is done by assembling an additional mechanism, as shown in figure 62c. This is analogous to PLSM constraining rotation in single leaf spring to give on the translational motion. To make the connections, the two EE of both the parallel mechanisms has to be connected from outside the plane of flexures. The 3D CAD model is shown in figure 63.

- To further maintain the support stiffness, design as shown in figure 64 is made. The black color is the primary stage that moves without any parasitic motion. The stages in grey color have parasitic motion. When the primary stage moves, flexures on one side deforms further and flexures on the other side straighten up. This will

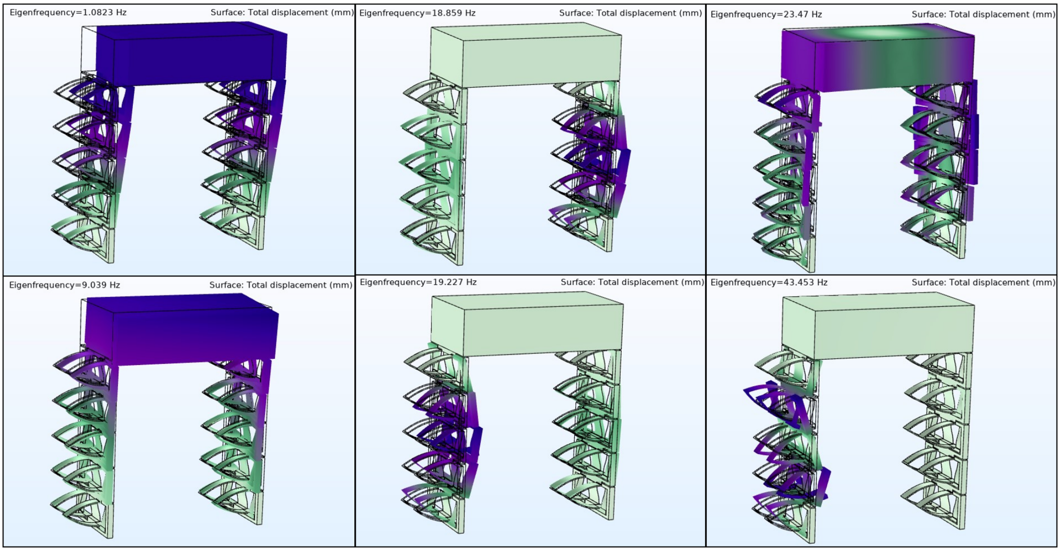


Figure 59: Mode shapes of the CM made of wrong flexure design

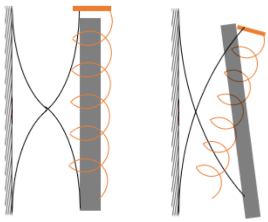

(a) Step 5: problem: Rotation between two EEs

(b) Step 6: problem: Translation between two EEs

Figure 60: Step 5 and 6: Relative motions between the two EEs should be constrained

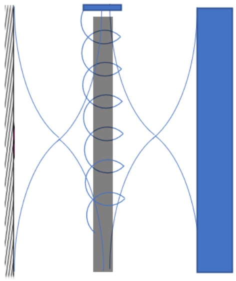

(a) Mechanism outline

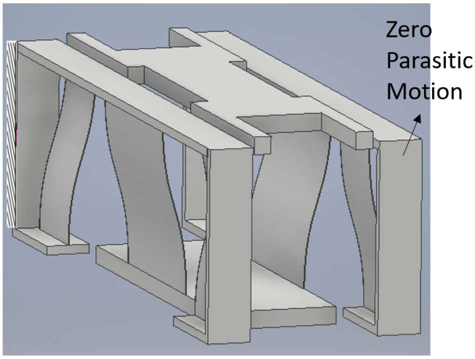


(b) 3D model

Figure 61: Step 5: solution: balancing actuator by additional set of flexures

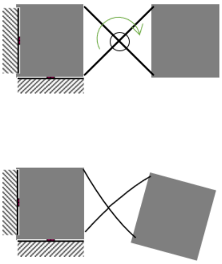

(a) Cross Pivot

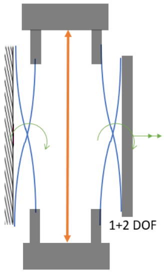


(b) Two axis of rotations and 1 translation

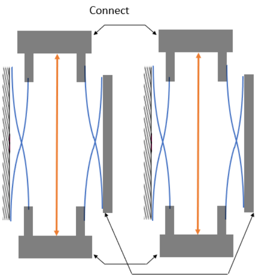


(c) Solution

Figure 62: Step 4: solution: additional mechanism in parallel to solve problem shown in figure 57

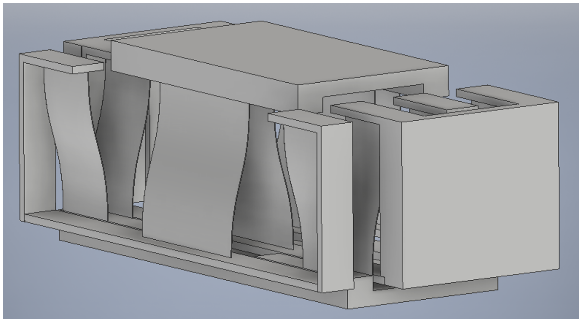

Figure 63: 3D model of the solution proposed in figure 62

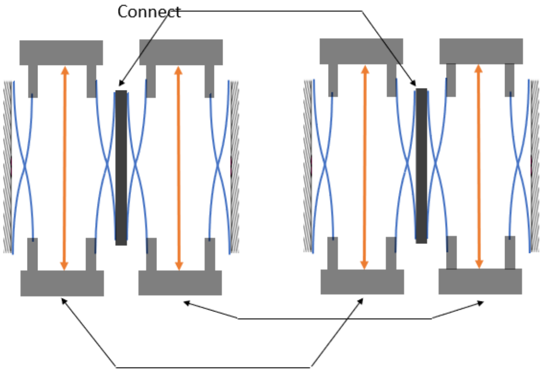


Figure 64: Design for zero parasitic motion and passive maintenance of support stiffness

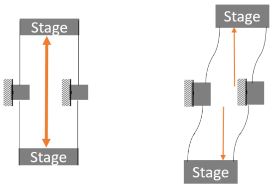


Figure 65: Step 6: problem remains: relative translation motion in transverse direction

maintain the axial stiffness passively as suggested in the literature discussed in appendix 2.1.

- Both the designs that are in figure 63 and 64 have problem of relative translation motion between secondary stage as shown by an analogy in 65. So to constrain this motion, a module of the mechanism is required as represented by green color in figure 66. This mechanism should allow translation of secondary stages towards each other so that the overall mechanism can actuate, but it should constrain relative translation motion in the transverse direction.

  At the end of 6 steps, 2 cell designs (66) have been developed. Further simplification leads to the third design that is proposed for future analysis.

A third design which is less complex than the above two designs (66) is shown in figure 67. It requires only one actuator. It has the same stiffening module between the two secondary stages. But it does not have the primary stage for zero parasitic motion. However, it can be the design of a cell in the flexure and an additional mechanism with more such flexures can be made to compensate for the parasitic motion.

Another design attempt is made by constraining rotation using the stiffening mechanism module as shown in 68. But the module only constraints relative translation motion and not the rotation. So this design of mechanism may have flaws.

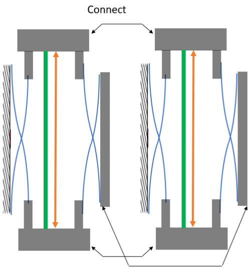


(a) In design shown in figure 63

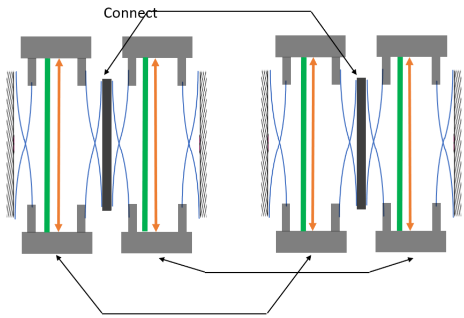


(b) In design shown in figure 64

Figure 66: Step 6: solution: solving the problem of relative translation

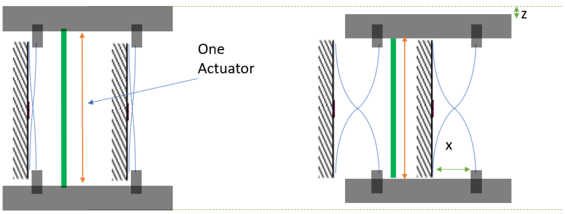


(a) Mechanism outline

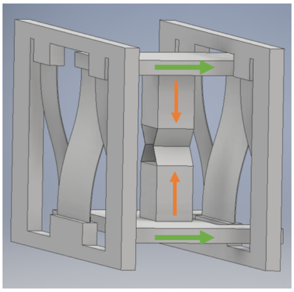

(b) 3D model

Figure 67: Third design

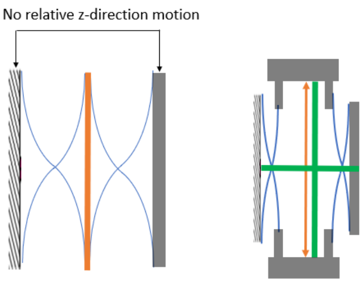


(a) Mechanism outline

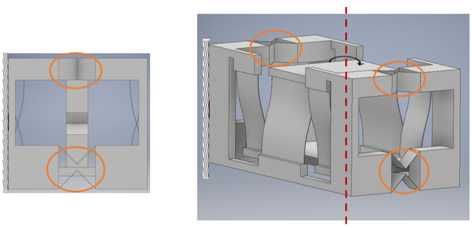

(b) 3D model

Figure 68: Fourth design

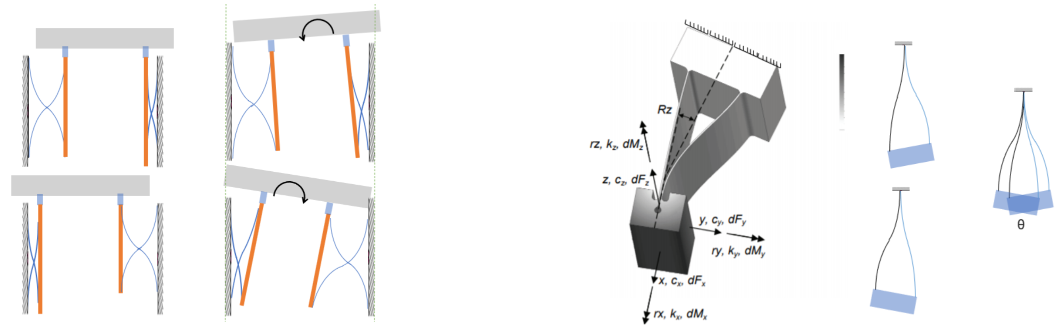


(a) Mechanism outline

(b) Analogous design

Figure 69: Rotational DOF Design

For the sake of completeness in discussing methods of adding parallel mechanism to constrain rotation, a design as shown in figure 69 is made. The left side of the figure outlines that actuator works in out of phase to translate the top stage. But what happens is, due to parasitic motion in flexures, the stage rotates as shown in next figure. This is analogues to design of pre-curved flexures for rotation. In literature, longitudinal direction stiffness is maintained by using two pre-curved flexures having a common EE. But this design is about having the pre-curved flexure with a common base. So it could be used for providing rotational DOF and not the translational DOF.